THERMOECONOMIC ANALYSIS OF SOLAR ORGANIC RANKINE CYCLE WITH ZEOTROPIC MIXTURE FOR POWER GENERATION

THORANIS DEETHAYAT

DOCTOR OF PHILOSOPHY
IN ENERGY ENGINEERING

GRADUATE SCHOOL
CHIANG MAI UNIVERSITY
DECEMBER 2015

THERMOECONOMIC ANALYSIS OF SOLAR ORGANIC RANKINE CYCLE WITH ZEOTROPIC MIXTURE FOR POWER GENERATION

THORANIS DEETHAYAT

A THESIS SUBMITTED TO CHIANG MAI UNIVERSITY IN PARTIAL FULFILLMENT OF THE REQUIREMENTS FOR THE DEGREE OF DOCTOR OF PHILOSOPHY IN ENERGY ENGINEERING

GRADUATE SCHOOL, CHIANG MAI UNIVERSITY
DECEMBER 2015

THERMOECONOMIC ANALYSIS OF SOLAR ORGANIC RANKINE CYCLE WITH ZEOTROPIC MIXTURE FOR POWER GENERATION

THORANIS DEETHAYAT

THIS THESIS HAS BEEN APPROVED TO BE A PARTIAL FULFILLMENT OF THE REQUIREMENTS FOR THE DEGREE OF DOCTOR OF PHILOSOPHY IN ENERGY ENGINEERING

Examination Committee:

....Chairman
(Asst. Prof. Dr. Nat Vorayos)

....Member
(Prof. Dr. Tanongkiat Kiatsiriroat)

....Member
(Asst. Prof. Dr. Det Damrongsak)

....Member
(Assoc. Prof. Dr. Sate Sampattagul)

....Member
(Dr. Atipoang Nuntaphan)

Advisory Committee:

....Advisor
(Prof. Dr. Tanongkiat Kiatsiriroat)

....Co-advisor
(Asst. Prof. Dr. Det Damrongsak)

....Co-advisor
(Assoc. Prof. Dr. Sate Sampattagul)

28 December 2015

ACKNOWLEDGEMENTS

The author wishes to express his utmost gratitude to his adviser, Professor Dr.Tanongkiat Kiatsiriroat for the constructive guidance, suggestion, comments and discussions throughout every phase of the study. Grateful acknowledgements are made to the members of the Doctoral Program Committee, Asst. Prof. Dr. Nat Vorayos, Asst. Prof. Dr. Det Damrongsak, Assoc. Prof. Dr. Sate Sampattagul and Dr. Atipong Nuntaphan for their valuable comments.

The author is greatly indebted to Prof. Dr. Chi-Chuan Wang from College of Engineering, National Chiao Tung University, Taiwan for supporting and assistance during his external training program.

Thanks to the Graduate School, School of Renewable Energy, Maejo University and Department of Mechanical Engineering, Chiang Mai University for supporting the test facilities.

Finally, I would like to thank my mother, my father, my family, my friends and the staffs of Thermal Systems Research Unit Laboratory for all of the support, guidance, care and love throughout my life especially during my doctoral research work.

Thoranis Deethayat

หัวข้อดุษฎีนิพนธ์	การวิเคราะห์เศรษฐศาสตร์อุณหภาพของวัฏจักรแรงคินอินทรีย์รังสีอาทิตย์ด้วยสารผสมซีโอโทรปิกสำหรับผลิตไฟฟ้า
ผู้เขียน	นายธรณิศวร์ ดีทายาท
ปริญญา	ปรัญชาดุษฎีบัณฑิต (วิศวกรรมพลังงาน)
คณะกรรมการที่ปรึกษา	ศ.ดร. ทนงเกียรติ เกียรติศิริโรจน์ อาจารย์ที่ปรึกษาหลัก รศ.ดร. เศรษฐ์ สัมภัตตะกุล อาจารย์ที่ปรึกษาร่วม ผศ.ดร.เดช ดำรงศักดิ์ อาจารย์ที่ปรึกษาร่วม

บทคัดย่อ

งานวิจัยนี้เป็นการศึกษาการวิเคราะห์เศรษฐศาสตร์อุณหภาพของวัฏจักรแรงคินสารอินทรีย์รังสีอาทิตย์ด้วยสารผสมซีโอโทรปิกสำหรับผลิตไฟฟ้า กลุ่มตัวแปรไร้มิติ “Figure of Merit, FOM” ได้นำมาใช้ในการพิจารณาประสิทธิภาพทางความร้อนของวัฏจักรแรงคินสารอินทรีย์ที่อุณหภูมิต่ำ โดยใช้สารทำงานซีโอโทรปิกดังนี้ R245fa/R152a, R245fa/R227ea, R245fa/R236ea, R245ca/R152a, R245ca/R227ea และR245ca/R236ea เป็นสารทำงาน สมการจากความสัมพันธ์ระหว่างประสิทธิภาพทางความร้อนและ FOM สำหรับทุกสารทำงานที่อุณหภูมิควบแน่น 25-40ºC และอุณหภูมิระเหย 80-130ºC ได้ถูกพัฒนาขึ้น พบว่าผลการทำนายจากสมการเมื่อนำไปเปรียบเทียบกับผลการทดลองและข้อมูลงานวิจัยอื่นพบว่ามีค่าใกล้เคียงกัน

สำหรับการศึกษาศักยภาพการผลิตไฟฟ้าโดยวัฏจักรแรงคินสารอินทรีย์แบบทั่วไปและแบบผลิตความร้อนร่วม (CHP-ORC) ซึ่งผลิตไฟฟ้าอย่างเดียวและผลิตไฟฟ้าและความร้อนร่วม ทำการวิเคราะห์โดยใช้การวิเคราะห์เศรษฐศาสตร์อุณหภาพ แหล่งความร้อนของวัฏจักรแรงคินสารอินทรีย์ได้จากชีวมวลหลายชนิดและน้ำมันไบโอดีเซล กำลังของวัฏจักรเท่ากับ 20 และ 100 kWe และของไหลซีโอโทรปิกทำงานภายในวัฏจักรคือ R245fa/R152a ที่สัดส่วน 70/30% ชั่วโมงการทำงาน 12 ชั่วโมง สำหรับชีวมวล ต้นทุนการผลิตไฟฟ้าของ 20 และ 100 kWe วัฏจักรแรงคินารอินทรีย์ที่มีการ

ผลิตความร้อนร่วม มีราคาถูกกว่าวัฏจักรแรงคินสารอินทรีย์แบบทั่วไป ต้นทุนการผลิตไฟฟ้าจากทะลายปาล์มของวัฏจักรแรงคินารอินทรีย์ที่มีการผลิตความร้อนร่วม 20 และ 100 kWe มีราคาเท่ากับ 2.91 บาท/kWh และ 2.73 บาท/kWh ตามลำดับ ที่ราคาต้นทุนน้ำมันไบโอดีเซลเท่ากับ 5 บาท/ลิตร (กำหนดให้น้ำมันพืชใช้แล้วได้มาฟรี) ต้นทุนการผลิตไฟฟ้าของวัฏจักรแรงคินสารอินทรีย์ที่มีการผลิตความร้อนร่วม 20 และ 100 kWe มีราคาเท่ากับ 5.92 บาท/kWh and 5.74 บาท/kWh ตามลำดับ

การวิเคราะห์ค่าความไวของราคาต้นทุนทะลายปาล์ม ชั่วโมงการทำงานและอัตราดอกเบี้ยต่อต้นทุนการผลิตฟ้าพบว่าต้นทุนทะลายปาล์มและอัตราดอกเบี้ยมีค่าความไวสูงสุดและต่ำสุด สำหรับนำมันไบโอดีเซล การวิเคราะห์ค่าความไวของราคาต้นทุนน้ำมันไบโอดีเซล ชั่วโมงการทำงานและอัตราดอกเบี้ยต่อต้นทุนการผลิตฟ้าพบว่าราคาต้นทุนไบโอดีเซลมีค่าความไวมากที่สุด

การวิเคราะห์เศรษฐศาสตร์อุณหภาพของวัฏจักรแรงคินสารอินทรีย์ร่วมกับตัวเก็บรังสีอาทิตย์แบบหลอดแก้วสุญญากาศและพลังงานชีวภาพเป็นแหล่งความร้อนเพื่อการผลิตไฟฟ้าภายใต้ภูมิอากาศเชียงใหม่ กำลังของวัฏจักรเท่ากับ 20 และ 100 kWe ชั่วโมงการทำงานสำหรับผลิตไฟฟ้าเริ่มจาก 8.30 ถึง 20.30 น. พื้นที่ตัวเก็บรังสีอาทิตย์ระหว่าง 100 ถึง 900 ตารางเมตร ชีวมวลที่ใช้คือทะลายปาล์ม ผลการศึกษาพบว่าต้นทุนการผลิตไฟฟ้า จากพลังงานไฮบริด 20 และ 100 kWe มีค่าอยู่ในช่วง 4.38 ถึง 6.54 บาท/kWh และอยู่ในช่วง 3.86 ถึง 4.39 บาท/kWh ตามลำดับ ในกรณีวัฏจักรแรงคินสารอินทรีย์ที่มีการผลิตความร้อนร่วม พบว่าต้นทุนการผลิตไฟฟ้า 20 และ 100 kWe มีค่าอยู่ในช่วง 3.74 ถึง 4.84 บาท/kWh และอยู่ในช่วง 2.93 ถึง 3.17 บาท/kWh ตามลำดับ

สำหรับพลังงานไฮบริด ตัวเก็บรังสีอาทิตย์พื้นที่ระหว่าง 100 และ 900 ตารางเมตร ร่วมกับน้ำมันไบโอดีเซล เมื่อต้นทุนราคาน้ำมันไบโอดีเซลเท่ากับ 5 บาท/ลิตร ต้นทุนการผลิตไฟฟ้า จากพลังงานไฮบริด 20 และ 100 kWe มีค่าอยู่ในช่วง 8.39 ถึง 10.19 บาท/kWh และอยู่ในช่วง 7.97 ถึง 8.34 บาท/kWh ตามลำดับ ในกรณีวัฏจักรแรงคินสารอินทรีย์ที่มีการผลิตความร้อนร่วม พบว่าต้นทุนการผลิตไฟฟ้า 20 และ 100 kWe มีค่าอยู่ในช่วง 6.40 ถึง 7.93 บาท/kWh และอยู่ในช่วง 6.07 ถึง 6.35 บาท/kWh ตามลำดับ

การปล่อย CO_2 สำหรับวัฏจักรแรงคินสารอินทรีย์ไฮบริดที่มีการผลิตความร้อนร่วม ร่วมกับทะลายปาล์ม 20 และ 100 kWe พบว่า การปล่อย CO_2 เมื่อมีการเพิ่มพื้นที่ของตัวเก็บรังสีอาทิตย์ และการปล่อย CO_2 มีค่าอยู่ในช่วง 3.96 ถึง1.44 kgCO_2e/kWh และค่าอยู่2.72 ถึง 1.90 kgCO_2e/kWh ตามลำดับ ซึ่งมีผลเหมือนกับน้ำมันไบโอดีเซล โดยการปล่อย CO_2 มีค่าอยู่ในช่วง 1.36 ถึง0.50 kgCO_2e/kWh และค่าอยู่ในช่วง 1.36 ถึง 1.11 kgCO_2e/kWh ตามลำดับ

เมื่อพิจารณาต้นทุนการผลิตไฟฟ้าสำหรับวัฏจักรแรงคินสารอินทรีย์ไฮบริดที่มีการผลิตความร้อนร่วมเมื่อรวมค่าต้นทุนส่วนเพิ่มของการลดก๊าซเรือนกระจก ในกรณีทะลายปาล์มและน้ำมันไบโอดีเซลต้นทุน 5 บาท/ลิตร พลังงานไฮบริดจะมีค่าต้นทุนไฟฟ้าแพงกว่า การใช้ชีวมวล 100% แต่ในกรณีน้ำมันไบโอดีเซล 20 บาท/ลิตร (ราคาตลาด) พลังงานไฮบริดที่มีพื้นที่ตัวเก็บรังสีอาทิตย์ที่เหมาะสมสามารถให้ราคาต้นทุนที่ถูกกว่าการใช้เชื้อเพลิงชีวภาพเพียงอย่างเดียว

Dissertation Title	Thermoeconomic Analysis of Solar Organic Rankine Cycle with Zeotropic Mixture for Power Generation
Author	Mr. Thoranis Deethayat
Degree	Doctor of Philosophy (Energy Engineering)
Advisory Committee	Prof. Dr. Tanongkiat Kiatsiriroat Advisor Assoc. Prof. Dr. Sate Sampattakul Co-advisor Asst. Prof. Dr. Det Damrongsak Co-advisor

ABSTRACT

This research studies thermoeconomic analyses of a modular organic Rankine cycle (ORC) with solar collectors and biofuels as heat sources for power generation. A dimensionless term “Figure of Merit, FOM” was used to investigate thermal performance of low temperature organic Rankine cycle having zeotropic mixtures which are R245fa/R152a, R245fa/R227ea, R245fa/R236ea, R245ca/R152a, R245ca/R227ea and R245ca/R236ea as working fluids. An empirical correlation to estimate the cycle efficiency from the FOM for all working fluids at the condensing temperature of 25-40ºC and the evaporating temperatures of 80-130ºC was developed. It could be found that the simulation results could validate and fit very well with the experimental data and other researcher information.

Studies on potentials of power generation by a basic ORC and an CHP-ORC to generate only electricity and both electricity and thermal were performed by thermoeconomic analyses. The heat sources of the ORCs came from various kinds of biomass and biodiesel. The power outputs of ORC were 20 and 100 kWe and the ORC zeotropic working fluid was R245fa/R152a at 70/30% composition. Hour for power generation was 12 hours. For biomass, the unit costs of electricity from the 20 kWe and 100 kWe CHP-ORCs were cheaper than those of the basic ORCs. It was found that with the palm fruit bunch as the energy source, the UCEs for the 20 kWe and 100 kWe CHP-ORCs were 2.91 Baht/kWh and 2.73 Baht/kWh, respectively. At capital cost of biodiesel of 5 Baht/liter (assumed free used cooking oil), the UCEs for the 20 kWe and 100 kWe CHP-ORCs were 5.92 Baht/kWh and 5.74 Baht/kWh, respectively.

The sensitivities on the UCE which were palm fruit bunch unit cost, operating hour and real debt interest rate on the UCE were considered. The results showed that the palm fruit bunch unit cost and the real debt interest gave the most and least effects on the UCE.

For biodiesel, the sensitivities on the UCE which were biodiesel capital cost, operating hour and real debt interest rate on the UCE were considered. It was found that the biodiesel capital cost gave the most sensitivity on the UCE.

Thermoeconomic analysis of a modular organic Rankine cycle with evacuated-tube solar collectors and bioenergy as heat source for power generation was considered. The ambient temperature and solar radiation data of Chiang Mai, Thailand were taken as the calculation inputs. The power outputs of the ORC power were 20 and 100 kWe. Working period for power generation was between 8.30 AM to 8.30 PM and the area of the evacuated-tube solar collector was between 100-900 m^2. Palm fruit bunch was the biofuel used in the simulation. The results showed that the unit cost of electricity from the hybrid energy source for 20 and 100 kWe ORCs, with solar collector area between 100 and 900 m^2 and biofuels, were found to be in a range of 4.38 to 6.54 Baht/kWh and in a range of 3.86 to 4.39 Baht/kWh, respectively. In cases of 20 and 100 kWe CHP-ORCs, the UCEs were found to be in a range of 3.74 to 4.84 Baht/kWh and in a range of 2.93 to 3.17 Baht/kWh, respectively.

For the hybrid energy for solar collector area between 100 and 900 m^2 with biodiesel, when the biodiesel cost was at 5 Baht/liter, the UCEs of basic 20 and 100 kWe ORCs were found to be in a range of 8.39 to 10.19 Baht/kWh and in a range of 7.97 to 8.34 Baht/kWh respectively. The UCEs of 20 and 100 kWe CHP-ORC were also found to be in a range of 6.40 to 7.93 Baht/kWh and in a range of 6.07 to 6.35 Baht/kWh for solar collector area between 100 and 900 m^2, respectively.

The CO_2 emission of the hybrid power plants with palm fruit bunch for 20 and 100 kWe CHP-ORCs, it was found that the CO_2 emission was decreased with the increase of solar collector area and the CO_2 emissions were found to be in a range of 3.96 to 1.44 kgCO_2e/kWh and in a range of 2.72 to 1.90 kgCO_2e/kWh, respectively.

Similarly with biodiesel, the CO_2 emissions were found to be in a range of 1.36 to 0.50 $kgCO_2e/kWh$ and in a range of 1.36 to 1.11 $kgCO_2e/kWh$, respectively.

Considering the UCEs of the CHP-ORCS when the external cost on GHG emission was included, in cases of palm fruit bunch and biodiesel at 5 Baht/liter (Free feed stock), the hybrid energy gave more expensive cost than those of the 100 % biomass but in case of biodiesel at 20 Baht/liter (Market price), the hybrid energy with some suitable collector areas could get cheaper price than that of the biofuel only.

CONTENTS

	Page
Acknowledgements	c
Abstract in Thai	d
Abstract in English	g
List of Tables	m
List of Figure	o
Chapter 1 Introduction	1
1.1 Rationale	1
1.2 Literature Review	4
1.3 Objective of the Present Study	6
1.4 Scope of the Study	7
1.5 Benefit of the study	7
1.6 Keywords	7
Chapter 2 Theory	8
2.1 Organic Rankine Cycle (ORC)	8
2.2 Improvement of ORC Efficiency by Zeotropic Working Fluid	11
2.3 The Solar ORC with Bio-oil or Biomass as Auxiliary Heat Source	13
2.4 ORC for Combined Heat and Power	19
2.5 Thermo-economics	20
Chapter 3 Parametric Analysis on Modular Organic Rankine Cycle Performance	24
3.1 ORC Thermodynamics Cycle	25
3.2 Working fluids	28
3.3 Results and Discussion	30

3.4 Conclusion 38

Chapter 4 Thermoeconomic Analysis of a Modular Organic Rankine Cycle with Biofuel as Heat Source 39

4.1 Organic Rankine Cycle with Bioenergy as Heat Source 39
4.2 Working Fluid 40
4.3 Combined Heat and Power (CHP) 41
4.4 Biomass and Biodiesel 42
4.5 Exergy Costing 43
4.6 Results and Discussion 46
4.7 Conclusion 55

Chapter 5 Thermoeconomic Analysis of a Modular Organic Rankine Cycle with Hybrid Solar Collectors/Biofuels as Heat Source 56

5.1 Organic Rankine Cycle with Hybrid Solar Collectors/Biofuels 56
5.2 Conditions for Analysis 59
5.3 System Performance 60
5.4 Thermoeconomic Analysis 64
5.5 CO_2 Emission of Hybrid Power Plant 68
5.6 Conclusion 72

Chapter 6 Conclusions 74

6.1 Parametric Analysis on Modular Organic Rankine Cycle Performance 74
6.2 Thermoeconomic Analysis of a Modular Organic Rankine Cycle with Biofuels as Heat Source. 74
6.3 Thermoeconomic Analysis of a Modular Organic Rankine Cycle with Hybrid Solar Collectors/Biofuels as Heat Source. 75
6.4 Commendation for future works 76

References 77

Appendix 83

Appendix 1 83

Appendix 2 86

Appendix 3 88

Curriculum Vitae 140

LIST OF TABLES

Page

Table 1.1	Thailand CO_2 emission by sector from 2010-2013 [Energy Policy and Planning Office, 2013].	2
Table 1.2	Renewable Energy Development Plan Targets in 2021[Department of Alternative Energy Development and Efficiency, 2013].	2
Table 3.1	The conditions for calculating ideal ORC performance.	28
Table 3.2	Physical and environmental data of the working fluids. [Tchanche, 2009]	29
Table 3.3	Physical data of the zeotropic working fluids. [REFPROP, 2013]	29
Table 3.4	The specification of the commercial modular ORC	32
Table 3.5	Testing data of the commercial modular ORC	32
Table 3.6	Comparison of the results from the proposed method with real cycle efficiency.	33
Table 3.7	Comparison of the results calculated from this study with Saleh, 2007.	34
Table 3.8	Gliding temperatures when the evaporation temperature was at 80-130ºC. The condensing temperature was at 25-40ºC.	35
Table 3.9	Comparison of the results calculated from this study with Li 2014.	38
Table 4.1	Heating values and prices of biomass residues [Biomass, 2013].	42
Table 4.2	Cost data used for the thermoeconomic analyses of basic ORC and CHP-ORC for biomass as heat source.	44
Table 4.3	Cost data used for the thermoeconomic analyses of basic ORC and CHP-ORC for biodiesel as heat source.	45
Table 5.1	Cost data used for the thermoeconomic analysis of CHP-ORC for solar collectors and biomass as heat source.	64

Table 5.2 Cost data used for the thermoeconomic analysis of CHP-ORC for solar collectors and biodiesel as heat source. 65

LIST OF FIGURES

Page

Figure 1.1	Historic and projected Thailand energy consumption, 1990-2030 [Ministry of Energy, 2013].	1
Figure 2.1	ORC basic components.	8
Figure 2.2	T-s diagram of the ideal ORC [Mago et al. 2008]	9
Figure 2.3	Figure 2.3 T-s diagram of the actual ORC [Saleh et al. 2007].	10
Figure 2.4	T-s Diagrams compared between single working fluid (dotted line) and zeotropic fluid (solid line).	12
Figure 2.5	T-s diagrams of an ORC (a) zeotropic mixtures of Hexane/Pentane 0.5/0.5 (b) Pentane [Chys et al. 2012].	13
Figure 2.6	Diagram of solar ORC with bio-oil or biomass as auxiliary heat source.	13
Figure 2.7	Flat-plate solar collector and evacuated-tube solar collector [Solar collector, 2014].	15
Figure 2.8	Components of evacuated-tube solar collector [Solar collector, 2014].	16
Figure 2.9	A CHP ORC system with solar energy and bio-oil or biomass as energy input.	19
Figure 2.10	Basic ORC system.	21
Figure 2.11	CHP ORC system.	22
Figure 3.1	Thermodynamic cycles of ideal ORC for single and zeotropic working fluids.	26
Figure 3.2	The correlation between the ideal cycle efficiency and the FOM for various single working fluids, condensing and evaporating temperatures.	31
Figure 3.3	The correlation between the ideal cycle efficiency with $FOM_{zeotropic}$ for zeotropic refrigerants.	35

Figure 3.4 The deviations of FOM for all zeotropic working fluids in this studies from that of single fluid. 36
Figure 3.5 The correlation of the cycle efficiency with the $FOM_{zeotropic}$for R245fa/R152a and R245ca/R152a at various compositions. 37
Figure 4.1 Organic Rankine cycle with biofuel as heat source. 40
Figure 4.2 T-s diagram of zeotropic fluid R245fa/R152a at composition of 70:30. 40
Figure 4.3 A basic ORC system. 41
Figure 4.4 A CHP-ORC system. 41
Figure 4.5 Heat rate input at various values of evaporating temperature for 20kWe ORC. 47
Figure 4.6 Heat rate input at various values of evaporating temperature for 100kWe ORC. 47
Figure 4.7 UCEs from various kinds of biomass at operating hour of 12hr/day, id=6% for the 20 kWe basic ORC. 48
Figure 4.8 UCEs from various kinds of biomass at operating hour of 12hr/day, id=6%, the 100 kWe basic ORC. 49
Figure 4.9 UCEs from various kinds of biomass at operating hour of 12hr/day, id=6% for the 20 kWe basic ORC and CHP-ORC. 49
Figure 4.10 UCEs from various kinds of biomass at operating hour of 12hr/day, id=6% for the 100 kWe basic ORC and CHP-ORC. 50
Figure 4.11 Sensitivity analyses on UCE with varying unit costs of biomass, operating hours and interest rates. 52
Figure 4.12 UCEs from various values of biodiesel price at operating hour of 12hr/day, id=6% for the basic ORCs and the CHP-ORCs. 53
Figure 4.13 Sensitivity analyses on UCE with varying unit costs of biodiesel, operating hours and interest rates. 54
Figure 5.1 Organic Rankine cycle with solar collectors with biofuels as auxiliary heat. 57
Figure 5.2 T-s diagram of ORC 57

Figure 5.3	The temperature histories of the storage water temperature for 20 kWe ORC with 500m2 of the solar collectors. T-s diagram of ORC	60
Figure 5.4	The supplied heat inputs from solar energy and biomass energy in each month for the 20 kWe ORC with 200 and 700 m^2 of solar collector areas.	61
Figure 5.5	The annual solar fraction of the 20 kWe ORC with various solar collector areas.	62
Figure 5.6	The supplied heat inputs from solar energy and biomass energy in each month for the 100 kWe ORC with 200 and 700 m^2 of solar collector areas.	63
Figure 5.7	The annual solar fraction of the 100 kWe ORC with various solar collector areas.	63
Figure 5.8	UCEs from palm fruit bunch at operating hour of 12hr/day, id=6% for the basic ORCs and the CHP-ORCs at 20kWe and 100 kWe versus solar collector area.	67
Figure 5.9	UCEs from biodiesel at operating hour of 12hr/day, id=6% for the basic ORCs and the CHP-ORCs at 20kWe and 100 kWe versus solar collector area.	68
Figure 5.10	CO2 emissions for 20 kWe and 100 kWe ORC with hybrid solar and biofuel energy at various solar collector areas.	69
Figure 5.11	The UCE for 20 and 100 kWe CHP-ORC with hybrid solar and biofuel energy at various solar collector areas include with the external cost of GHG emission.	70
Figure 5.12	The UCE for 20 kWe CHP-ORC with hybrid solar and biodiesel (Capital cost 20 Baht/liter) at various solar collector areas include with the external cost of GHG emission.	71
Figure 5.13	The UCE for 100 kWe CHP-ORC with hybrid solar and biodiesel (Capital cost 20 Baht/liter) at various solar collector areas include with the external cost of GHG emission.	72

ข้อความแห่งการริเริ่ม

1) วิทยานิพนธ์นี้ได้นำเสนอกลุ่มตัวแปรไร้มิติ “Figure of Merit, FOM” ในการพิจารณาประสิทธิภาพของวัฏจักรแรงคินสารอินทรีย์ที่อุณหภูมิต่ำ โดยใช้สารทำงานซีโอโทรปิก เป็นสารทำงาน สมการจากความสัมพันธ์ระหว่างประสิทธิภาพทางความร้อนและ FOM ได้ถูกพัฒนาขึ้นเพื่อใช้หาประสิทธิภาพวัฏจักรโดยไม่ต้องใช้สมบัติทางเธอร์โมไดนามิกส์ในการวิเคราะห์

2) ศักยภาพการผลิตไฟฟ้าโดยวัฏจักรแรงคินสารอินทรีย์แบบทั่วไปและแบบผลิตความร้อนร่วม (CHP-ORC) ซึ่งผลิตไฟฟ้าอย่างเดียวและผลิตไฟฟ้าและความร้อนร่วม ทำการวิเคราะห์โดยใช้การวิเคราะห์เศรษฐศาสตร์อุณหภาพ แหล่งความร้อนได้จากชีวมวลหลายชนิดและน้ำมันไบโอดีเซล ได้มีการศึกษาในงานวิจัยนี้

3) มีการวิเคราะห์เศรษฐศาสตร์อุณหภาพของวัฏจักรแรงคินสารอินทรีย์ร่วมกับตัวเก็บรังสีอาทิตย์แบบหลอดแก้วสุญญากาศและพลังงานชีวภาพเป็นแหล่งความร้อนเพื่อการผลิตไฟฟ้าภายใต้ภูมิอากาศเชียงใหม่

4) วิทยานิพนธ์นี้ได้พิจารณาต้นทุนการผลิตไฟฟ้าสำหรับวัฏจักรแรงคินสารอินทรีย์ไฮบริดที่มีการผลิตความร้อนร่วมเมื่อรวมต้นทุนส่วนเพิ่มของการลดก๊าซเรือนกระจก

STATEMENT OF ORIGINALITY

1) This study proposed a dimensionless term “Figure of Merit, FOM” which could be used to investigate thermal performance of low temperature organic Rankine cycle having zeotropic mixtures as working fluids. An empirical correlation to estimate the cycle efficiency from the FOM was developed to evaluate cycle efficiency without any information of thermodynamic properties.

2) Potentials of power generation by a basic ORC and an CHP-ORC to generate only electricity and both electricity and thermal were performed by thermoeconomic analyses. The heat sources of the ORCs came from various kinds of biomass and biodiesel.

3) Thermoeconomic analysis of a modular organic Rankine cycle with evacuated-tube solar collectors and bioenergy as heat sources for power generation was considered. The ambient temperature and the solar radiation data of Chiang Mai, Thailand were taken as the calculation inputs.

4) This research considered the unit cost of electricity, UCE of the CHP-ORC when the external cost on GHG emission was included.

CHAPTER 1

INTRODUCTION

1.1 Rationale

Thailand energy situation in the last 20 years from 1990, the final energy consumption was increased rapidly with a growth rate of 4.4 percent per year. At 2010, the final energy consumption was 2.32 times of that at 1990 or around 71.2 Mtoe. The energy demand in the next 20 years from 2010 to 2030 will be more than double from 71.2 Mtoe to 162.7 Mtoe as shown in Figure 1.1.

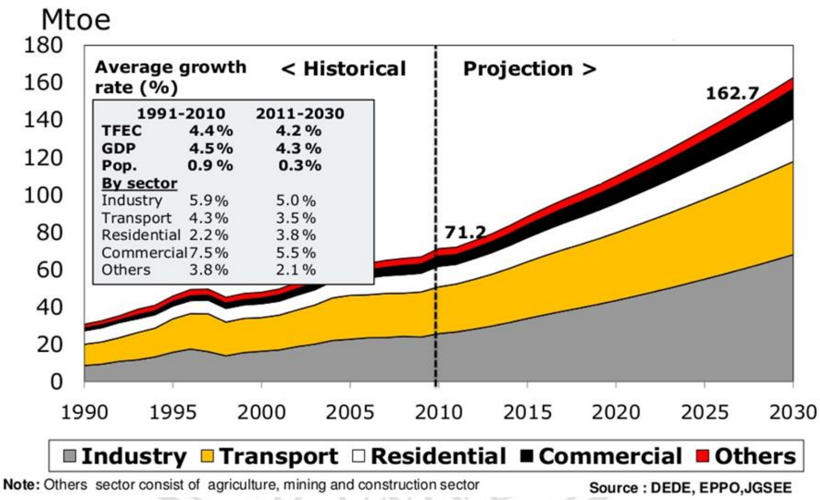

Figure 1.1 Historic and projected Thailand energy consumption, 1990-2030 [Ministry of Energy, 2013].

At present, electricity generation from steam Rankine cycle is still the major way and usually based on fossil fuels such as coal and natural gas to be energy sources. Heat supplied from fossil fuel has caused many environmental problems such as air pollution and global warming which are Carbon Dioxide (CO_2) , Carbon Monoxide (CO), Methane (CH_4), Sulfur Dioxide (SO_2) and Nitrogen Dioxide (NO_x).

From Table 1.1, for Thailand CO_2 emission by sector from 2010-2013, it could be found that electricity sector released CO_2 emission higher than any sector and CO_2 is also the main cause of global warming.

Table 1.1 Thailand CO_2 emission by sector from 2010-2013 [Energy Policy and Planning Office, 2013].

Sector	2010	2011	2012	2013
Electricity	89,965	87,719	95,996	96,414
Transportation	57,587	59,246	61,071	62,430
Industrial Process	54,173	57,547	62,015	62,313
other*	18,6578	19,873	21,414	19,561

Unit: 1,000 tons

Ministry of Energy is targeting to replace 30 percent of total fossil fuel consumption with renewable and alternative energies by the end of 2036. From Table 1.2, it could be found that the Government has tried to promote electricity produced mostly from solar energy, hydro power and biomass and also promoted the communities to generate electricity which could be managed and maintained by themselves.

Table 1.2 Renewable Energy Development Plan Targets in 2036 [Department of Alternative Energy Development and Efficiency, 2015].

Electricity	**Capacity**	**Unit**
MSW	500	MW
Waste from Industry	50	MW
Biomass	5,570	MW
Biogas	1,280	MW
Mini Hydro Power Plant	376	MW
Wind	3,002	MW
Solar	6,000	MW
Mega Hydro Power Plant	2,906	MW
Thermal	**Capacity**	**Unit**
Waste	495	ktoe
Biomass	22,100	ktoe
Biogas	1,283	ktoe
Solar	1,200	ktoe
Others	10	ktoe
Biofuels	**Capacity**	**Unit**
Biodiesel	14	ml/day
Ethanol	11.3	ml/day
Pyrolysis Oil	0.53	ml/day
CBG	4,800	ton/day
Others	10	ktoe

Solar radiation in Thailand seems to be high but Thailand is in the monsoon area where the diffuse solar radiation is around 40-50 % of the global radiation. The annual direct normal solar radiation is in a range of 1,350-1,400 kWh/m^2-yr [Department of Alternative Energy Development and Efficiency, 2013] which is not high enough for concentrating solar power (CSP) to generate electrical power.

Non-Concentration solar collector such as flat-plate and evacuated tube solar collectors could generate heat in a range of 90-120ºC. At this range, these collectors could be taken as heat sources for organic Rankine cycle (ORC).

Organic Rankine cycle (ORC) is a kind of Rankine cycle of which the working fluid has a low boiling point thus the unit could operate with a low heat source temperature such as low temperature waste heat, geothermal heat, solar heat or biomass combustion for generating electricity.

During heat exchanging at the evaporator and the condenser of the ORC cycle, there were temperature differences between the heat exchanging fluids which generate irreversibilities at the cycle components then some part of the cycle available work was destroyed.

Use of zeotropic fluid in the ORC is one method to reduce the temperature differences during the heat exchanges. The temperature of the zeotropic fluid is changing during a phase change then the temperature of the cycle working fluid could follow those of the heat source and the heat sink streams at the evaporator and the condenser, respectively. With smaller temperature differences compared with the single working fluid, consequently, the irreversibilities during the heat exchanges are less and higher cycle work output could be obtained.

In this research work, improvement of solar organic Rankine cycle performance was performed with zeotropic mixture as working fluid in organic Rankine cycle. A dimensionless “figure of merit” was proposed for screening suitable zeotropic working fluid based on thermal efficiency. In addition, integration of bioenergy such as biomass and biodiesel to be hybrid energy source is also investigated. Thermo-economic analysis of solar organic Rankine cycle with zeotropic mixture for power generation was also considered.

1.2 Literature Reviews

The literature review was divided into 2 sections. The first section gave a review on the organic Rankine cycle and its working fluid. The second section gave a review on the potential of the organic Rankine cycle with zeotropic working fluid.

1.2.1 The Organic Rankine Cycle and Working Fluid

Increase of fossil fuel consumption has caused environmental problems such as ozone depletion, global warming and air pollution. A solution for these problems is to use technology which is environment friendly such as renewable energy to generate electricity. Organic Rankine cycle (ORC) is also an alternative method which can be used with geothermal energy [Hettiarachchi, 2006], solar thermal energy [Marion, 2012] and waste heat in a form of combined heat and power (CHP) [Donghong, 2006].

Selection of ORC working fluids based on available heat source, safety and technical feasibility have been reported by many researchers. Maizza and Maizza, 2001, Saleh et al. 2007 and Drescher and Bruggemann 2007 analyzed performances and properties of different working fluids for an ORC application. Some important properties of a good working fluid were low specific volumes, low toxicity, low ozone depletion potential (ODP), low global warming potential (GWP) and low flammability. Tchanche et al. 2009 presented R134a was the most suitable for small scale solar application with maximum temperature heat source 90ºC. R152a, R600a, R600 and R290 also offered good performances but needed safety precautions. Another property that must be considered is saturation vapor line of working fluid. The slope of the saturation line in the T-s diagram depends on the fluid types. Mago et al. 2008 reported a dry and isentropic fluid gave better thermal efficiencies because they did not condense during the fluid went through the turbine.

To screen out the appropriate working fluid for ORC system, many specific thermos-physical properties have to be considered. Kuo et al. 2009 proposed a dimensionless "figure of merit (FOM)" which was defined as FOM $= Ja^{0.1}\left(\frac{T_{cond}}{T_{evap}}\right)^{0.8}$. This term was used to screen working fluid at various condensing/evaporation temperatures. The thermal efficiency decreased with the increase of FOM.

Some researchers proposed many methods to improve the performance of ORC, Mago et al. 2008 analyzed and compared regenerative cycle with basic ORC using dry fluids, The regenerative ORC gave higher thermal efficiency compared with the basic ORC and also decreased heat input to produce the same power. Somayaji et al. 2006 reported the effect of superheating of dry fluid on the thermal efficiency of basic ORC. It was noted that the thermal efficiency was slightly decreased or remains approximately constant with the increment of the turbine inlet temperature.

1.2.2 Organic Rankine Cycle Performance with Zeotropic Working Fluid

During heat exchanging at the evaporator and the condenser of the ORC cycle, there were temperature differences between the streams of the heat source and the heat sink with the ORC working fluid, respectively. The temperature differences generate irreversibilities at the cycle components then some part of the cycle work was destroyed.

Use of a zeotropic fluid in the ORC is one method to reduce the temperature differences among those of the heat source and the heat sink with the ORC working fluid. Since the temperature of zeotropic fluid is changing during a phase change then the temperature of the working fluid could follow those of the heat source and the heat sink streams at the evaporator and the condenser, respectively with smaller temperature differences compared with the single working fluid. Consequently, the irreversibilities during the heat exchanges are less which results in higher cycle work output. Moreover, some working fluid blend might be friendlier to the environment. The ODP or GWP will be less than those of the single component.

Li et al. 2011 investigated the influence of evaporating temperature and internal heat exchanger. Three pure fluids (R123, R141b and R245ca) and one mixture (R141b/RC318) were used as working fluids. They concluded that the ORC efficiency of the mixture R141b/RC318 would be better than R141b after adding an internal heat exchanger. Wang and Zhao 2009 compared three different compositions by mass (0.9/0.1, 0.65/0.35 and 0.45/0.55) of R245fa/R152a to pure R245fa at a low temperature solar ORC. For zeotropic mixtures, a significant increase of thermal efficiencies could be obtained when the outlet of evaporator is superheated with IHE. Heberle et al. 2012 presented simulations for ORC with isobutene/isopentane and R227ea/R245fa mixtures as working fluids. The composition of mixture, heat source temperature and temperature difference of cooling water were the concerned parameters. The second law efficiency increased in a range of 4.3% to 15% for mixtures compared to pure fluids for a heat source temperature under 120ºC. Chys et al. 2012 used zeotropic as the working of ORC systems when the heat source temperatures were at 150ºC and 250ºC. They found a potential increment of 16% and 6% in the system efficiency, respectively. The power generation at optimal condition could be increased by 20% for the low temperature heat source comparing with the pure working fluids.

From the previous studies, it could be seen that ORC can be converting low temperature heat source to generate electricity and ORC operating with zeotropic fluids can achieve higher efficiencies compared to typical ORC with single fluids. In this study, thermoeconomic analysis and performance modeling of an ORC with hybrid solar/biofuel were carried out. The ORC in this study was a modular unit of 20 and 100 kWe output that could be implemented in an office or small community. Hot water to generate heat at ORC evaporator came from evacuated tube solar collectors, biofuel was burnt to generate an auxiliary heat when the solar radiation level was not high enough. Selection of zeotropic working fluid in the cycle was found out from the related parameter and the dimensionless "figure of merit" was developed to screen suitable zeotropic working fluid.

1.3 Objective of the Present Study

1.3.1 To study parameters which affect the zeotropic organic Rankine cycle performance, both the first and the second laws of thermodynamics and find out the suitable zeotropic fluid for the ORC.

1.3.2 To generate thermoeconomic analysis of an ORC with hybrid solar/biofuel as energy source and find out the unit cost of the output.

1.4 Scope of This Study

1.4.1 ORC capacity was not over 100 kWe.

1.4.2 Evaporating temperature was between 80-130 ºC.

1.4.3 The weather data of the Chiang Mai, Thailand were taken as the input information for the simulation.

1.4.4 Evacuated tube solar collector was used in the simulation.

1.5 Benefit of This Study

1.5.1 A dimensionless “figure of merit” to screen zeotropic fluid for ORC system was presented.

1.5.2 Thermoeconomic analysis of an ORC with hybrid solar and biofuel and the unit cost of the output could be carried out.

1.6 Keywords

Organic Rankine cycle, Zeotropic fluid, Solar collector, Power Generation, Thermoeconomic analysis, Figure of Merit.

CHAPTER 2

THEORY

2.1 Organic Rankine Cycle (ORC)

Organic Rankine cycle (ORC) is a kind of Rankine cycle of which the working fluid has a low boiling point thus the unit could operate with a low heat source temperature. ORC is a well-known technology since the early 70's [Hung et al., 1997]. Most of ORC power plants have been built and the heat sources mainly come from low temperature waste heat, geothermal heat, solar energy or biomass combustion for generating electricity.

2.1.1 ORC Thermodynamics Cycle

A diagram of the basic ORC system is shown in Figure 1. The system consists of an evaporator, a turbine, a condenser and a pump. The working fluid leaves the condenser is designated as saturated liquid (state 1) and the pump supplies the working fluid to the evaporator (state 2) where it is heated and vaporized by a heat source. The generated high pressure vapor or high pressure superheated vapor (state 3) flows through the turbine to produce power. The low pressure vapor then exits the turbine (state 4) and enters into the condenser to reject heat to a heat sink. The condensed working fluid at the condenser outlet is pumped back to the evaporator.

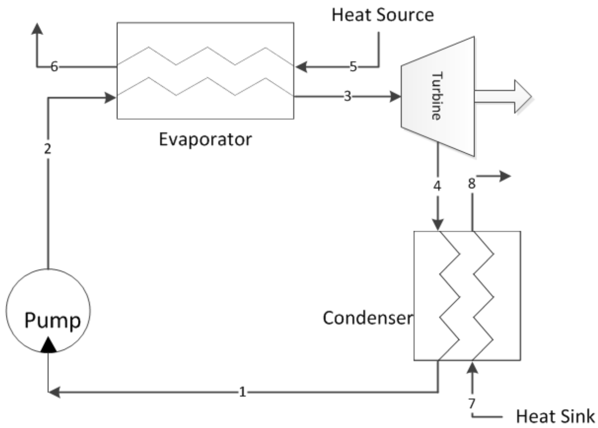

Figure 2.1 ORC basic components.

The slope of the saturation curve in the T-s diagram depends on the type of working fluid. An isentropic fluid has infinitely large slope; a wet fluid has a negative slope, while a dry fluid has a positive slope. Dry and isentropic fluids show better thermal efficiencies because they do not condense after the fluid goes through the turbine as opposed to wet fluids that produce condensates after the fluid expansion. The comparisons of the temperature-entropy diagram for isentropic, wet and dry fluids are shown in Figure 2.2.

Figure 2.2 shows T-s diagrams of the ideal ORC. The process 1-2 is isentropic compression for liquid pumping and the process 3-4 is isentropic expansion in the turbine. But in practice, there are effects of heat loss and friction on the cycle performance therefore, the actual exit states of the pump and the turbine become states 2a and 4a, respectively as shown in Figure 2.3.

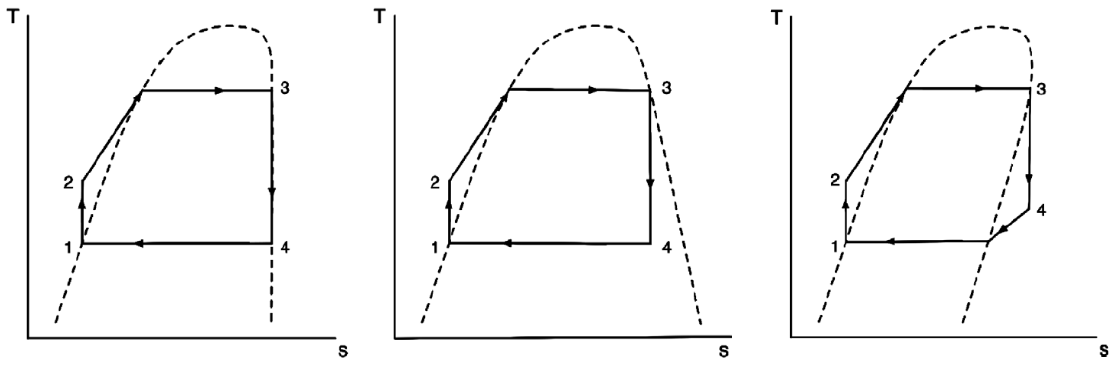

(a) Isentropic Fluid. (b) Wet Fluid. (c) Dry Fluid.

Figure 2.2 T-s diagram of the ideal ORC [Mago et al. 2008].

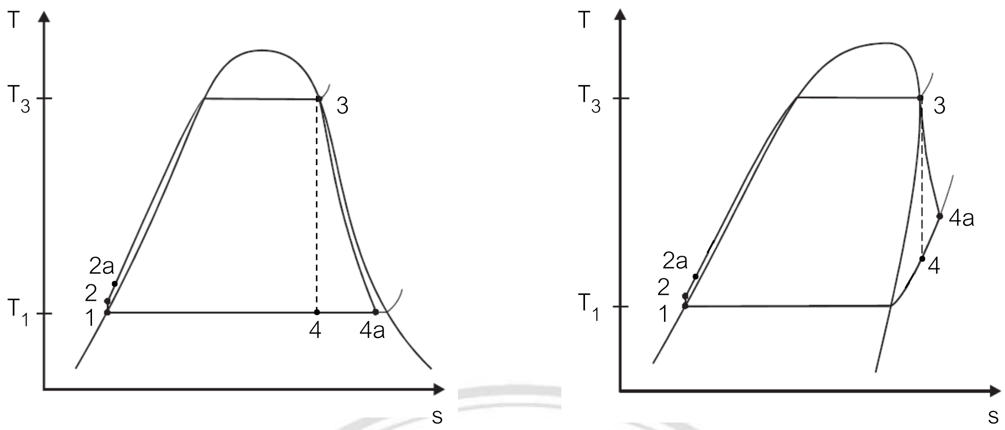

(a) Wet Fluid. (b)Dry Fluid.

Figure 2.3 T-s diagram of the actual ORC [Saleh et al. 2007].

2.1.2 Thermodynamics Analysis

Detailed analysis of the ORC system is summarized as follows:

Pump

$$\dot{W}_p = \frac{\dot{m}_R v_1 (P_2 - P_1)}{\eta_P} \tag{2.1}$$

$$\dot{W}_p = \dot{m}_R (h_{2a} - h_1). \tag{2.2}$$

Where $\dot{W}_p$ = Work rate from pump (kW)

$\dot{m}_R$ = Mass flow rate of refrigerant (kg/s)

P_1 = Pressure at state 1 (kPa)

P_2 = Pressure at state 2 (kPa)

η_P = Isentropic efficiency of pump

h_1 = Enthalpy at state 1 (kJ/kg)

h_{2a} = Enthalpy at state 2a (kJ/kg).

Evaporator

$$\dot{Q}_E = \dot{m}_R(h_3 - h_{2a}). \tag{2.3}$$

Where $\dot{Q}_E$ = Heat rate for evaporator (kW)

h_3 = Enthalpy at state 3(kJ/kg).

Turbine

$$\dot{W}_T = \dot{m}_R(h_3 - h_4)\eta_T. \tag{2.4}$$

Where $\dot{W}_T$ = Work rate from turbine (kW)

h_4 = Enthalpy at state 4(kJ/kg).

Condenser

$$\dot{Q}_C = \dot{m}_R(h_{4a} - h_1). \tag{2.5}$$

Where $\dot{Q}_C$ = Heat loss from condenser (kW)

h_{4a} = Enthalpy at state 4a (kJ/kg).

Cycle Efficiency

1st law efficiency

$$\eta_I = \frac{\dot{W}_T - \dot{W}_P}{\dot{Q}_E}. \tag{2.6}$$

2.2 Improvement of ORC Efficiency by Zeotropic Working Fluid

During heat exchanging in the evaporator and the condenser of the ORC cycle, there were temperature differences between the streams of the heat source and the heat sink with the ORC working fluid, respectively. The temperature differences generate irreversibilities at the cycle components then some part of the cycle work was destroyed.

Use of zeotropic fluid in the ORC is one method to reduce the temperature differences between the heat source and the heat sink with the ORC working fluid at the evaporator and the condenser. Since the temperature of the zeotropic fluid is changing during a phase change then the temperature of the working fluid could follow those of the heat source and the heat sink streams at these components, respectively with smaller temperature differences compared with the single working fluid. Consequently, the irreversibilities during the heat exchanges are less which results in higher cycle work output. Moreover, some working fluid blend might be friendlier to the environment. The ODP or GWP will be less than those of the single component [Wang et al. 2010].

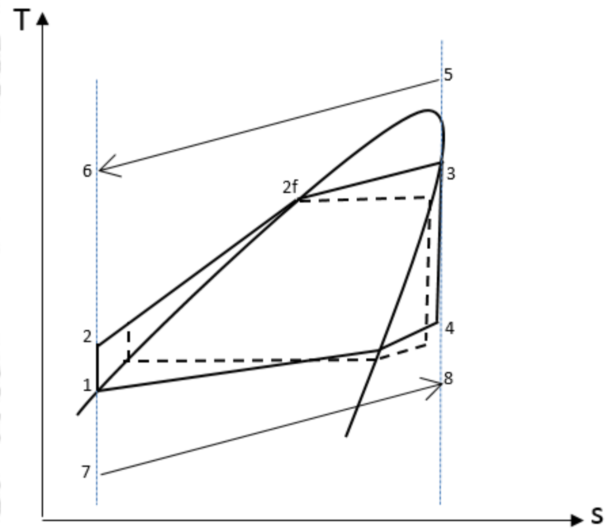

Figure 2.4 T-s Diagrams compared between single working fluid (dotted line) and zeotropic fluid (solid line).

Chys et al. 2012 analyzed performance of a low temperature ORC using Hexane/Pentane compared with Pentane as shown in Figure 2.5 The results showed that the zeotropic gave better performance since there were gliding temperatures during heat exchanges in the evaporator and the condenser thus the total area in the T-s diagram which represented the total work output was higher than that of the single fluid.

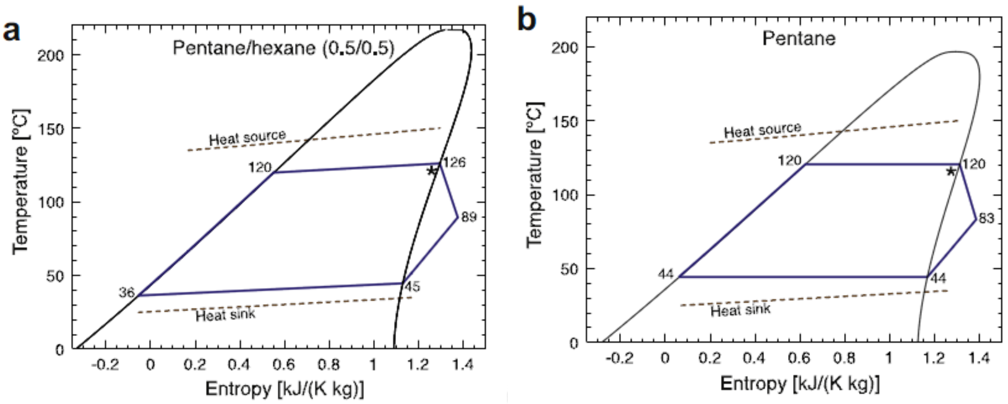

Figure 2.5 T-s diagrams of an ORC (a) zeotropic mixtures of Hexane/Pentane 0.5/0.5 (b) Pentane [Chys et al. 2012].

2.3 The Solar ORC with Bio-oil or Biomass as Auxiliary Heat Source

Figure 2.6 shows a diagram of an ORC with solar collectors and bio-oil and biomass as energy source for generating hot water to the ORC.

There is a water closed loop to extract heat from the solar thermal system and the heat is transferred to the ORC evaporator. If the heat rate and the hot water temperature are not high enough the auxiliary heat will be generated from bio-oil or biomass combustion in a furnace.

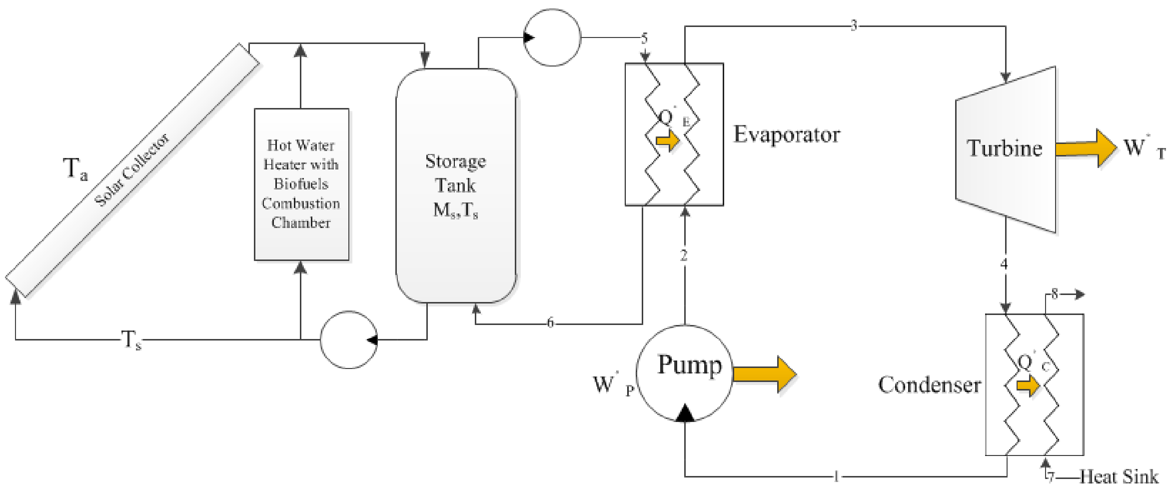

Figure 2.6 Diagram of solar ORC with bio-oil or biomass as auxiliary heat source.

2.3.1 Solar Collector

Solar collector is an equipment that absorbs and transforms solar energy into thermal energy to working fluid, liquid or air, which is moving in the collector.

There are 2 types of solar collector: a non-concentrating solar collector and a concentrating solar collector. At present, concentrating solar power (CSP) technology can be exploited through three different systems, i.e. the parabolic trough system, the tower system and the dish/Stirling engine system. All the CSP technologies will be appropriate for countries having high direct normal solar radiation. There were some reports showed that the average direct normal solar radiation values for the power generation should be above 1500 kWh/m^2-year [IEA, 2003].

For Thailand, the annual direct normal solar radiation was in a range of 1350-1400 kWh/m^2-year [Potentials of solar power, 2006], which was rather low for the CSP technologies.

Wibulswas, P. 1998 and Vorayos, N. et al. 2009 reported the diffuse component of the solar radiation in Thailand was quite high since the country was in the monsoon area and it was about 50% of the total radiation. A solution for this problem (low annual direct normal solar radiation) was the use of evacuated-tube solar collectors instead of solar concentrators as a heat source to generate hot water for running organic Rankine cycle (ORC) to generate electrical power.

Non–concentrating collector such as flat- plate solar collector and evacuated-tube solar collector are shown in Figure 2.7.

Figure 2.7 Flat-plate solar collector and evacuated-tube solar collector

[Solar collector, 2014].

An evacuated-tube solar collector in Figure 2.8 is composed of a set of vacuum glass tubes. The air between the absorber and the glass tube is pumped out, generating a vacuum. This mechanism creates excellent insulation, trapping the heat inside and makes the solar collector performance be highly efficient.

Each absorber tube is a heat pipe which contains the substance that could vaporize at low temperature. When the tube absorbs solar energy, the vapor will float up to the bulb heat exchanger which is inserted into a water passage tube outside the glass tube to heat the hot water that circulating in the system. After heating the hot water, the substance will condense and return back to the heat pipe tube to reabsorb the solar heat.

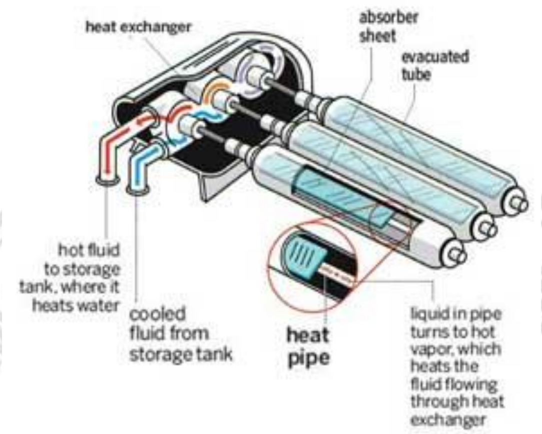

Figure 2.8 Components of evacuated-tube solar collector [Solar collector, 2014].

For solar collector, the heat gain rate from the solar collector can be calculated from

$$\dot{Q}_{coll} = A_c\left[I_T(\tau\alpha) - U_L(T_{pm} - T_a)\right]. \quad (2.7)$$

Where $\dot{Q}_{coll}$ = the heat gain rate from the solar collector (kW)

A_c = the area of solar collector (m^2)

I_T = the total solar radiation on the tilted surface (W/m^2)

$\tau\alpha$ = the optical efficiency of collector

U_L = the overall heat loss coefficient (W/m^2. K)

T_{pm} = the average absorbing plate temperature (°C)

T_a = the ambient temperature (°C).

In practice, the value of the average absorbing plate temperature is rather difficult to get the exact value, therefore, the average fluid temperature (T_{fm}) is used instead. The above equation could be modified as

$$\dot{Q}_{coll} = A_c F'\left[I_T(\tau\alpha) - U_L\left(T_{fm} - T_a\right)\right]. \tag{2.8}$$

Where F' is the collector efficiency factor which is the ratio of actual heat gain to that when the average temperature of the absorber plate is the same as T_{fm} which is

$$T_{fm} \cong \frac{(T_{fi} - T_{fo})}{2}. \tag{2.9}$$

Where T_{fi} = the temperature of fluid entering solar collector (°C)

T_{fo} = the temperature of fluid leaving solar collector (°C).

The equation could also be rewritten in the form of

$$\dot{Q}_{coll} = A_c F_R\left[I_T(\tau\alpha) - U_L(T_{fi} - T_a)\right]. \tag{2.10}$$

Where F_R is called the heat removal factor which is the ratio of actual heat gain to that when the absorber plate has a temperature of T_{fi}.

2.3.2 Thermal Energy Storage

A set of solar collectors with a thermal energy storage supplies heat for thermal applications. An energy balance for the non-stratified thermal energy storage and the temperature of water in the thermal energy storage can be evaluated from

$$M_s C_p \frac{dT_s}{dt} = \dot{Q}_{coll} - \dot{Q}_{useful} - \dot{Q}_{loss}. \tag{2.11}$$

Where

$$\dot{Q}_{useful} = \dot{m}_W C_p (T_{TL} - T_{FL}), \tag{2.12}$$

$$\dot{Q}_{loss} = UA(T_s - T_a). \tag{2.13}$$

Substitute equations (2.10), (2.12) and (2.13) into equation (2.11), the temperature of water in the storage tank can be calculated from

$$T_s^{t+\Delta t} = T_s^t + \frac{\Delta t}{M_s C_p}\left\{A_c F_R\left[I_T(\tau\alpha) - U_L(T_{fi} - T_a)\right] - \dot{m}_W C_p (T_{TL} - T_{FL}) - UA(T_s - T_a)\right\}. \tag{2.14}$$

Where M_s = the mass of water in thermal energy storage (kg)

C_p = the specific heat of water (kJ/kg.K)

T_s^t = the temperature of water at time *t* (°C)

$T_s^{t+\Delta t}$ = the temperature of water at time $t + \Delta t$ (°C)

t = time (s).

2.3.3 Solar Fraction

The solar fraction (SF) is the amount of heat supplied by solar thermal system divided by the total heat demanded by the ORC system. It could be expressed as

$$SF = \frac{\sum(\dot{Q}_{solar}\Delta t)}{\sum(\dot{Q}_{load}\Delta t)}. \tag{2.15}$$

Where

$\sum \dot{Q}_{solar}\,\Delta t$ = the total heat supplied by the solar thermal system

$\sum \dot{Q}_{load}\,\Delta t$ =the total heat load for supplying to the ORC.

2.4 **ORC for Combined Heat and Power**

Combined Heating and Power (CHP) is a system that simultaneously generates electricity and useful heating from a combustion fuel or other kinds of heat sources. In this system, modular organic Rankine cycle having low temperature heat from solar energy coupled with bio-oil or biomass as auxiliary could be used for power generation, the exhausted gas from biomass or bio-oil combustion could be used for water heating, therefore, higher overall efficiency could be obtained compared with conventional heat engine.

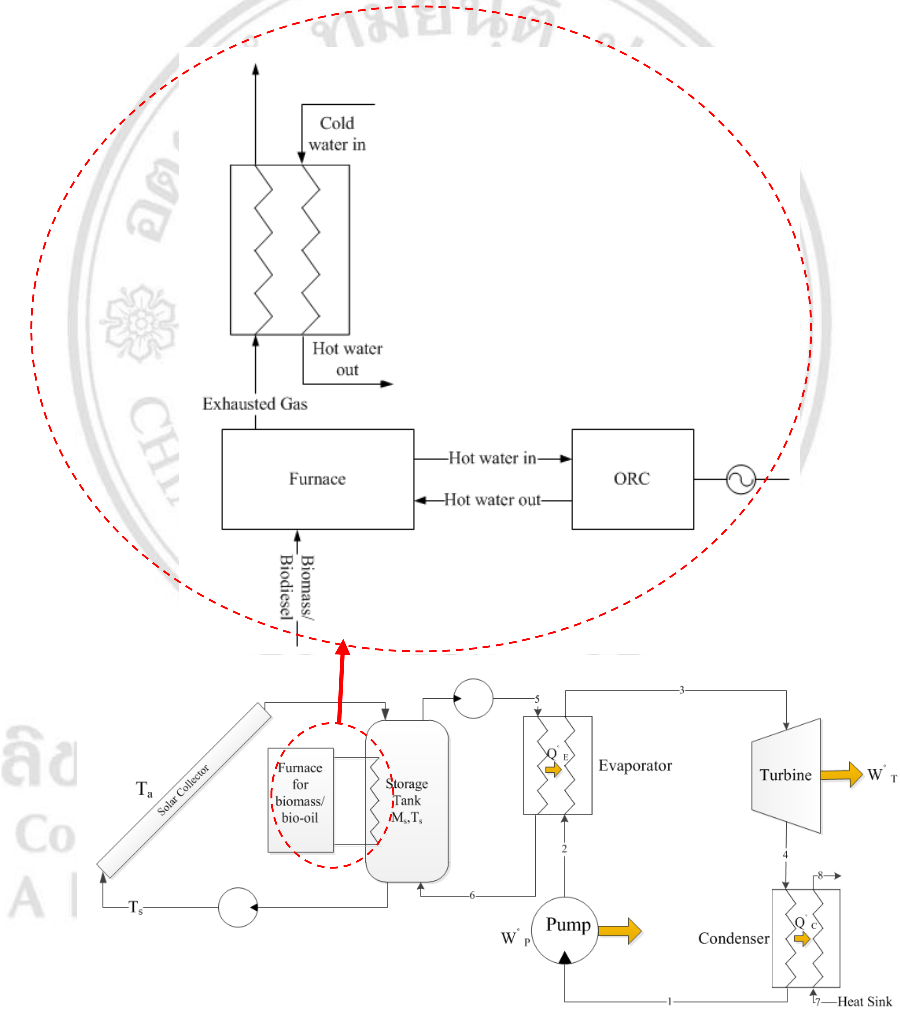

Figure.2.9 A CHP ORC system with solar energy and bio-oil or biomass as energy input.

From Figure 2.9, the combined heat and power ORC unit could generate both electricity and heating then the total efficiency could be calculated by

$$\eta_{CHP} = \frac{E_{net}+(\dot{Q}_{HWout} \times \Delta t)}{H_T A_c + \sum(m_{biomass,bio\ oil}\ HHV)}. \tag{2.16}$$

Where $\dot{Q}_{HWout}$ is the useful heat for other thermal applications (kW), Δt is the operating hour.

It could be noted from equation (2.16) that the overall efficiency of the CHP is higher than that of the ORC for power generation only.

2.5 Thermo-economics

Thermo-economics is a combination of exergy analysis and economic principle to provide the effective cost of the products or useful energy outputs with different qualities.

Thermo-economic balance for any unit based on exergy and cost balances could be formulated as [Thermoeconomics, 2005]

$$\dot{C}_p = \dot{C}_{in} + \dot{C}_{out} + \dot{Z}_{O\&M}. \tag{2.17}$$

Where $\dot{C}_p$ is the cost rate of power, $\dot{C}_{in}$ and $\dot{C}_{out}$ are the cost rates according to inlet and outlet streams and $\dot{Z}_{O\&M}$ is the capital investment and operating & maintenance cost.

With exergy costing, each of the cost rates is evaluated in term of the associated rate of exergy transfer and unit cost as

$$c_p \dot{E}_p = c_{in} \dot{E}_{in} + c_{out} \dot{E}_{out} + \dot{Z}. \tag{2.18}$$

Where c = Cost per unit of exergy (Baht/s)

$\dot{E}$ = Rate of exergy (kW)

$\dot{Z}$ = Cost rate of investment and operating & maintenance cost (Baht/s).

In the study, electrical energy and useful heat are the required outputs of the ORC as shown in Figure 2.10 and 2.11.

Basic ORC system

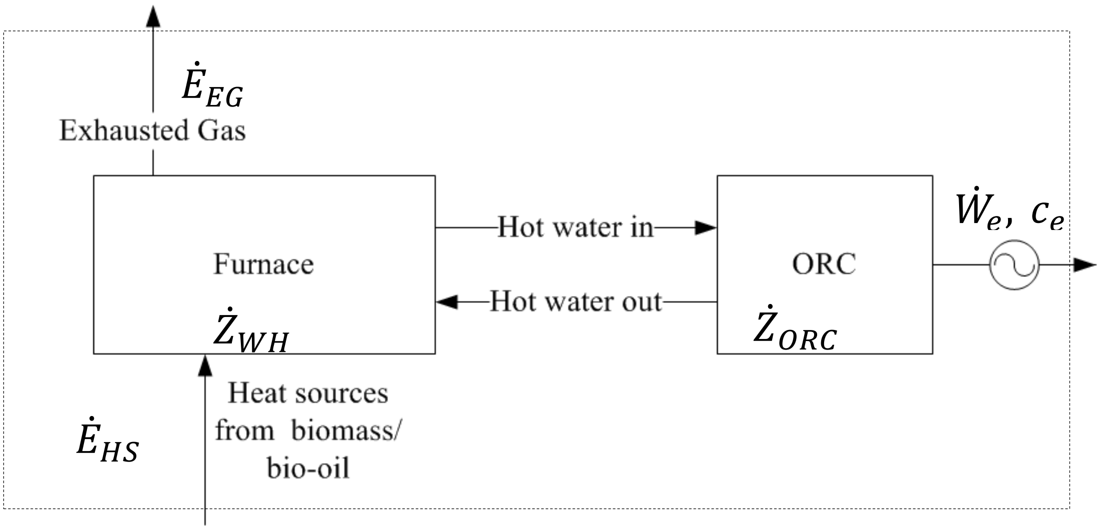

Figure 2.10 Basic ORC system.

For basic ORC as shown in Figure 2.10, we consider a control volume enclosing the system. Heat from solar energy or biomass or bio-oil enters the water heater and there is exhausted gas leaving the furnace. The total cost to produce the electricity and exhausted gas equals the cost of the entering heat sources plus the investment cost and the operating maintenance cost of the water heater and the ORC. This could be expressed by.

$$\dot{C}_e + \dot{C}_{EG} = \dot{C}_{HS} + \dot{Z}_{WH} + \dot{Z}_{ORC} + \dot{Z}_{O\&M} \tag{2.19}$$

Where $\dot{C}$ = the cost rate of the respective stream

$\dot{Z}_{WH}$ = the cost rate of investment in water heater

$\dot{Z}_{ORC}$ = the cost rate of investment in ORC

$\dot{Z}_{O\&M}$ = the cost rate of investment in operating & maintenance.

For simplicity, we assume the exhausted gas is discharged directly to the surrounding with negligible cost. Thus equation (2.19) could be reduced as follow

$$\dot{C}_e = \dot{C}_{HS} + \dot{Z}_{WH} + \dot{Z}_{ORC} + \dot{Z}_{O\&M}. \tag{2.20}$$

Then, with equation (2.20), the above equation could be

$$c_e\dot{W}_e = c_{HS}\dot{E}_{HS} + \dot{Z}_{WH} + \dot{Z}_{ORC} + \dot{Z}_{O\&M}. \tag{2.21}$$

CHP ORC system

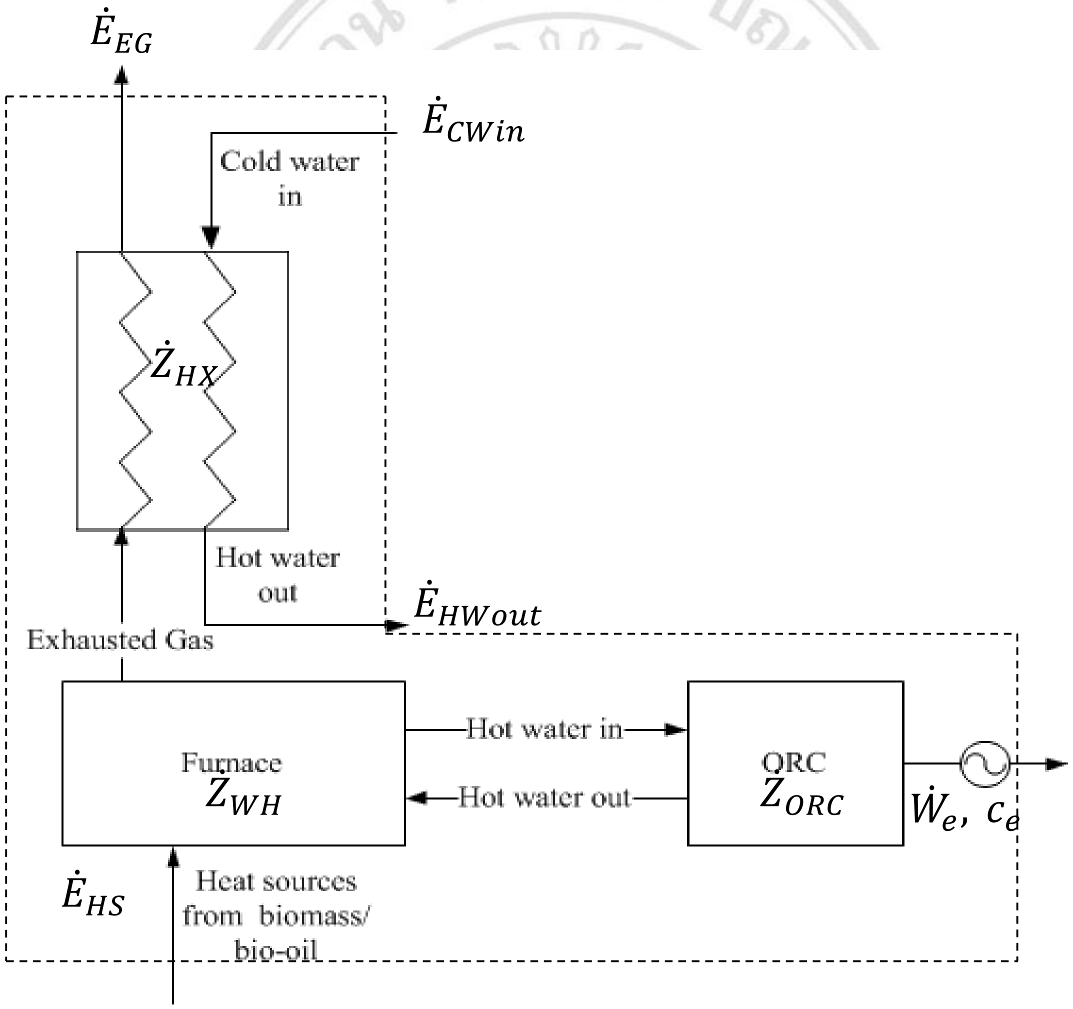

Figure 2.11 CHP ORC system.

In our CHP ORC as shown in Figure 2.11, the gas from biomass or bio-oil combustion could be used for water heating, therefore, higher overall efficiency could be obtained compared with the basic ORC.

The total cost to produce the electricity including the costs of exhausted gas and hot water equals the cost of the entering heat sources which are the cost of cold water plus the cost of investment and operating & maintenance and the cost of water heater, the cost of heat exchanger and the cost of ORC. This could be expressed by

$$\dot{C}_e + \dot{C}_{EG} + \dot{C}_{HWout} = \dot{C}_{HS} + \dot{C}_{CWin} + \dot{Z}_{HX} + \dot{Z}_{WH} + \dot{Z}_{ORC} + \dot{Z}_{O\&M} \quad (2.22)$$

Where $\dot{C}$ is the cost rate of the respective stream and $\dot{Z}_{HX}$, $\dot{Z}_{WH}$, $\dot{Z}_{ORC}$, $\dot{Z}_{O\&M}$ are the cost rate of investment in heat exchanger, water heater, ORC and operating & maintenance, respectively.

For simplicity, we assumed the cold water entering the heat exchanger with negligible exergy and cost, the exhaust gas was discharged directly to the surrounding with negligible cost. Thus equation (2.22) could be reduced as

$$\dot{C}_e + \dot{C}_{HWout} = \dot{C}_{HS} + \dot{Z}_{HX} + \dot{Z}_{WH} + \dot{Z}_{ORC} + \dot{Z}_{O\&M}. \quad (2.23)$$

It could be noted that the exergy costings of the power and the exergy in the generated hot water were assumed to be similar. Therefore, with (2.24) we have

$$c_e\left(\dot{W}_e + \dot{E}_{HWout}\right) = c_{HS}\dot{E}_{HS} + \dot{Z}_{WH} + \dot{Z}_{ORC} + \dot{Z}_{HX} + \dot{Z}_{O\&M}. \quad (2.24)$$

The exergy analysis was used to explain the outputs which were useful heat and power obtained from CHP ORC in following Chapters.

CHAPTER 3

PARAMETRIC ANALYSIS ON MODULAR ORGANIC RANKINE CYCLE PERFORMANCE

To improve ORC efficiency, a concept of a zeotropic working fluid of which the temperatures during boiling and condensation are changing with the temperatures of heat source and heat sink, respectively, could be applied. Due to the temperature differences during heat exchanging were less than those of the single working fluid then the thermodynamic irreversibilities in these components could be reduced which resulted in higher work output. Wang et al. 2010 compared performance of low temperature ORC using pure fluid (R245fa) and its mixture (R245fa/R152a) based on the experimental study. It could be found that thermal efficiency of the zeotropic fluid was higher than that of pure R245fa. Similar results was found by Dong et al. 2014 who investigated the performance of a high-temperature ORC (heat source at 280^{o}C) with zeotropic mixtures of siloxanes as working fluids. Chys et al. 2012 also considered thermal performances of ORC systems having zeotropic mixture as working fluid for heat source at temperature of 150 - 250 ^{o}C. The cycle efficiency could be increased about 6 - 16%. Heberle et al. 2012 presented the second law efficiency of an ORC with isobutane/isopentane and R227ea/R245fa as working fluids. The second law efficiency increased 4.3% to 15% for the zeotropic mixtures compared with fluids.

The thermal efficiency of an ORC system was completely related to many thermophysical properties. Recently Kuo et al. 2009 studied relationships of thermodynamic properties of many working single fluids which affected ORC thermal efficiency. The properties could be consolidated in a dimensionless group called Figure of Merit, FOM which included Jacob number, evaporation and condensing temperatures. Lower the FOM value, higher the ORC thermal efficiency could be achieved. The FOM could also be used to screen working fluid to get high ORC performance.

In this chapter, a technique proposed by Kuo et al. 2009 was modified to find out a correlation between the cycle efficiency and FOM of small-scale ORC at evaporating temperature of 80-130ºC and condensing temperature of 25-40ºC with zeotropic mixtures in case of ideal cycle. The correlation data could also be used to estimate the cycle efficiency for real cycles. It could be noted that only dry fluid having positive slope of saturated vapor line in T-s diagram or isentropic fluid were considered.

3.1 ORC Thermodynamics Cycle

Fig. 3.1 (a) shows the ORC configuration which is consisted of a pump, an evaporator, an expander and a condenser. The working fluid leaves the condenser as saturated liquid (state 1) and it is pumped to the evaporator (state 2) to be heated and vaporized by various heat sources such as waste heat, hot water from solar heat or geothermal energy, etc. The generated high pressure vapor (state 3) flows into the expander to generate power and thereafter the low pressure vapor exits the expander (state 4) to the condenser where the vapor is condensed by rejecting heat to cooling water. The condensed working fluid at the condenser outlet is pumped back to the evaporator, and a new cycle begins. All the above described processes are shown in temperature-entropy diagrams for ideal ORCs with single and zeotropic working fluids as shown in Figs. 3.1 (b) and (c), respectively.

In Fig. 3.1 (c) it could be seen that during heat exchanging at the evaporator and the condenser of the ORC, there were temperature differences between the streams of the heat source and the heat sink with the ORC working fluid, respectively. The temperature differences generate irreversibilities at the cycle components then some part of the available cycle work was destroyed.

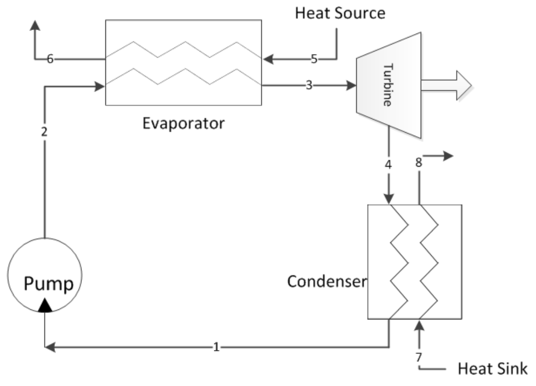

a. ORC basic components.

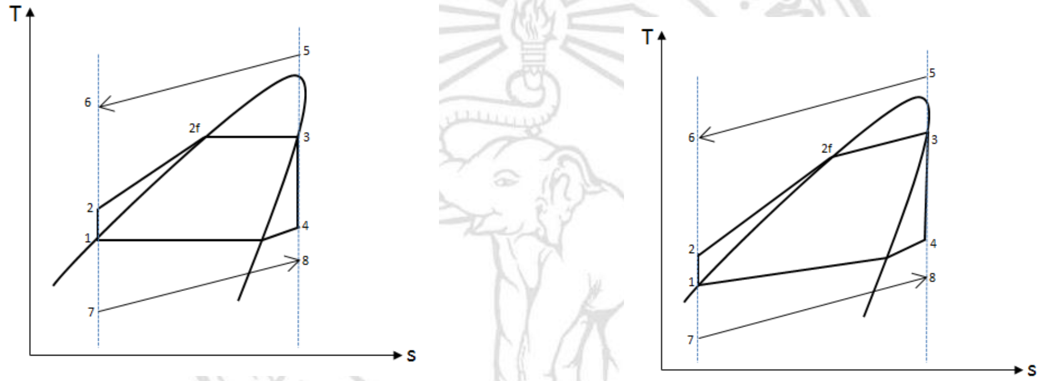

b. T-s diagram of ORC for single fluid. c. T-s diagram of ORC for zeotropic fluid.

Figure 3.1 Thermodynamic cycles of ideal ORC for single and zeotropic working fluids.

The energy balance at each component could be summarized as follows:

Pump:

$$\dot{W}_p = \frac{\dot{m}v_1(P_2 - P_1)}{\eta_P} \tag{3.1}$$

$$\dot{W}_p = \dot{m}(h_2 - h_1). \tag{3.2}$$

Evaporator:

$$\dot{Q}_E = \dot{m}(h_3 - h_2). \tag{3.3}$$

Turbine:

$$\dot{W}_T = \dot{m}(h_3 - h_4)\eta_T. \tag{3.4}$$

Condenser:

$$\dot{Q}_C = \dot{m}(h_{4a} - h_1). \tag{3.5}$$

Thermal efficiency:

$$\eta_{th} = \frac{\dot{W}_T - \dot{W}_P}{\dot{Q}_E}. \tag{3.6}$$

For ideal cycle, the expansion work and the compression work are isentropic. The states of the working fluid entering the expander and the pump are saturated.

In real practice, the isentropic efficiencies during expansion and the compression are less than 100%. For simplicity, the compression work is rather small and it could be neglected then the actual cycle efficiency could be calculated by

$$\eta_{actual\ cycle} = \eta_{th\ ideal} \times \eta_{isentropic\ turbine} \tag{3.7}$$

The cycle efficiency for each working fluid could be calculated from the above equations at various evaporating and condensing temperatures.

Kuo et al. 2009 consolidated the related parameters which affected the ORC thermal efficiency. A term called "Figure of Merit, FOM" was defined as

$$Figure\ of\ Merit\ (FOM) = Ja^{0.1}\left(\frac{T_{cond}}{T_{evap}}\right)^{0.8}. \tag{3.8}$$

This dimensionless term includes the Jacob number, evaporating and condensing temperatures. Jacob number is defined as $Ja = \frac{C_p \Delta T}{h_{fg}}$, C_p represents the average specific heat evaluated from the mathematical mean of the condensing and evaporating temperature, ΔT is the temperature difference between evaporator and condenser temperatures, where h_{fg} denotes the latent heat at evaporation temperature.

FOM increases when the evaporating temperature decreases or the condensing temperature increases. These also result to the decreases in the output work and the cycle efficiency.

The cycle efficiency could be calculated from thermodynamics properties following equations (3.1-3.7) at various condensing and evaporating temperatures. It could be noted that the cycle efficiency depended strongly on the FOM from eqn (3.8). Lower the value of FOM, higher the thermal efficiency of the ORC could be achieved.

In this study, various single and zeotropic working fluids were considered. The conditions for the calculation of ideal ORC were given in Table 3.1.

Table 3.1 The conditions for calculating ideal ORC performance.

Parameter	Data
Isentropic efficiency of pump (η_p)	1
Isentropic efficiency of turbine (η_T)	1
Evaporating temperature	80-130ºC
Condensing temperature	25-40ºC
The ambient temperature	25ºC

3.2 Working fluids

For low temperature ORC, the heat source could come from low temperature waste heat, geothermal heat, solar heat or biomass combustion to generate hot water stream having temperature of about 80-130ºC. The hot water supplies heat at the ORC evaporator. The ORC working fluids could be screened out from its environment impacts: low ozone depression potential, ODP; low global warming potential, GWP and low atmospheric life time, ALT; its chemical stability in the operating temperature range and its thermal stability. Five working fluids, R245fa, R152a, R227ea, R245ca and R236fa and their blendings in form of zeotropic fluids were selected. The fluids physical properties and the environmental data of each single and zeotropic working fluids were shown in Tables 3.2 and 3.3, respectively. The thermodynamic properties of the single fluids and their mixtures could be obtained from REFPROP, 2013.

Table 3.2 Physical and environmental data of the working fluids. [Tchanche, 2009]

Substance	Physical Data				Environmental Data			Type
	M (kg/kmol)	T_{cri} (ºC)	P_{cri} (Mpa)	T_b (ºC)	ALT (yr)	ODP	GWP (100 yr)	
R245fa	134.05	154.01	3.65	15.14	7.6	0	710	Dry
R245ca	134.05	174.42	3.93	25.13	6.2	0	693	Dry
R236ea	152.04	139.29	3.5	6.19	8	0	710	Dry
R227ea	170.03	101.75	2.925	-16.34	34.2	0	3220	Dry
R152a	66.05	113.3	4.52	-24	1.4	0	124	Wet
R123	152.93	183.7	3.67	27.8	1.3	0.02	77	Isentropic

Table 3.3 Physical data of the zeotropic working fluids. [REFPROP, 2013]

Substance	**Mass Fraction**	**Physical Data**		
		M (kg/kmol)	T_{crit} (ºC)	P_{crit} (Mpa)
R245fa/R152a	90/10	121.54	147.44	3.91
R245fa/R152a	80/20	111.16	141.36	4.07
R245fa/R152a	70/30	102.42	136.29	4.20
R245fa/R227ea	90/10	136.95	149.57	3.65
R245fa/R227ea	80/20	139.97	144.86	3.63
R245fa/R227ea	70/30	143.13	139.89	3.59
R245ca/R236ea	90/10	135.65	170.98	3.93
R245ca/R236ea	80/20	137.3	167.42	3.90
R245ca/R236ea	70/30	138.98	163.77	3.85
R245ca/R227ea	90/10	136.95	169.37	3.98
R245ca/R227ea	80/20	139.97	163.64	3.97
R245ca/R227ea	70/30	143.13	157.35	3.94
R245ca/R152a	90/10	121.54	166.05	4.30
R245ca/R152a	80/20	111.16	157.57	4.49

Substance	Mass Fraction	Physical Data		
		M (kg/kmol)	T_{crit} (ºC)	P_{crit} (Mpa)
R245ca/R152a	70/30	102.42	149.19	4.57
R245fa/R236ea	90/10	135.65	151.88	3.63
R245fa/R236ea	80/20	137.3	149.82	3.61
R245fa/R236ea	70/30	138.98	147.85	3.58

3.3 Results and Discussion

Single Fluids

Ideal Cycles:

Fig. 3.2 shows correlation between the ideal cycle efficiency calculated from equations (3.1-3.6) and the FOM for various single working fluids, when the evaporating and the condensing temperatures are prescribed. With a selected working fluid, Ja could be estimated followed by the FOM. It could be seen that lower the FOM resulted in higher the thermal efficiency. Thus the term FOM could also be used to screen working fluid to get high thermal efficiency at the same evaporating and condensing temperatures.

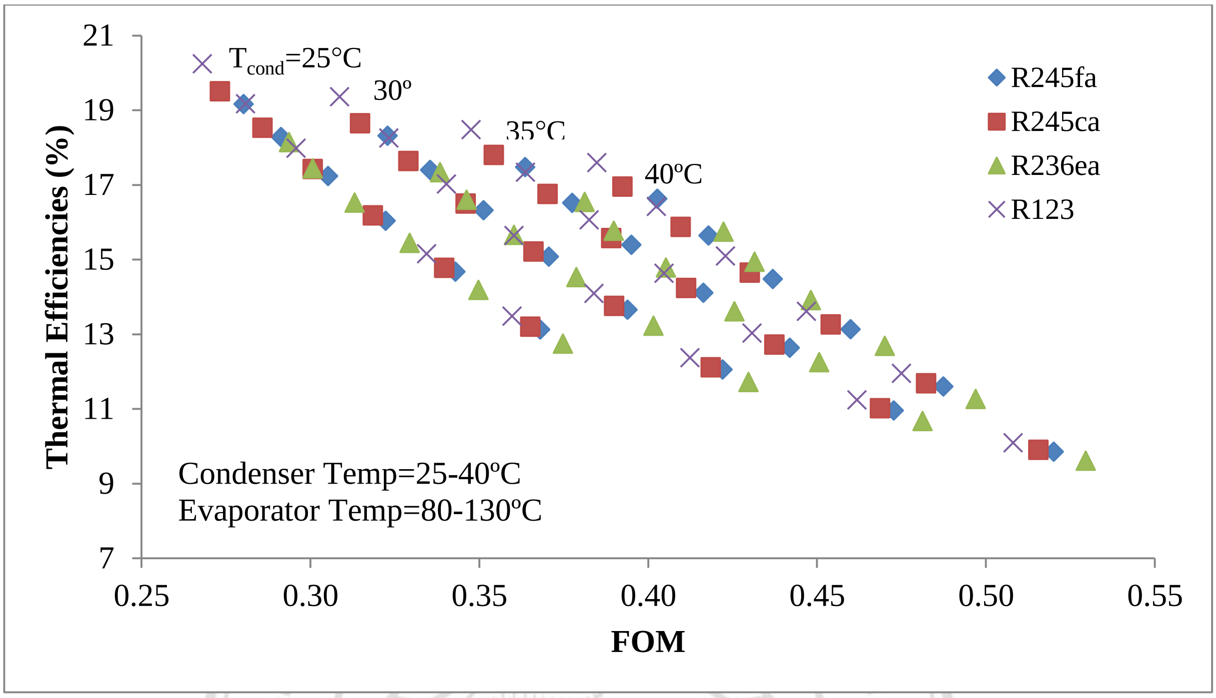

Figure 3.2 The correlation between the ideal cycle efficiency and the FOM for various single working fluids, condensing and evaporating temperatures.

From Fig. 3.2, the thermal efficiency (η_{th}) could be expressed as a function of the condensing temperature (T_{cond}) and FOM as

$$\eta_{th\ ideal} = [40.44 - 0.17T_{cond} + 0.0035T_{cond}^2] + [-132.76 + 3.604T_{cond} - 0.0428T_{cond}^2]FOM. \quad (3.9)$$

Experimental Cycle

Single Fluid:

From equation (3.7), the actual thermal efficiency for single fluids could be evaluated by multiplying $\eta_{th\ ideal}$ by the isentropic efficiency of expander. A set of experimental data from a commercial modular ORC was taken to verify the calculation from the proposed method. The specification of the commercial modular ORC was given in Table 3.4 The testing results were shown in Table 3.5

Table 3.4 The specification of the commercial modular ORC.

ORC type	R245fa hot water source, 3P 380V 50HzInduction generator	
	Gross power:20kW	Net power:16 kW
Refrigerant	R245fa	
Expander	Semi-hermetic twin screw type expander with direct drive induction generator	
	Model:RC2-300	300CMH displacement volume
Evaporator	SUS 316 plate type heat exchanger, Z400H x 136	
	Hot water inlet 110ºC	flow rate:150LPM
	Capacity:260kW	Hot water connection:3" JIS10K
Condenser	Shell and tube heat exchanger	
	Shell: Carbon steel 12" x 3000mmL	
	Tube:3/4" copper tube with inner and outer low fin tube	
	Cooling water: inlet 30ºC	Outlet 35ºC
	Flow rate: 810 LPM	Water connection:4" Flange

Table 3.5 Testing data of the commercial modular ORC.

Descriptions	Condition 1	Condition 2	Condition 3	Unit
Evaporator				
Hot water inlet	116	107.8	97	ºC
Heat source capacity	244	238.3	228.8	kW
Condenser				
Cool water inlet	28	28	28	ºC
Heat sink capacity	219	215.6	210.9	kW
Expander				
Expander inlet pressure	1097.1	1120	1074	kPa-Abs
Expander outlet pressure	227.4	227.4	227	kPa-Abs
Expander inlet temperature	93.7	94.6	92.8	ºC
Expander outlet temperature	37.1	37	37	ºC
Isentropic Efficiency of	71.4	67.9	56.6	%

Descriptions	Condition 1	Condition 2	Condition 3	Unit
The Expander				
Cycle Efficiency	9.40	8.81	7.37	%

From equation (9), the ideal ORC cycle efficiencies at the same conditions as given in Table 3.3 were found to be 12.92%, 13.08%, 12.80% respectively. With the isentropic efficiencies at the expander, the actual cycle efficiencies were found to be close to those of the real cycle. The deviations of the results from the real values were shown in Table 3.6.

Table 3.6 Comparison of the results from the proposed method with real cycle efficiency.

Descriptions	Condition 1	Condition 2	Condition 3	Unit
Ideal Cycle Efficiency from eqn.(3.9)	12.92	13.08	12.8	%
Isentropic Efficiency of The Expander	71.4	67.9	56.6	%
Cycle Efficiency (from the present method)	9.23	8.88	7.25	%
% Difference from Real Cycle from Table 3.4.	1.81	0.79	1.63	%

The results by this method were also compared with those given by Saleh et al. [13] as shown in Table 3.7 and very good agreements of these results were found.

Table 3.7 Comparison of the results calculated from this study with Saleh, 2007.

Working Fluid	η_{th}		% Difference from Saleh et al.
	Saleh et al.	This study	
R245fa	12.52	12.89	2.96
R245ca	12.79	13.13	2.66
R152a	8.82	8.59	2.61
R227ea	9.2	8.90	3.26
R236ea	12.02	12.46	3.66

Operating conditions: The evaporating temperatures for R245fa, R245ca and R236ea was 100ºC, the evaporating temperatures for R152a and R227ea were 72.59ºC and 83.88ºC, respectively. The condensing temperature was 30 ºC and the isentropic efficiency of turbine was 0.85.

Zeotropic Mixture

Ideal Cycle

In this studies, 6 zeotropic mixtures, R245fa/R152a, R245fa/R227ea, R245fa/R236ea, R245ca/R152a, R245ca/R227ea and R245ca/R236ea were considered. The mass fractions of R245fa and R245ca were recommended not to be less than 70% [5, 12]. Fig. 3.3 shows the correlation between the ideal cycle efficiency with $FOM_{zeotropic}$ for these zeotropic refrigerants compared with that for R245fa. The evaporating temperature and the condensing temperature for the $FOM_{zeotropic}$ calculation were taken from saturated liquid at the evaporating pressure and saturated vapor at the condensing pressure, respectively. It could be seen that high disorders of the data points were found with the zeotropic working fluids.

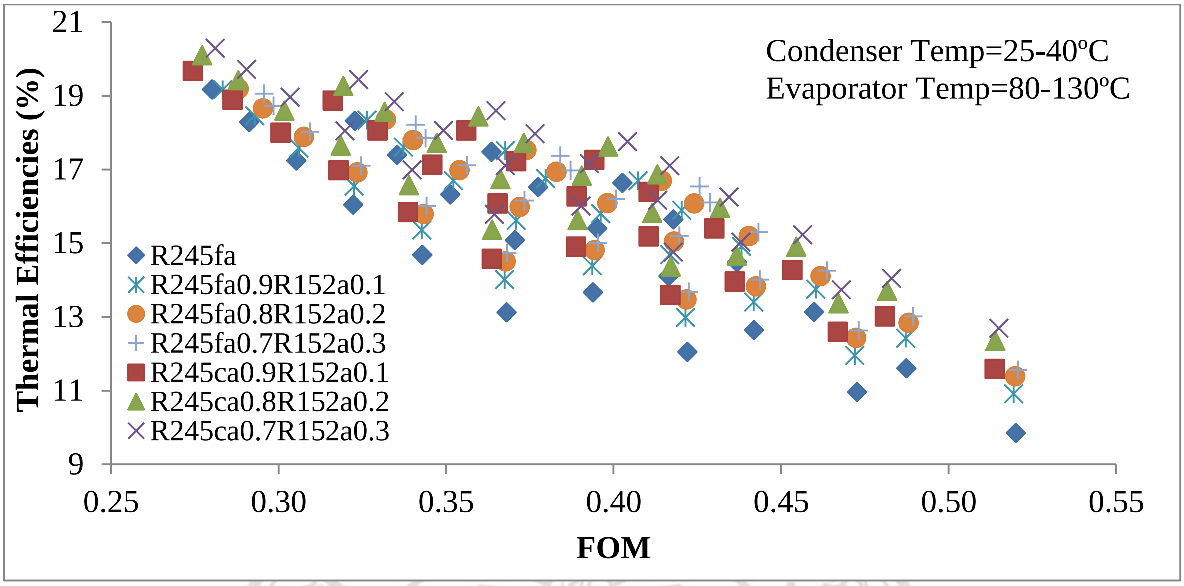

Figure 3.3 The correlation between the ideal cycle efficiency with $FOM_{zeotropic}$ for zeotropic refrigerants.

The deviation of cycle efficiency from the single fluid was mainly due to gliding temperatures of the zeotropic fluids as shown in Table 3.8.

Table 3.8 Gliding temperatures when the evaporation temperature was at 80-130ºC. The condensing temperature was at 25-40ºC.

Working Fluid	**Mass Fraction**	**Evaporation temperature (ºC)**					
		80	90	100	110	120	130
R245fa/R152a	90/10	6.66	6.12	5.56	4.96	4.29	3.48
R245fa/R152a	80/20	8.76	8.02	7.23	6.35	5.32	3.99
R245fa/R152a	70/30	8.92	8.12	7.23	6.22	4.99	3.20
R245fa/R227ea	90/10	3.19	2.92	2.64	2.36	2.05	1.71
R245fa/R227ea	80/20	5.19	4.75	4.29	3.79	3.25	2.59
R245fa/R227ea	70/30	6.25	5.69	5.09	4.45	3.70	2.73
R245ca/R236ea	90/10	1.44	1.36	1.28	1.20	1.11	1.01
R245ca/R236ea	80/20	2.35	2.22	2.09	1.94	1.79	1.61
R245ca/R236ea	70/30	2.81	2.66	2.49	2.31	2.11	1.89
R245ca/R227ea	90/10	5.43	5.06	4.69	4.31	3.93	3.51

Working Fluid	Mass Fraction	Evaporation temperature (ºC)					
		80	90	100	110	120	130
R245ca/R227ea	80/20	8.93	8.34	7.73	7.09	6.41	5.66
R245ca/R227ea	70/30	10.94	10.21	9.43	8.60	7.67	6.61
R245ca/R152a	90/10	11.63	10.90	10.14	9.33	8.46	7.50
R245ca/R152a	80/20	15.08	14.12	13.08	11.93	10.64	9.14
R245ca/R152a	70/30	15.36	14.29	13.11	11.78	10.24	8.34
R245fa/R236ea	90/10	0.46	0.43	0.39	0.35	0.31	0.27
R245fa/R236ea	80/20	0.69	0.63	0.58	0.52	0.46	0.38
R245fa/R236ea	70/30	0.74	0.68	0.61	0.55	0.48	0.40

Figure 3.4 shows the deviation of $FOM_{zeotropic}$ for zeotropic working fluids from *FOM* for single fluid. Higher the gliding temperature resulted in higher deviation from the single fluid. The deviation D could be empirically related with the gliding temperature as

$$D = 0.0004{T_g}^2 + 0.0004T_g + 0.0047. \tag{3.10}$$

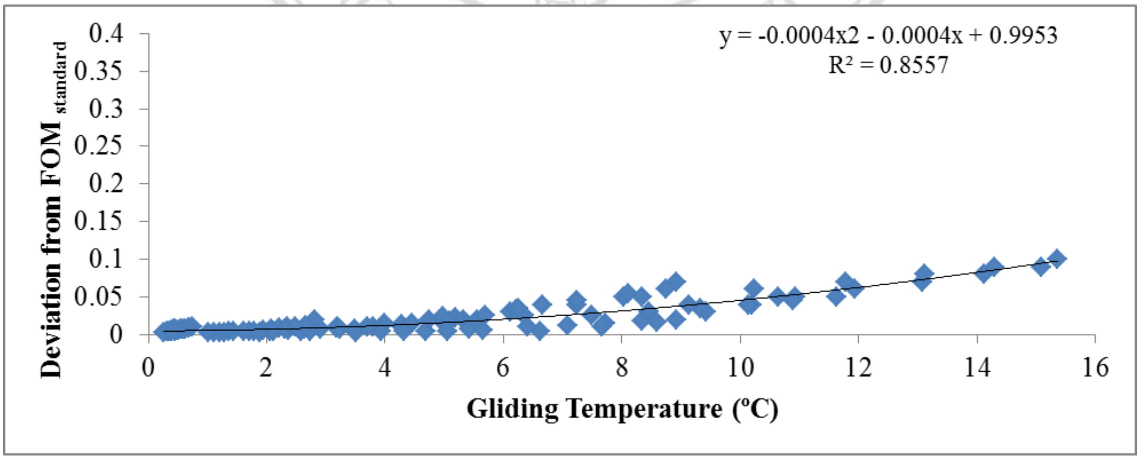

Figure 3.4 The deviations of *FOM* for all zeotropic working fluids in this studies from that of single fluid.

The $FOM_{zeotropic}$ for zeotropic mixture then could be modified as

$$FOM_{zeotropic} = F(FOM_{single}). \tag{3.11}$$

Where F is the correction factor: $F = (1 - D) = [1 - (-0.0004{T_g}^2 - 0.0004T_g + 0.9953)]$.

From equation 3.11, a correlation between the ideal thermal efficiency and the $FOM_{zeotropic}$ at various condensing temperatures and evaporating temperatures could be presented and the results were shown in Fig. 3.5. Now the data points could be presented orderly. Again, it could be seen that lower the $FOM_{zeotropic}$ resulted in higher the thermal efficiency.

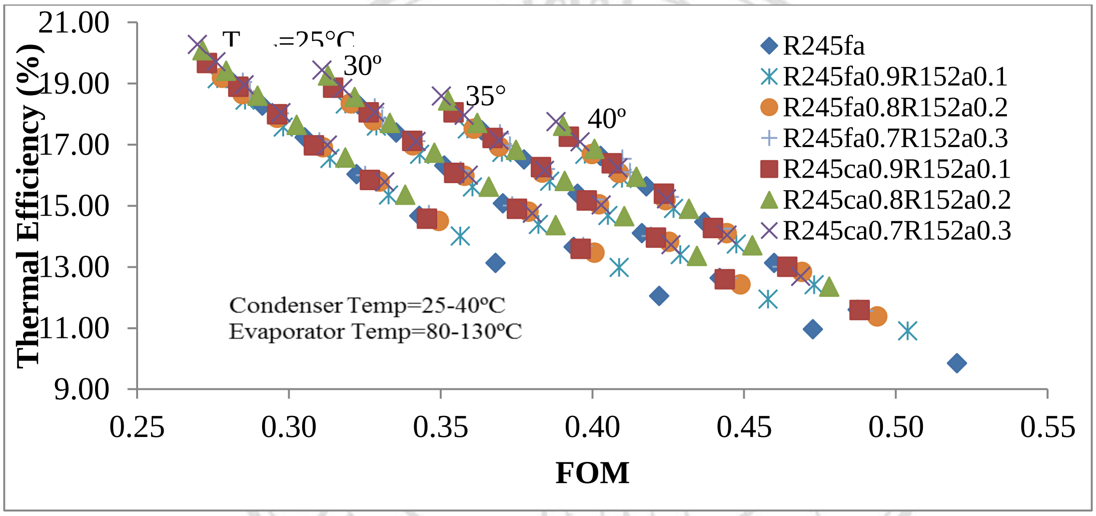

Figure 3.5 The correlation of the cycle efficiency with the $FOM_{zeotropic}$ for R245fa/R152a and R245ca/R152a at various compositions.

We could express the thermal efficiency (η_{th}) as a function of the condensing temperature (T_{cond}) and the $FOM_{zeotropic}$ as

$$\eta_{th} = [40.44 - 0.17T_{cond} + 0.0035T_{cond}^2] + [-132.76 + 3.604T_{cond} - 0.0428T_{cond}^2]FOM_{zeotropic}. \quad (3.12)$$

For zeotropic working fluids, the calculated efficiency from equation (3.12) was compared with the results of Li et al. [14]. The ORC used a zeotropic mixture which was R245fa/R152a (0.8/0.2) at evaporating temperature of 90-110 ºC and condensing temperature of 25 ºC. The efficiencies were calculated from thermodynamic properties. Very good agreements between our results from equation (3.12) with those of the literature were found as shown in Table 3.9.

Table 3.9 Comparison of the results calculated from this study with Li 2014.

Evaporating Temperature (ºC)	η_{th}		% Difference from Li et al.
	Li et al. [14]	This study	
90	11.65	10.97	5.86
100	12.45	12.00	3.61
110	13.12	12.83	2.20

3.4 Conclusion

The thermal efficiency of an ORC system could be indicated by a dimensionless term, Figure of Merit (*FOM*) which covered parameters such as Jacob number, evaporating and condensing temperatures of the ORC. The *FOM* could be used to screen the working fluids to get high thermal efficiency at prescribed evaporating and condensing temperatures. Lower the *FOM* resulted in higher thermal efficiency.

For zeotropic working fluid, *FOM* must be modified by multiplying a correction factor *F* which relied on the gliding temperature of the zeotropic mixture.

A model to predict the zeotropic ORC efficiency was developed. The results could be fitted very well with those from the literature.

CHAPTER 4

THERMOECONOMIC ANALYSIS OF A MODULAR ORGANIC RANKINE CYCLE WITH BIOFUEL AS HEAT SOURCE

In this chapter, a study on potentials of power generation by a basic ORC and an ORC to generate only electricity and both electricity and thermal energy (combined heat and power, CHP-ORC) was performed by thermoeconomic analysis. The heat sources of the ORCs came from various kinds of biomass and biodiesel.

4.1 Organic Rankine Cycle with Bioenergy as Heat Source

Figure 4.1 shows a schematic diagram of an organic Rankine cycle with biofuel which is biomass or biodiesel as heat source. The system was consisted of a water heater having a combustion chamber for biofuel burning. The hot water at a suitable temperature was fed and transferred heat to the ORC evaporator and after that returned back to the heater. For the ORC cycle , the working fluid left the condenser as saturated liquid (state 1) and it was pumped to the evaporator (state 2) where it was heated and left the evaporator as saturated vapor at high pressure (state 3). The fluid expanded through the turbine to generate work and entered the condenser (state 4). After heat rejection to a heat sink, the condensed working fluid was at state 1 and the new cycle restarted.

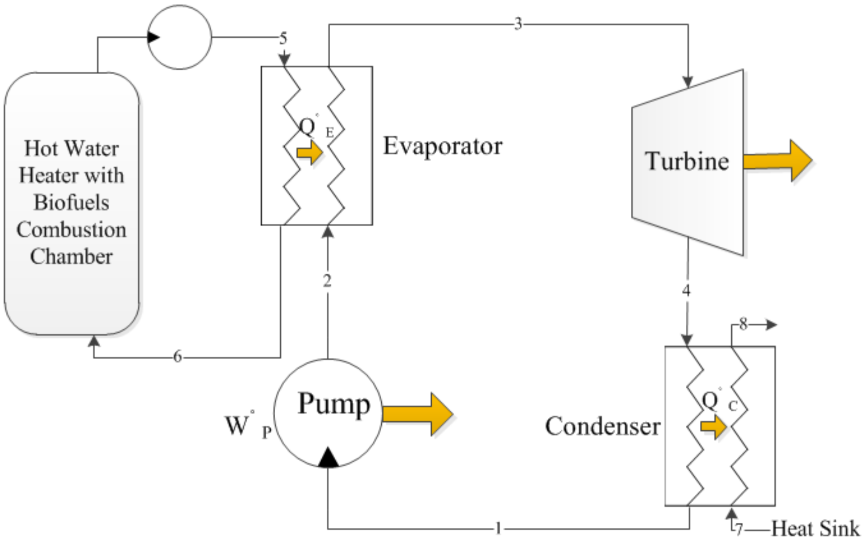

Figure 4.1 Organic Rankine cycle with biofuel as heat source.

4.2 Working Fluid

From Chapter 3, it could be found that the zeotropic working fluid R245fa/R152a at the composition of 70/30% was appropriate for Thailand climate to get high thermal efficiency and the fluid at this composition was carried out throughout this study. The T-s diagram of the ORC for this working fluid was given in Fig. 4.2.

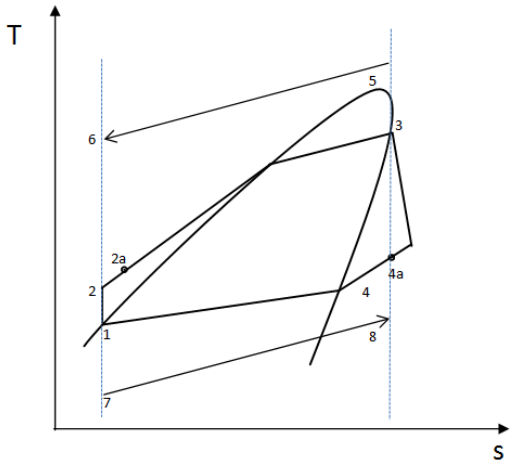

Figure 4.2 T-s diagram of zeotropic fluid R245fa/R152a at composition of 70:30.

4.3 Combined Heat and Power (CHP)

From basic ORC in Figure 4.3 the exhaust gas from biofuel combustion could be recovered to generate hot water for other thermal processes as a combined heat and power (CHP) in Fig. 4.4. Now the CHP could simultaneously generate electricity and useful heat thus higher overall efficiency could be obtained.

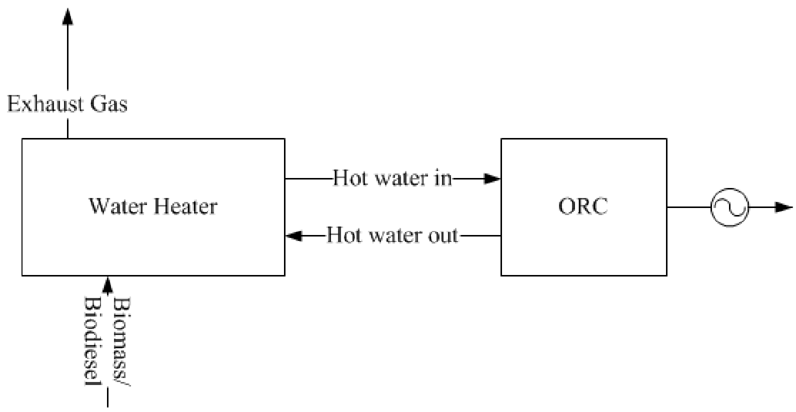

Figure 4.3 A basic ORC system.

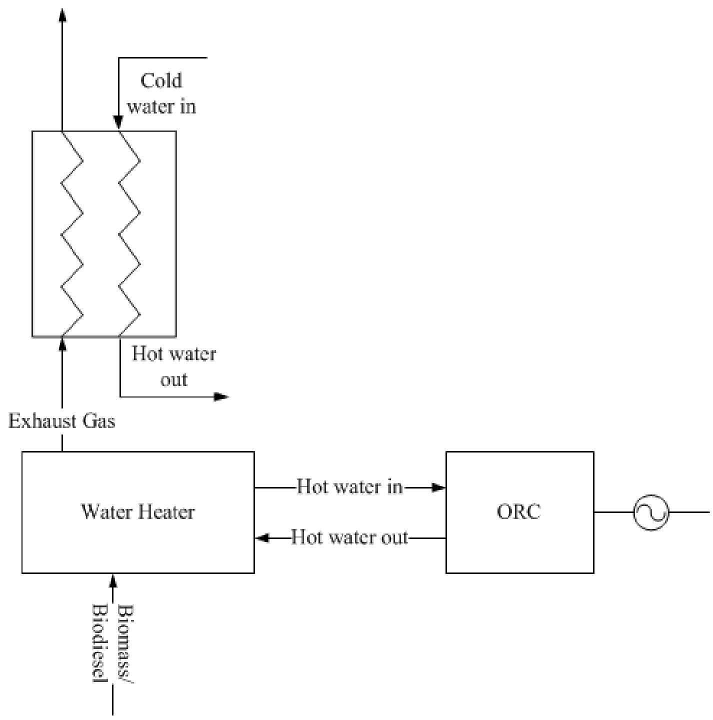

Figure 4.4 A CHP-ORC system.

4.4 Biomass and Biodiesel

Biofuel could be converted into energy by various processes such as direct combustion and gasification, etc. In this study, thermal heat from direct burning of biomass or biodiesel to generate hot water for the ORC was performed.

Various kinds of biomass for direct combustion were shown in Table 4.1. The heating values and the prices of the residues were also given.

Table 4.1 Heating values and prices of biomass residues [Biomass, 2013].

Type of Biomass	Ash (%)	Higher heating value (kJ/kg)	Lower heating value (kJ/kg)	Price (Baht/ton)
Rice Husk	12.65	14,755	13,517	1,600
Rice Straw	10.39	13,650	12,330	1,225
Sugar Cane Leaves and Tops	6.10	16,794	15,479	1,125
Rubber wood	1.59	10,365	8,600	1,300
Palm Fruit Bunch	2.03	9,196	7,240	514
Corncob	0.9	11,298	9,615	1,100
Cassava	1.5	7,451	5,494	950
Eucalyptus Bark	2.44	6,811	4,917	700

The biodiesel used in this study was produced from used cooking oil and its heating value was around 39,310 kJ/kg. [Ngammuang, 2015]

The heat rate at the ORC evaporator ($\dot{Q}_E$) was assumed to be the same as the heat rate from fuel combustion($\dot{Q}_{heater}$) which could be calculated by

$$\dot{Q}_{heater} = n_{WH}\left(\dot{m}_{biofuel}HHV\right). \tag{4.1}$$

Where n_{WH} is the combustion efficiency of biofuel burning (decimal), $\dot{m}_{biofuel}$ is the biofuel consumption (kg/s) and HHV is the higher heating value of biomass (kJ/kg).

4.5 Exergy Costing

Exergy costing is generally taken as a tool to analyze energy quality of thermal systems including the energy cost in term of exergy cost rate or exergy costing.

For basic ORC

$$c_e\dot{W}_e = c_{fuel}\dot{E}_{fuel} + \dot{Z}_{ORC} + \dot{Z}_{O\&M} \tag{4.2}$$

Where c_e, c_{fuel} are the exergy costing of the power and biofuel (Baht/kWh), $\dot{W}_e$is the electrical power output from cycle (kW),$\dot{E}_{fuel}$ is the exergy rate of biofuel (kW) and $\dot{Z}_{ORC}$, $\dot{Z}_{O\&M}$ are the cost rates of net investment in ORC including salvage value and the operating & maintenance (Baht/h), respectively.

For CHP ORC

$$c_e\left(\dot{W}_e + \dot{E}_{HWout}\right) = c_{fuel}\dot{E}_{fuel} + \dot{Z}_{ORC} + \dot{Z}_{HX} + \dot{Z}_{O\&M} \tag{4.3}$$

Where c_e, c_{fuel} are the exergy costing of the power and biofuel (Baht/kWh), $\dot{W}_e$ is the electrical power output from cycle (kW), $\dot{E}_{fuel}$, $\dot{E}_{HWout}$ are the exergy rates of biofuel and generated hot water from exhaust gas (kW) and $\dot{Z}_{ORC}$, $\dot{Z}_{HX}$, $\dot{Z}_{O\&M}$ are the cost rates of net investment of ORC, heat exchanger and operating & maintenance (Baht/h), respectively.

It could be noted that the exergy costings of the power and exergy in the generated hot water were assumed to be the same.

Table 4.2 Cost data used for the thermoeconomic analyses of basic ORC and CHP-ORC for biomass as heat source.

Investment cost for ORC 20kW	
ORC power plant 20 kW (Baht/unit) [1]	1,500,000
Biomass Furnace and heat exchanger (Baht/unit) [1]	200,000
Heat Exchanger for exhaust gas from biomass (Baht/unit) [1]	50,000
Land for ORC and feedstock storage (m^2) [2]	80
Investment cost for ORC 100kW	
ORC power plant 100 kW (Baht/unit) [1]	4,000,000
Biomass Furnace and heat exchanger (Baht/unit) [1]	2,700,000
Heat Exchanger for exhaust gas from biomass (Baht/unit) [1]	100,000
Land for ORC and feedstock storage (m^2) [2]	160
Operating & Maintenance (O&M) cost	
Operating & maintenance equipment cost (% of investment cost per year)[3]	1
Financial parameters	
Real debt interest rate, i_d (%) [4]	6
Salvage value (% of investment cost)	10
Depreciation period, n (year)	20

*Investment cost for land was 1250 Baht/m^2

Table 4.3 Cost data used for the thermoeconomic analyses of basic ORC and CHP-ORC for biodiesel as heat source.

Investment cost for ORC 20kW	
ORC power plant 20 kW (Baht/unit) [1]	1,500,000
Biodiesel burner and heat exchanger (Baht/unit) [1]	200,000
Heat Exchanger for exhaust gas from biodiesel (Baht/unit) [1]	50,000
Land for ORC and feedstock storage (m^2) [2]	40
Investment cost for ORC 100kW	
ORC power plant 100 kW (Baht/unit) [1]	4,000,000
Biodiesel burner and heat exchanger (Baht/unit) [1]	2,000,000
Heat Exchanger for exhaust gas from biodiesel (Baht/unit) [1]	100,000
Land for ORC and feedstock storage (m^2) [2]	80
Operating & Maintenance (O&M) cost	
Operating & maintenance equipment cost (% of investment cost per year) [3]	1
Financial parameters	
Real debt interest rate, i_d (%)[4]	6
Salvage value (% of investment cost)	10
Depreciation period, n (year)	20

*Investment cost for land was 1250 Baht/m^2 [2]

[1] Market cost

[2] Treasury Department, 2015

[3] Thawonngamyingsakul, 2013

[4] Karellas et al., 2011

The conditions for the basic ORC and the CHP-ORC analyses were

1. The total power output from the ORC were 20 kWe and 100kWe.
2. The furnace for water heating efficiency from biomass combustion was 70% [European Wood-Heating Technology Survey, 2014].
3. The burner for water heating efficiency from biodiesel combustion was 80% [European Wood-Heating Technology Survey, 2014].

4. Evaporating temperature were 80ºC to110ºC for 20 kWe and 100 kWe and condensing temperature was 40ºC.
5. Isentropic efficiency of turbine was 0.8.
6. Generator efficiency and mechanical efficiency were 0.9.
7. 50% of heat loss in the exhaust gas after combustion could be recovered and it was used to generate hot water for other thermal processes. The hot water temperature could be heated up to 80ºC from its inlet temperature at 28ºC in a heat exchanger having an effectiveness ($\boldsymbol{\varepsilon}$) of 0.85.
8. The ORC working fluid were R245fa and R245fa/R152a at composition 70/30%, the properties were based upon REFPROP [10].

4.6 Results and Discussion

4.6.1 Heat input

From eqn 3.12 in Chapter 3, with the prescribed values of the ORC evaporating and condensing temperatures then the cycle efficiency could be evaluated. For the electrical power outputs at 20 kWe and 100 kWe with the generator efficiency and the mechanical efficiency at the turbine, the heat rates at the evaporator $(\dot{Q}_E)$ could be estimated. The results were shown in Figures 4.5 and 4.6. Increase of the evaporating temperature resulted in higher the cycle efficiency then the input heat rate at the evaporator decreased. At the evaporating temperature of 110ºC, with R245fa working fluid, the heat rate inputs for $20kW_e$ and $100kW_e$ ORC were 213.16kW and 1,065.82kW, respectively. For R245fa/R152a zeotropic working fluid at 70:30 composition, the heat rate inputs were 201.80 kW and 1009 kW, respectively.

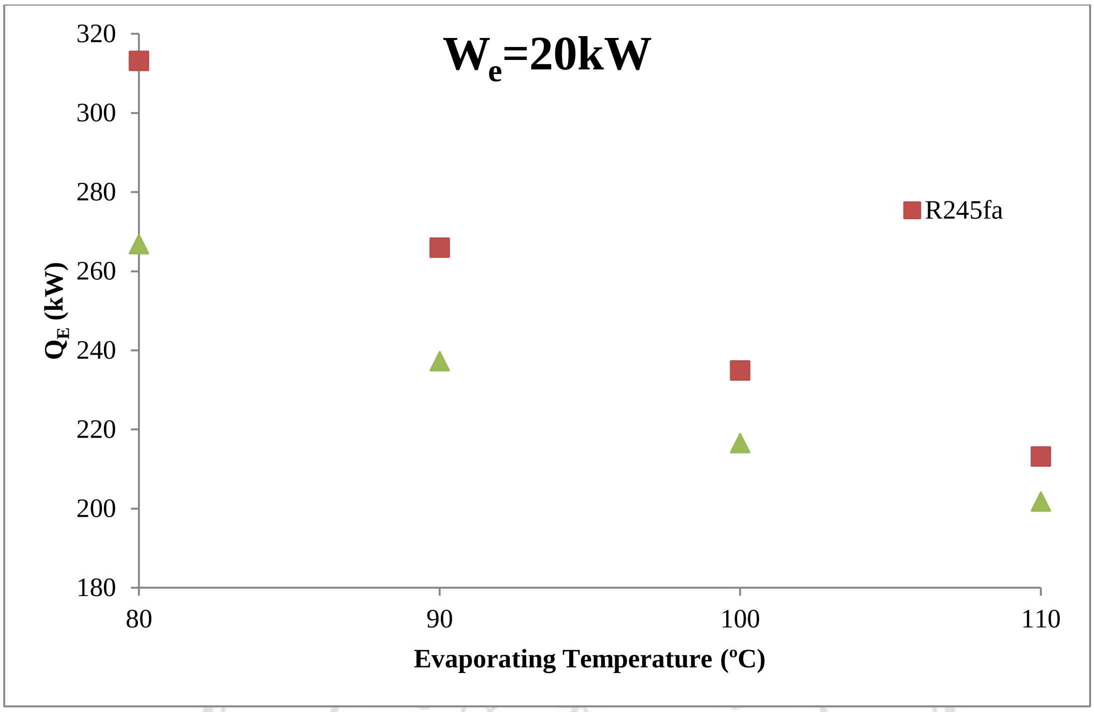

Figure 4.5 Heat rate input at various values of evaporating temperature for 20kWe ORC.

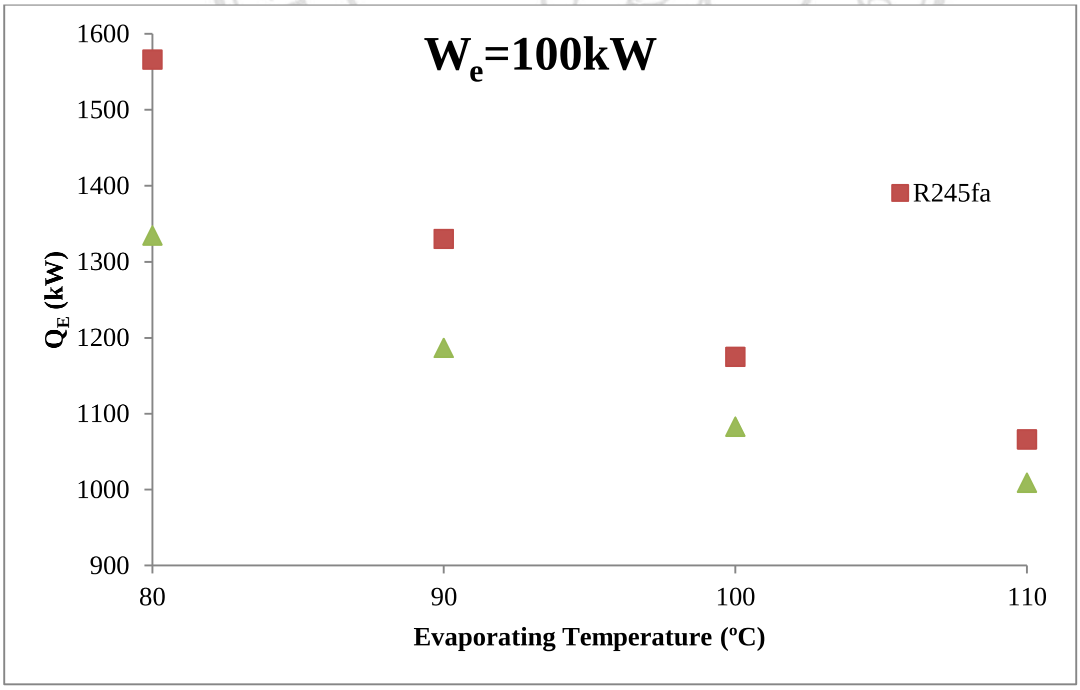

Figure 4.6 Heat rate input at various values of evaporating temperature for 100kWe ORC.

4.6.2 The values of unit cost of generated electricity (UCE) for the basic ORC and the CHP-ORC with biomass as heat source.

Figs. 4.7 and 4.8 show UCEs of 20 kW_e and 100 kW_e basic ORC, respectively. The daily operating hour was 12 hour per day, the real debt interest rate was 6% annually and the heat sources of ORC came from various kinds of biomass.

For 20 kW_e and 100 kW_e basic ORC with R245fa working fluid, it could be found that the UCE for palm fruit bunch was lowest as 4.15 and 3.74 Baht/kWh, respectively even the HHV of palm fruit bunch was low but the price per ton was cheapest as given in Table 4.1. For R245fa/R152a zeotropic fluid at composition of 70:30 with the palm fruit bunch, it was found that the UCEs could be decreased compared with the single fluid. At 20 kW and100kW ORC, the UCEs were 3.76 baht/kWh and 3.57 Baht/kWh, respectively.

In Figures 4.9 and 4.10, when the exhausted gas from biomass combustion was used to generate hot water in other process (CHP-ORC), for 20kW and 100 kW, it could be found that UCE was decreased. With palm fruit bunch, for the zeotropic fluid, the UCEs were decreased from 3.76 to 2.91 Baht/kWh and 3.57 to 2.73 Baht/kWh for the 20 and the 100kWe ORC, respectively.

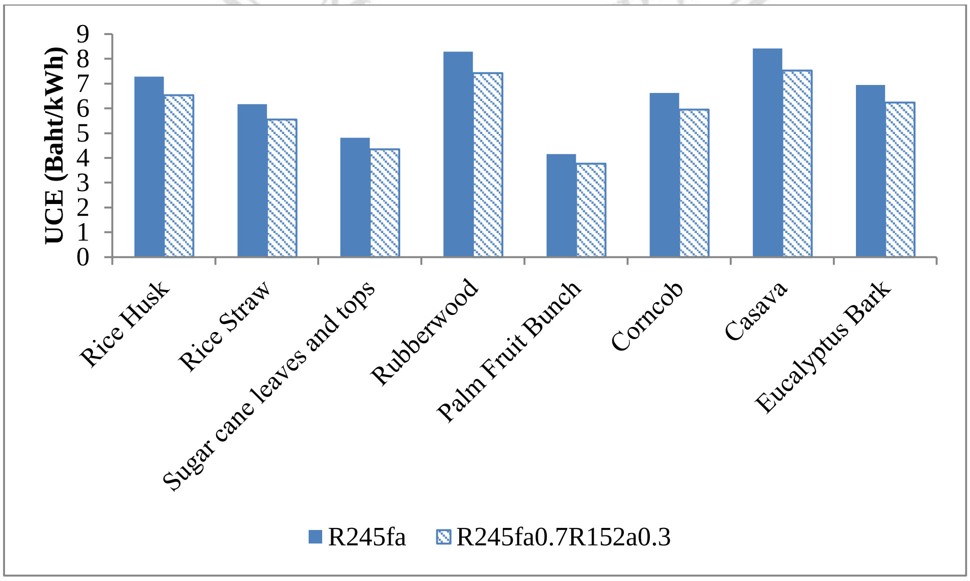

Figure 4.7 UCEs from various kinds of biomass at operating hour of 12hr/day, id=6% for the 20 kWe basic ORC.

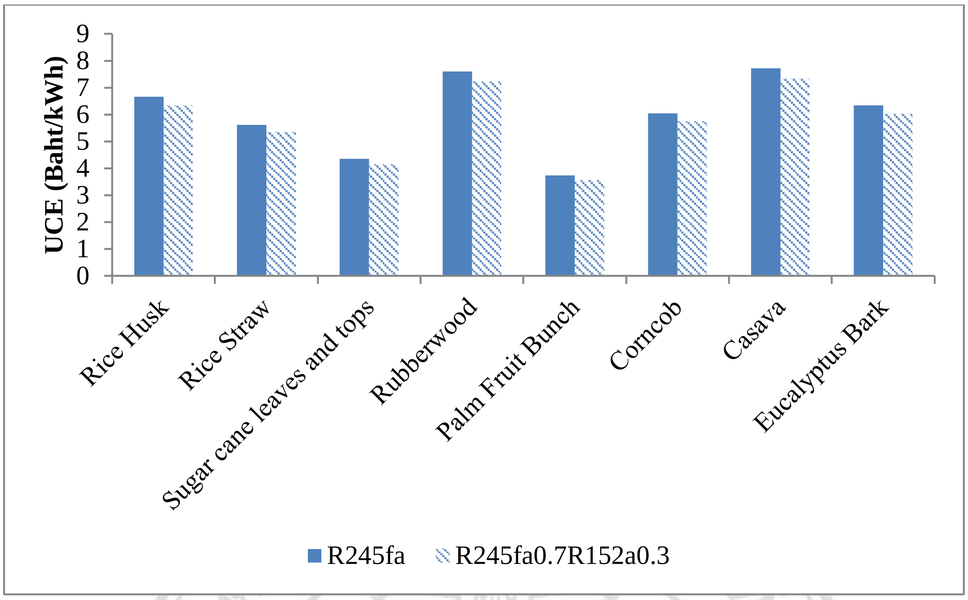

Figure 4.8 UCEs from various kinds of biomass at operating hour of 12hr/day, id=6%, the 100 kWe basic ORC.

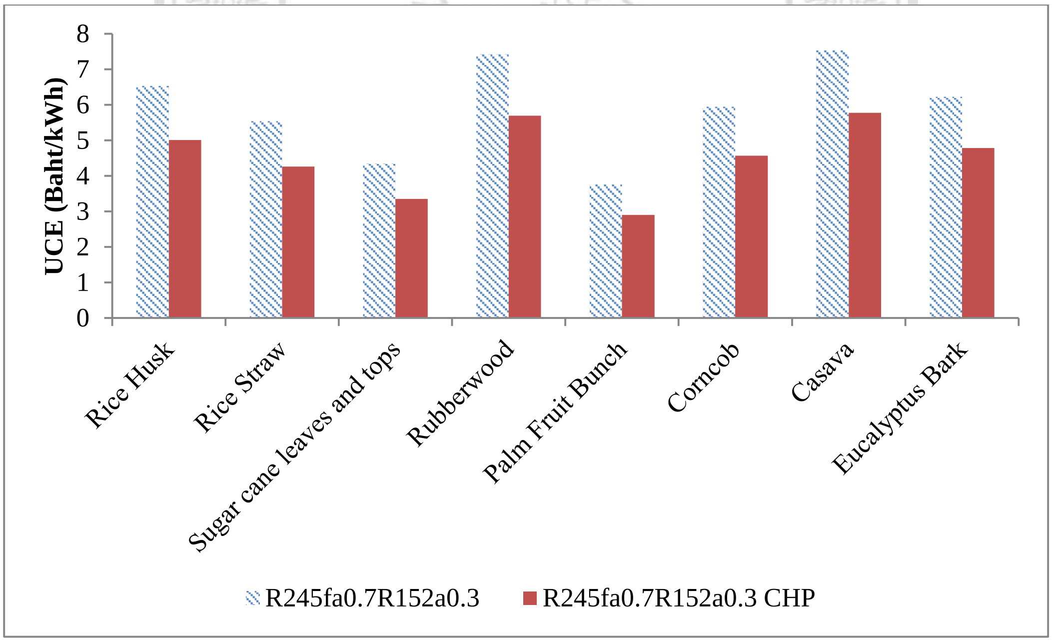

Figure 4.9 UCEs from various kinds of biomass at operating hour of 12hr/day, id=6% for the 20 kWe basic ORC and CHP-ORC.

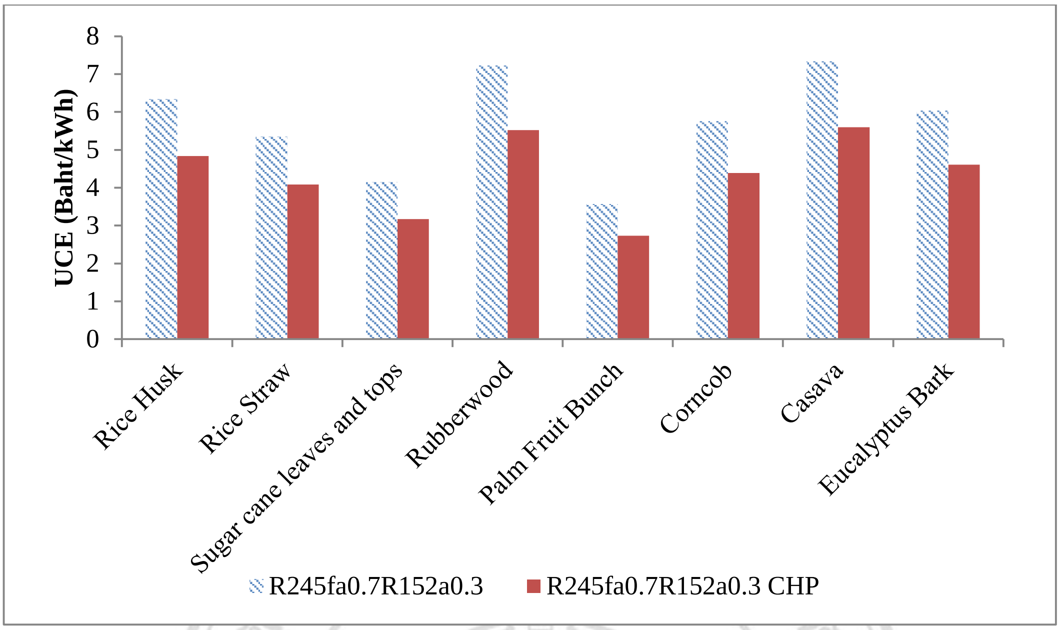

Figure 4.10 UCEs from various kinds of biomass at operating hour of 12hr/day, id=6% for the 100 kWe basic ORC and CHP-ORC.

4.6.4 Sensitivity Analysis

In this section, sensitivity analyses of the parameters those affect the electricity unit cost of the CHP-ORC system with the R245fa/R152a zeotropic fluid at composition of 70:30 were considered. The parameters were: the palm fruit bunch unit cost of 300-700 Baht/ton, the operating hour of 8-12 hour/day and the real debt interest rate of 4-8%. From Fig.4.11, it was found that the palm fruit bunch unit cost and the real debt interest gave the most and least effects on the UCE.

If the 20kWe and 100kWe CHP-ORCs operated at 12 hours/day, 6% real debt interest rate and palm fruit bunch unit cost of 300 Baht/ton, the unit cost of electricity was 2.82 Baht/kWh and 2.65 Baht/kWh, respectively.

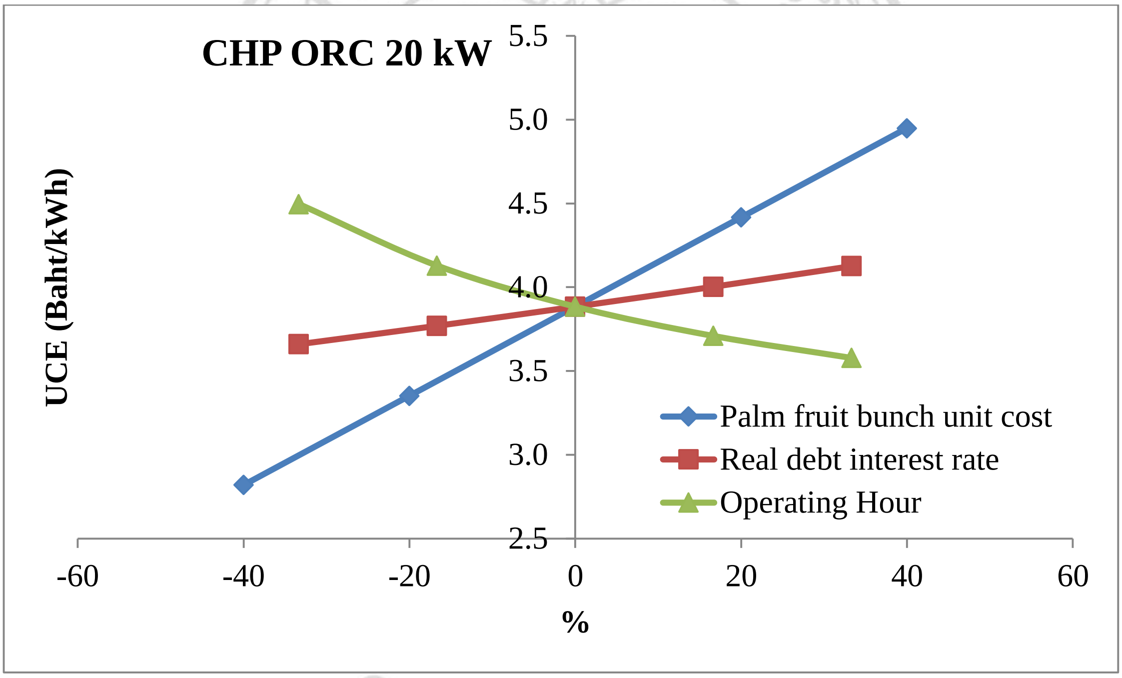

(a) CHP ORC 20 kW

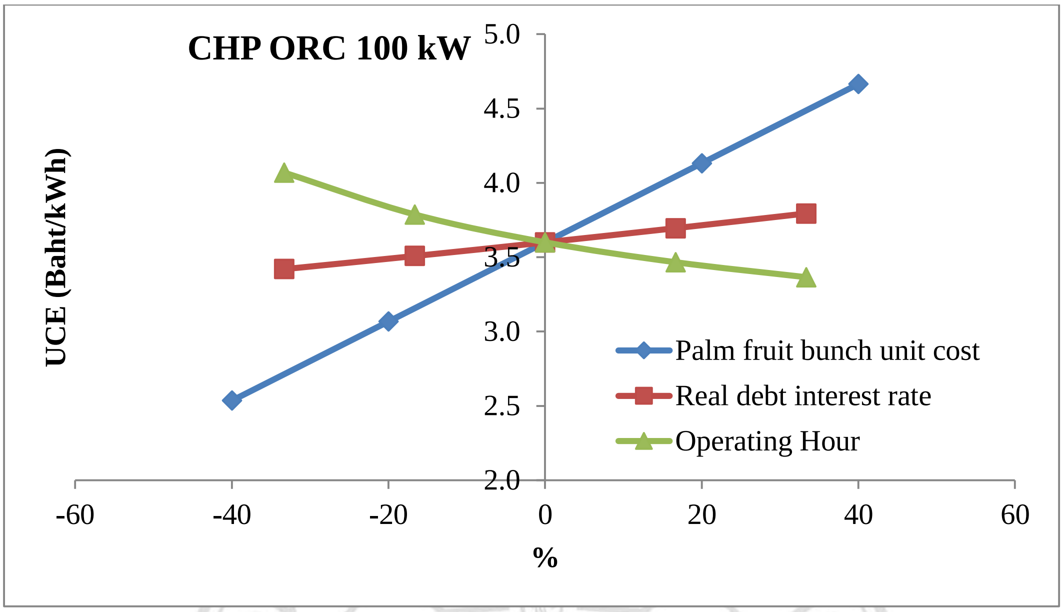

(b) CHP ORC 100 kW

Figure 4.11Sensitivity analyses on UCE with varying unit costs of biomass, operating hours and interest rates. The reference conditions are: Palm fruit bunch unit cost = 514 Baht/ton, operating hour= 12hr/day and real debt interest rate =6%. R245fa/R152a zeotropic fluid at composition of 70:30 was the ORC working fluid.

4.6.5 The values of unit cost of generated electricity (UCE) for the basic ORC and the CHP-ORC with biodiesel as heat source.

Fig. 4.12 shows UCEs of basic ORC andCHP-ORC 20 kW and100 kW, respectively. The working fluid was zeotropic fluid R245fa/R152a at composition 70/30%. The daily operating hour was 12hour per day, the real debt interest rate was 6% and heat sources of ORC came from biodiesel.

For basic ORC of 20 kW and 100 kW, it could be found that UCE with capital cost of biodiesel as 5 Baht/liter was 7.77 and 7.53 Baht/kWh, respectively.

When the exhaust gas from biodiesel burner was used to generate hot water in other process (CHP-ORC), for 20kW and 100 kW, it could be found that UCEs was decreased from 7.77 to 5.92 Baht/kWh and 7.53 to 5.74 Baht/kWh for 20 and 100 kWe ORC, respectively.

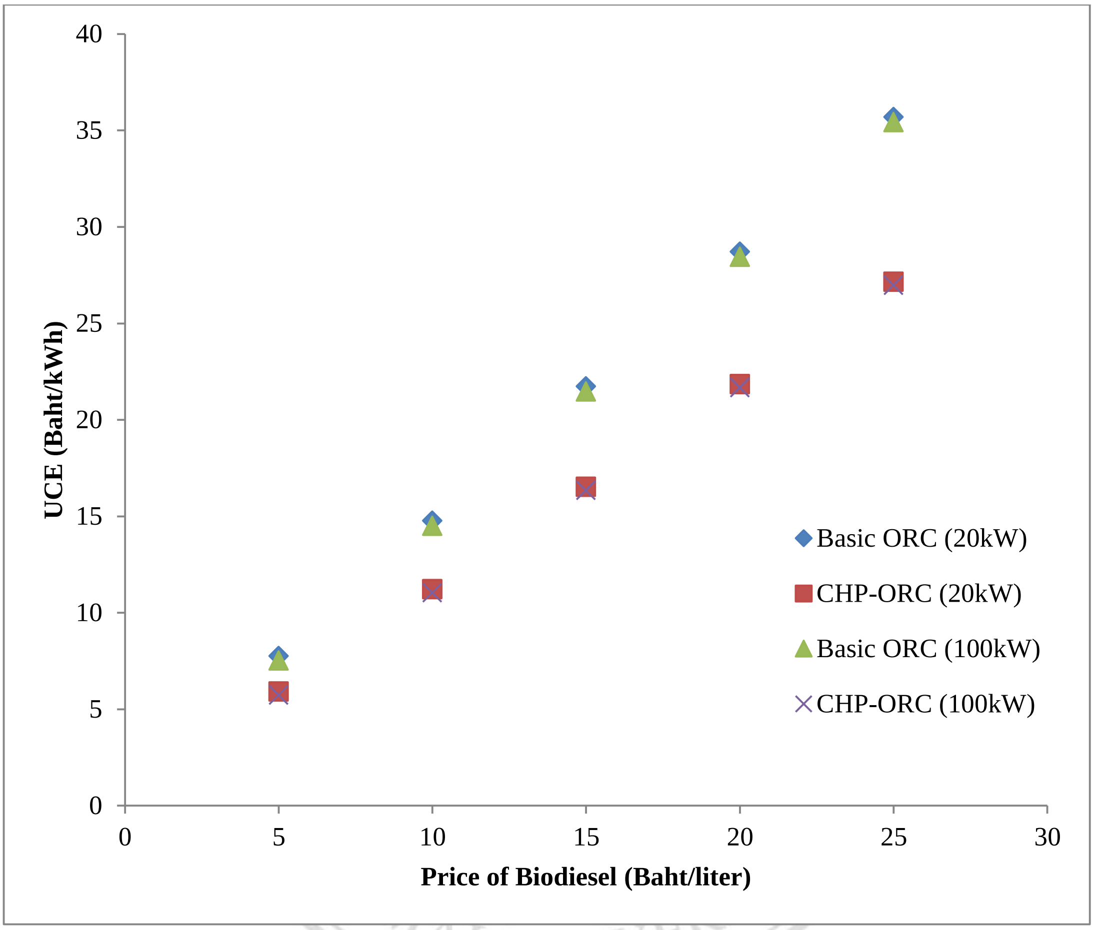

Figure 4.12 UCEs from various values of biodiesel price at operating hour of 12hr/day, id=6% for the basic ORCs and the CHP-ORCs. R245fa/R152a zeotropic fluid at composition of 70:30 was the ORC working fluid.

4.6.6 Sensitivity Analysis in Biodiesel as Heat source

Sensitivity analyses of the parameters those affect the electricity unit cost of the CHP-ORC system were considered. The parameters were the biodiesel capital cost of 5-25 Baht/liter, the operating hour of 8-12 hour/day and the real debt interest rate of 6-10%. From Fig.4.12, it was found that the biodiesel capital gave the most sensitivity on the UCE.

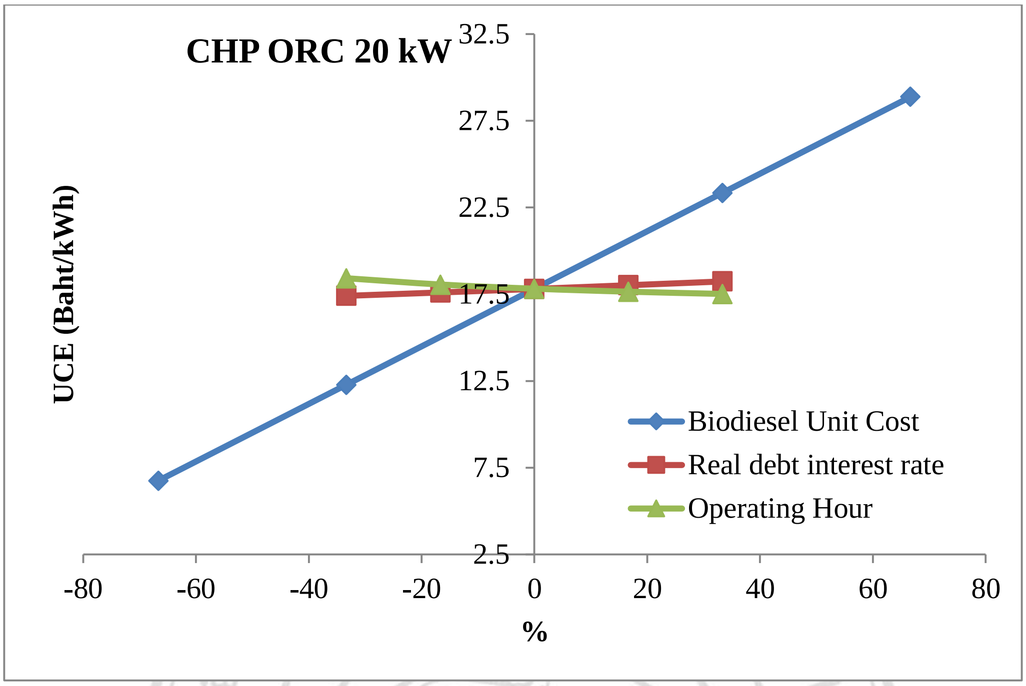

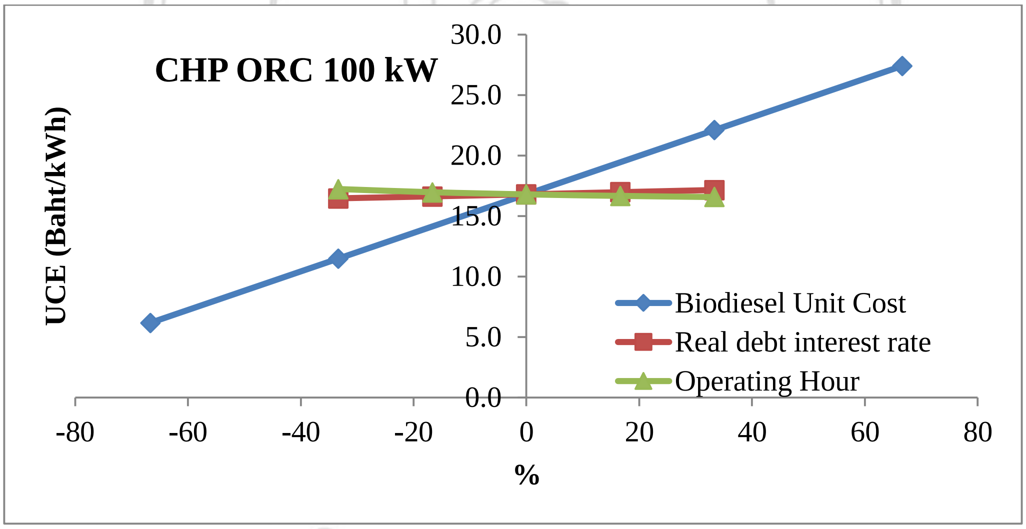

Figure 4.13 Sensitivity analyses on UCE with varying unit costs of biodiesel, operating hours and interest rates. The reference conditions are: biodiesel capital cost = 15 Baht/liter, operating hour= 12hr/day and real debt interest rate =6%.

4.7 Conclusion

For biomass and biodiesel, the unit costs of electricity from the 20 kWe and 100 kWe CHP-ORCs were cheaper than those of the basic ORCs. It was found that with the palm fruit bunch as the energy source, the UCEs for the 20 kWe and 100 kWe CHP-ORCs were 2.91Baht/kWh and 2.73 Baht/kWh, respectively. At capital cost of biodiesel of 5 Baht/liter, the UCEs for the 20 kWe and 100 kWe CHP-ORCs were 5.92 Baht/kWh and 5.74 Baht/kWh, respectively.

The sensitivities on the UCE which were palm fruit bunch unit cost, operating hour and real debt interest rate on the UCE were considered. The results showed that the palm fruit bunch unit cost and the real debt interest gave the most and least effects on the UCE.

For biodiesel, the sensitivities on the UCE which were biodiesel capital cost, operating hour and real debt interest rate on the UCE were considered. It was found that the biodiesel capital cost gave the most sensitivity on the UCE.

CHAPTER 5

THERMOECONOMIC ANALYSIS OF A MODULAR ORGANIC RANKINE CYCLE WITH HYBRID SOLAR COLLECTORS/BIOFUELS AS HEAT SOURCE

In this chapter, thermoeconomic analysis of a modular organic Rankine cycle with evacuated-tube solar collectors and bioenergy as heat source for power generation was presented. The ambient temperature and solar radiation data of Chiang Mai, Thailand were taken as the calculation inputs. Furthermore, CO_2 emission of an ORC with hybrid solar and biofuels was also investigated.

5.1 Organic Rankine Cycle with Hybrid Solar Collectors/Biofuels

Figure 5.1 shows a schematic diagram of an ORC which consists of a set of solar collectors with water storage and a biofuel combustion chamber. There was a water closed loop to extract heat from solar thermal system and the heat was transferred to the ORC evaporator (process 2-3). If the heat rate and the hot water temperature are not high enough the auxiliary heat will be generated from biodiesel or biomass combustion in the combustion chamber.

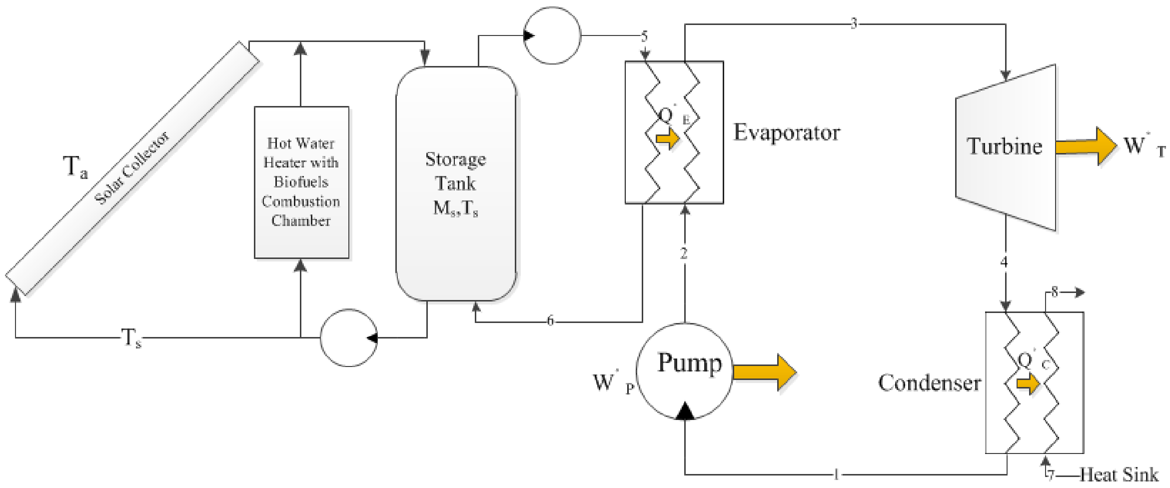

Figure 5.1 Organic Rankine cycle with solar collectors with biofuels as auxiliary heat.

For the ORC cycle, the working fluid left the condenser as saturated liquid (state 1) and it was pumped suppli es to the evaporator (state 2) where it was heated and left the evaporator as saturated vapor at high pressure (state 3). The fluid expanded through the turbine to generate electrical power and entered the condenser (state 4). After heat rejection to a heat sink, the condensed working fluid was at state 1 and the new cycle restarted. All the described processes were shown in a T-s diagram in Figure 5.2.

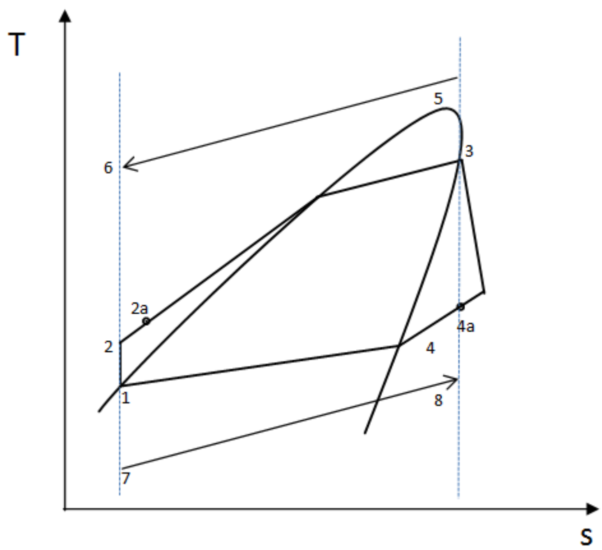

Figure 5.2 T-s diagram of ORC

For simplicity in the analysis, the pressure drops in the evaporator, the condenser, the solar collector, the heat exchanger and the piping system, were ignored. The energy equations of the all components were summarized in eqn. (2.1)-(2.6).

For evacuated-tube solar collector, the useful heat rate from the solar collector could be calculated from

$$\dot{Q}_{coll} = A_c F_R \left[I_T(\tau\alpha) - U_L(T_{fi} - T_a) \right]. \tag{5.1}$$

In case of collector connected in series, the values of $F_R(\tau\alpha)$ and $F_R U_L$ could be developed. Oonk et al. 1979 have shown in equations following:

$$F_R(\tau\alpha) = F_{R1}(\tau\alpha)_1 \left[\frac{1-(1-K)^N}{NK} \right] \tag{5.2}$$

$$F_R U_L = F_{R1} U_{L_1} \left[\frac{1-(1-K)^N}{NK} \right]. \tag{5.3}$$

where $K = \frac{A_1 F_{R1} U_{L_1}}{\dot{m} C_p}$ and N is the number of the solar collector units in series connection.

The suffix 1 refers to the values quoted from the tested data of the solar collector

The model for evaluating the temperature of water in the thermal energy storage was applied from lump model by considering the storage be non-stratified. With finite difference method, the temperature of water in the thermal energy storage could be evaluated from

$$T_s^{t+\Delta t} = T_s^t + \frac{\Delta t}{M_s C_p} \left(\dot{Q}_{coll} - \dot{Q}_{useful} - \dot{Q}_{loss} \right). \tag{5.4}$$

$$\dot{Q}_{useful} = \dot{m}_W C_p (T_{TL} - T_{FL}), \tag{5.5}$$

$$\dot{Q}_{loss} = UA(T_s - T_a). \tag{5.6}$$

5.2 Conditions for Analysis

In this study, a set of evacuated-tube solar collectors with $F_R(\tau\alpha)$ of 0.81, $F_R U_L$ of 2.551 W/m^2K (Thawonngamyingsakul C., 2013) was used for generating hot water. The power outputs of the system were 20 kWe and 100 kWe. The ORC working fluid was zeotropic working fluid R245fa/R152a at composition 70/30%. The weather data of Chiang Mai was taken as input data of the calculation and the time step (Δt) at 5 min was used for system simulation. The area of the solar collectors was between 100 and 900 m^2. Each row of the solar collector set had 5 units each of 2 m^2 in series connection. The solar collector was tilted at the angle from horizontal plane similar to the latitude of Chiang Mai and south facing. The working hour for power generation was 12 hours between 8.30 AM to 8.30 PM. The overall heat loss coefficient (UA) from the thermal energy storage was 5 W/K (Thawonngamyingsakul., 2013) and the pressure of the thermal energy storage was 5 bar for preventing water boiling in the storage tank.

The conditions for the basic ORC and the CHP-ORC analyses were

1. The total power outputs from the ORC were 20 kWe and 100kWe.
2. The furnace for water heating efficiency from biomass combustion was 70%[European Wood-Heating Technology Survey, 2014].
3. The burner for water heating efficiency from biodiesel combustion was 80%[European Wood-Heating Technology Survey, 2014].
4. The ORC will be operated when the supplied hot water was at 120 ºC.
5. Evaporating temperature of the ORC was 110ºC for 20 kWe and 100 kWe and the ORC condensing temperature was 40ºC.
6. The turbine isentropic efficiency was 0.8.
7. The generator efficiency and the mechanical efficiency at the turbine/generator each was 0.9.
8. 50% of heat loss in the exhaust gas after combustion could be recovered and it was used to generate hot water for other thermal processes. The hot water temperature could be heated up to 80ºC from its inlet temperature at 28ºC in a heat exchanger having an effectiveness $(\boldsymbol{\varepsilon})$ of 0.85.
9. The ORC working fluid was R245fa/R152a at a composition of 70/30% and the properties were based upon REFPROP 2013.

5.3 System Performance

The water in the storage tank was heated up by biomass energy first and the water temperature could reach 120ºC from the initial value of 28ºC. The biomass energy was prolonged till the solar energy was high enough to generate hot water for the ORC then the biomass combustion stopped and the auxiliary heat was carried out again when the solar energy intensity was not available.

Figure 5.3 shows an example of water storage temperature history of the 20 kWe ORC with hybrid solar energy/biomass as heat sources. It could be seen that the temperature generated by solar energy could be over 120ºC when the solar irradiation was rather high around 10:00 AM-01:30 PM. Before and after this period biomass energy was taken to maintain the temperature.

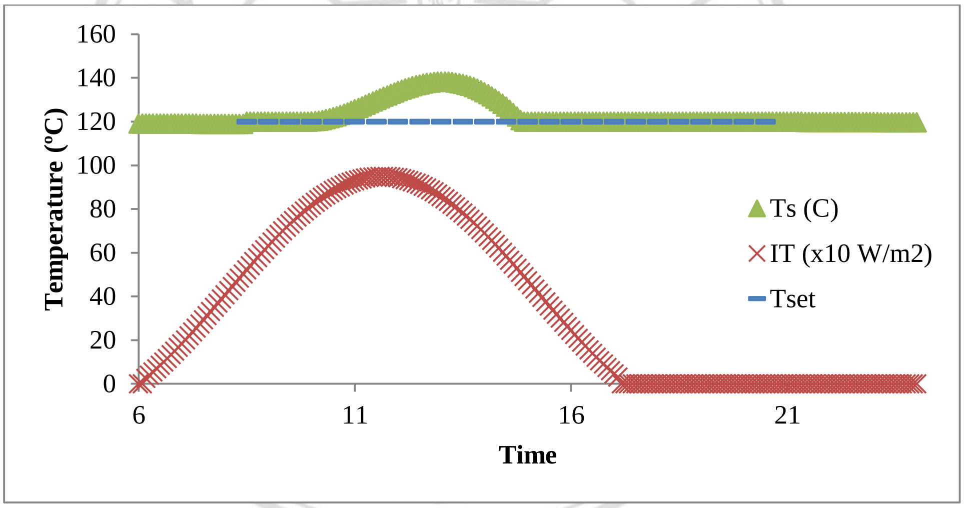

Figure 5.3 The temperature histories of the storage water temperature for 20 kWe ORC with 500m^2 of the solar collectors.

Figure 5.4 shows the energy supplies from solar energy and biomass (palm fruit bunch) energy in each month for the 20 kWe ORC with 200 m^2 and 700 m^2 solar collector areas. Higher the solar collector area resulted in lower the heat input from the biomass. It could be noted that high fraction of heat input from solar energy could be obtained during the 3rd – 4th months due to high solar energy intensity. Figure 5.5 also shows the annual solar fraction for the 20 kWe ORC of which the value was increased with the increment of the solar collector area.

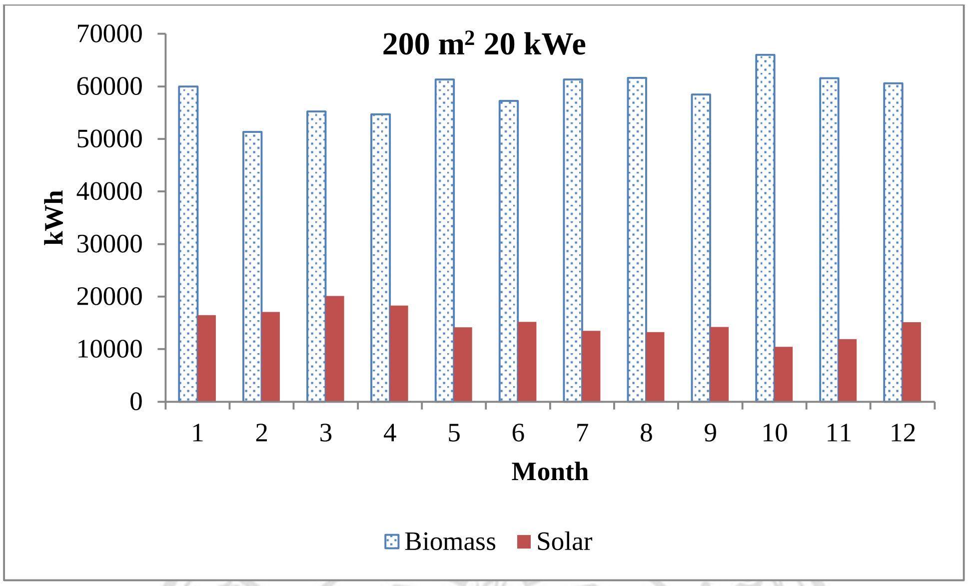

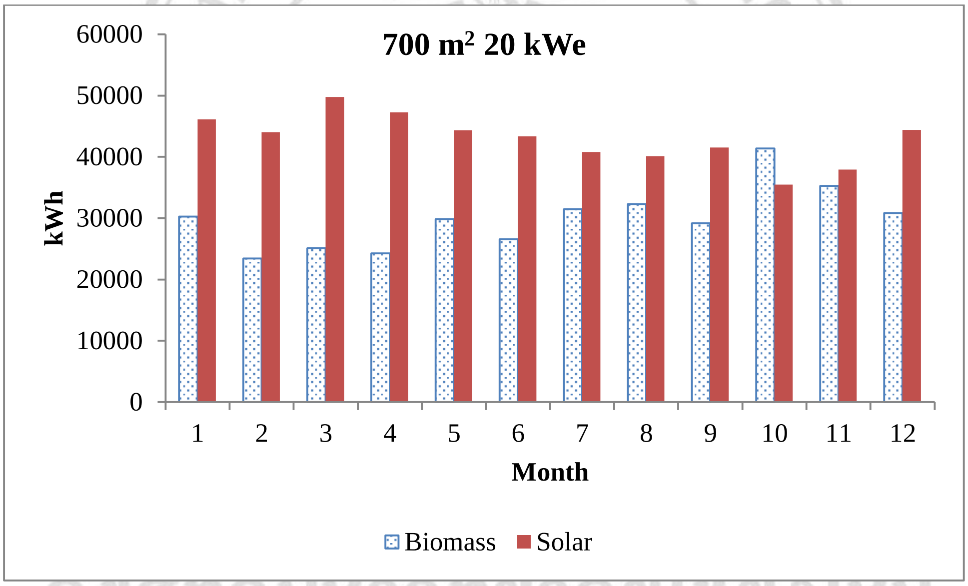

Figure 5.4 The supplied heat inputs from solar energy and biomass energy in each month for the 20 kWe ORC with 200 and 700 m^2 of solar collector areas.

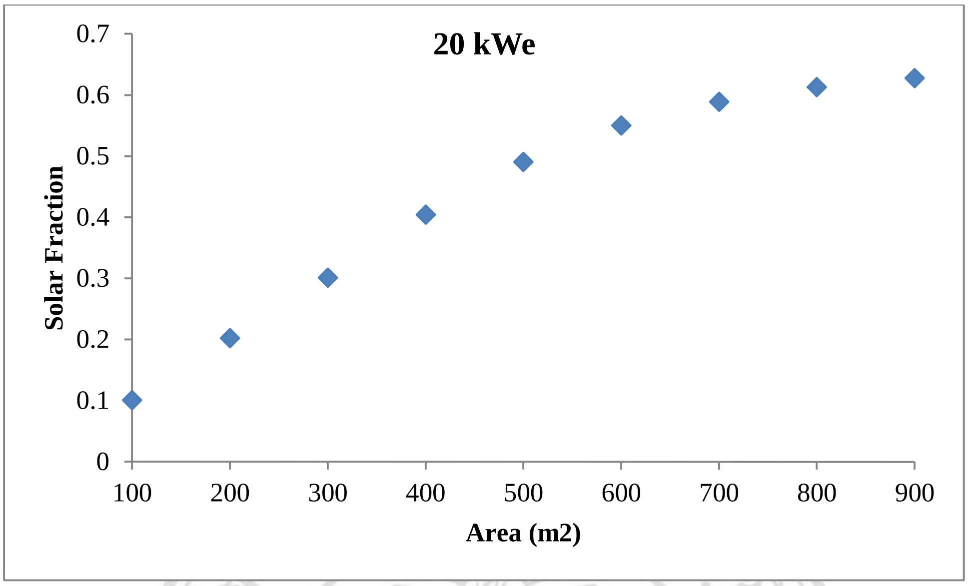

Figure 5.5 The annual solar fraction of the 20 kWe ORC with various solar collector areas.

The results for the 100 kWe ORC were similarly to those of the 20 kWe ORC as shown in Figures 5.6-5.7. Anyhow the solar fraction was less than that of the previous case.

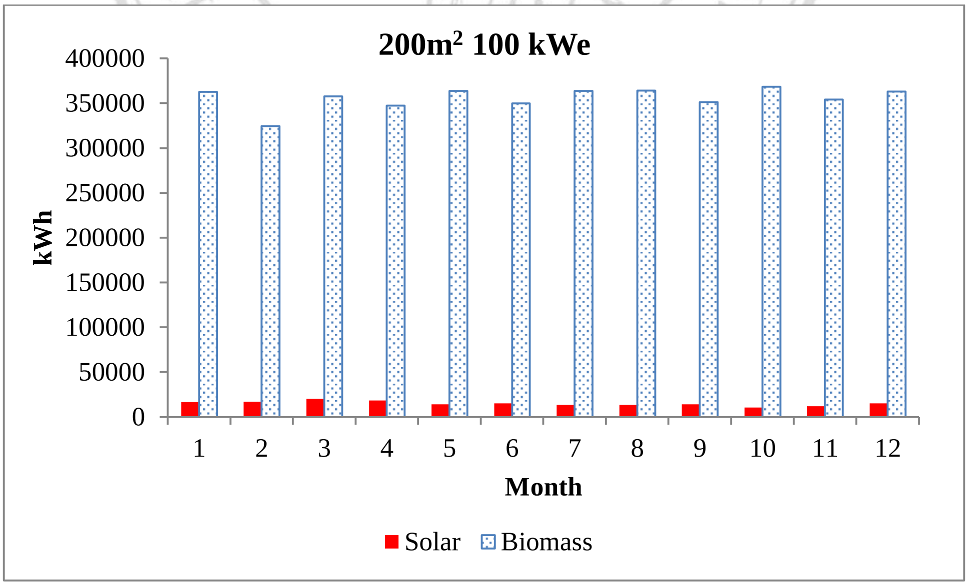

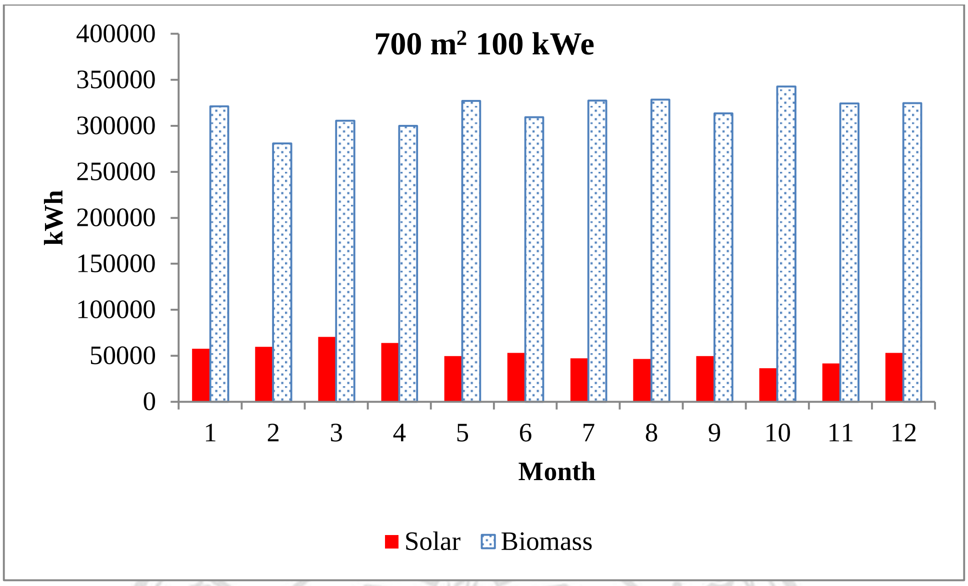

Figure 5.6 The supplied heat inputs from solar energy and biomass energy in each month for the 100 kWe ORC with 200 and 700 m^2 of solar collector areas.

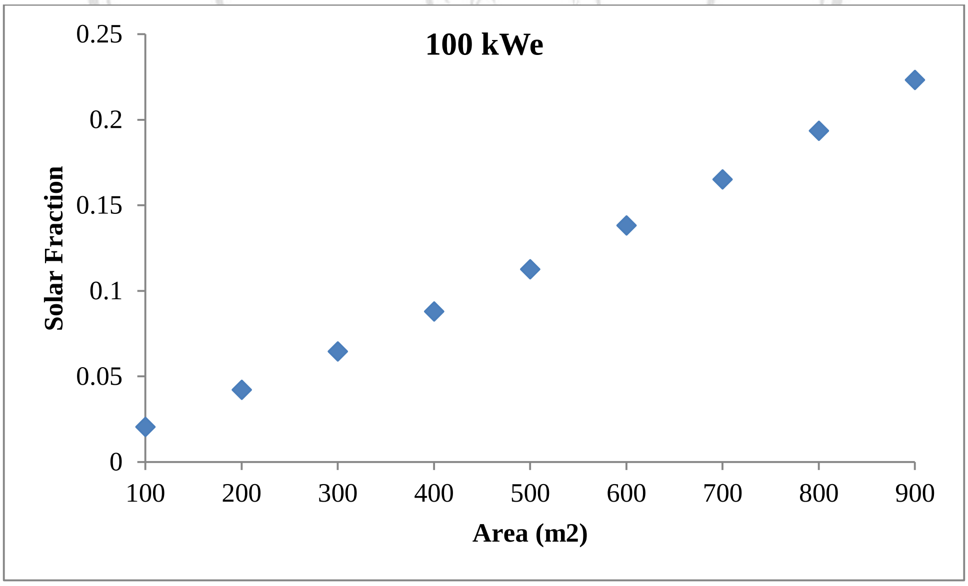

Figure 5.7 The annual solar fraction of the 100 kWe ORC with various solar collector areas.

5.4 Thermoeconomic Analysis

In this part, the thermoeconomic analyses of 20 and 100 kWe basic ORC and CHP-ORC with hybrid solar energy/ biofuel as heat source were carried out. The ORC working fluid was R245fa/R152a at a composition of 70/30%. The cost data information for the calculations were given in Tables 5.1 and 5.2.

Table 5.1 Cost data used for the thermoeconomic analysis of CHP-ORC for solar collectors and biomass as heat source.

Investment cost for ORC		
	20 kWe	**100 kWe**
ORC power plant (Baht/unit) [1]	1,500,000	4,000,000
Biomass Furnace and heat exchanger [1] (Baht/unit)	200,000	2,700,000
Thermal Storage (Baht/Unit) [1]	70,000	70,000
Heat Exchanger for exhaust gas from biomass (Baht/unit) [1]	50,000	100,000
Land for ORC and feedstock storage (m^2) [2]	80	160
Evacuated-tube solar collectors (Baht/m^2) [1]	5,000	
Operating & Maintenance (O&M) cost		
Operating & maintenance equipment cost (% of investment cost per year) [3]	1	
Palm Fruit bunch (Baht/ton) [4]	514	
Financial parameters		
Real debt interest rate, i_d (%)[5]	6	
Salvage value (% of investment cost)	10	
Depreciation period, (year)	20	

*Investment cost for land was 1250 Baht/m^2

Table 5.2 Cost data used for the thermoeconomic analysis of CHP-ORC for solar collectors and biodiesel as heat source.

Investment cost for ORC		
	20 kWe	**100 kWe**
ORC power plant (Baht/unit) [1]	1,500,000	4,000,000
Biodiesel burner and heat exchanger (Baht/unit) [1]	200,000	2,700,000
Heat Exchanger for exhaust gas from biodiesel (Baht/unit) [1]	50,000	100,000
Thermal Storage (Baht/Unit) [1]	70,000	70,000
Land for ORC and feedstock storage (m^2) [2]	40	80
Evacuated-tube solar collectors (Baht/m^2) [1]	5,000	
Operating & Maintenance (O&M) cost		
Operating & maintenance equipment cost (% of investment cost per year) [3]	1	
Biodiesel (Baht/liter) [6]	5	
Financial parameters		
Real debt interest rate, i_d (%)[5]	6	
Salvage value (% of investment cost)	10	
Depreciation period, (year)	20	

*Investment cost for land was 1250 Baht/m^2

[1] Market cost

[2] Treasury Department, 2015

[3] Thawonngamyingsakul, 2013

[4] Biomass Price, 2013

[5] Karellas et al., 2011

The unit cost of electricity from palm fruit bunch and biodiesel versus collector area were shown in Figures 5.8 and 5.9. It was found that the UCEs increased with the increase of the collector area and the UCE from palm fruit bunch was lower than that of the biodiesel. For biomass, the UCEs of basic ORC at 20 and 100 kWe from palm fruit bunch were found in a range of 4.38 to 6.54 Baht/kWh and in a range of 3.86 to 4.39 Baht/kWh for solar collector area between 100 and 900 m^2, respectively, the UCEs of CHP-ORC 20 and 100 kWe were found in a range of 3.74 to 4.84 Baht/kWh and in a range of 2.93 to 3.17 Baht/kWh for solar collector area between 100 and 900 m^2, respectively.

For biodiesel at capital cost of biodiesel as 5 Baht/liter (Assume feedstock), the UCEs of basic ORC 20 and 100 kWe were found in a range of 8.39 to 10.19 Baht/kWh and in a range of 7.97 to 8.34 Baht/kWh for solar collector area between 100 and 900 m^2, respectively, the UCEs of CHP-ORC 20 and 100 kWe were found in a range of 6.40 to 7.93 Baht/kWh and in a range of 6.07 to 6.35 Baht/kWh for solar collector area between 100 and 900 m^2, respectively.

It could be noted that the UCE from the CHP-ORC was lower than that of the basic ORC. Use of biodiesel was still more expensive than that of biomass fuel. The hybrid energy also gave higher UCE than the biofuel energy.

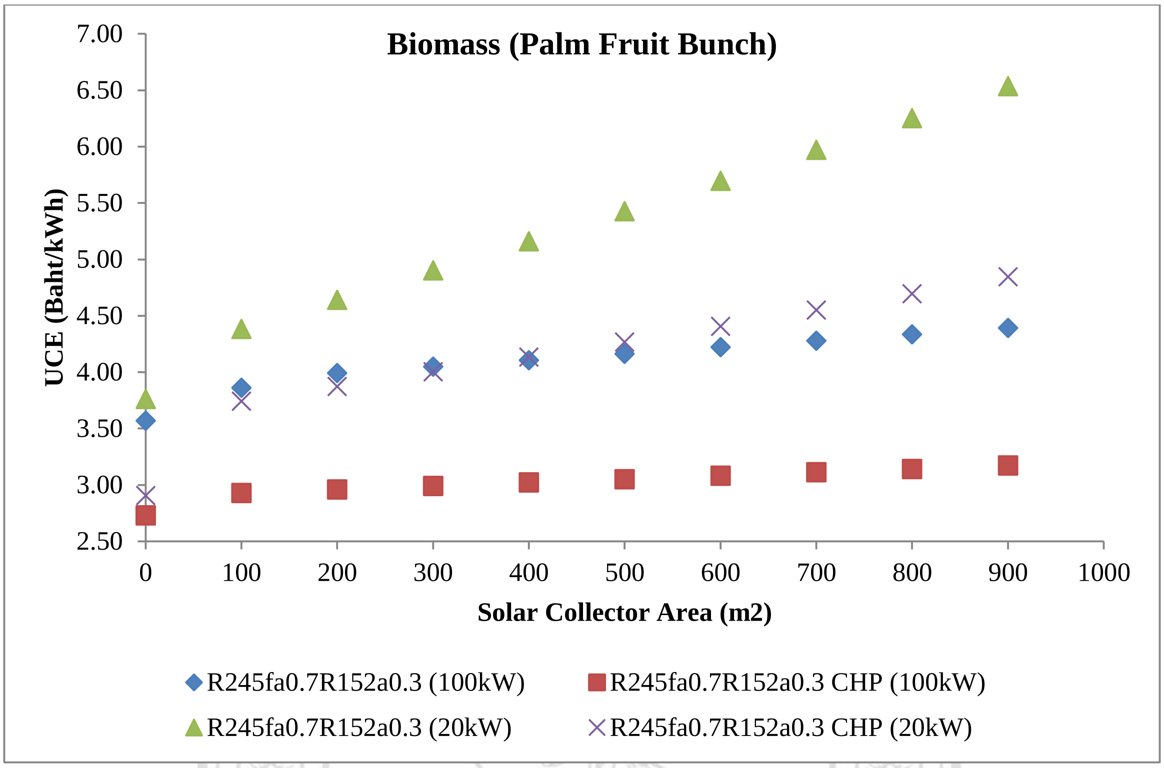

Figure 5.8 UCEs from palm fruit bunch at operating hour of 12hr/day, id=6% for the basic ORCs and the CHP-ORCs at 20kWe and 100 kWe versus solar collector area.

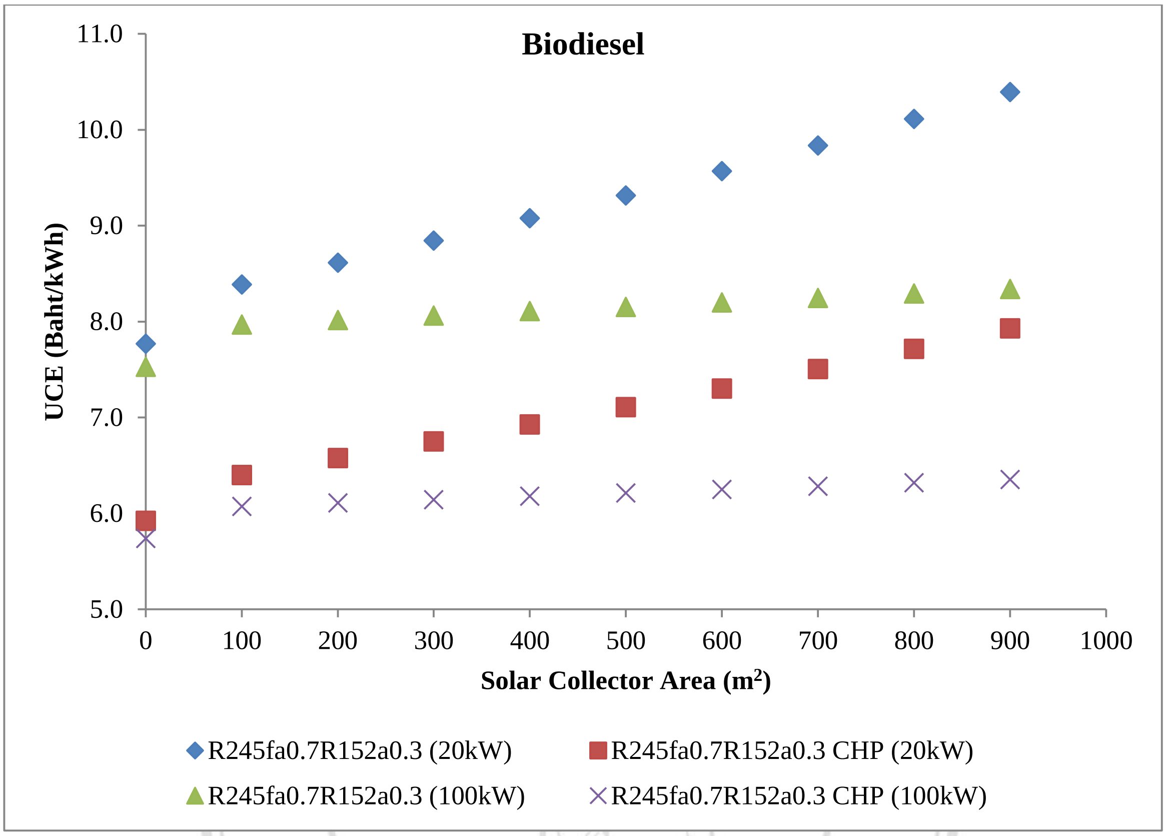

Figure 5.9 UCEs from biodiesel at operating hour of 12hr/day, id=6% for the basic ORCs and the CHP-ORCs at 20kWe and 100 kWe versus solar collector area.

5.5 CO_2 Emission of Hybrid Power Plant

To consider the CO_2 emission of the ORCs with hybrid solar and biofuel energy, from Thailand Greenhouse Gas Management Organization 2015, the carbon emission factors from biomass and biodiesel for boiler combustion were 0.693 $kgCO_2e/kg$ and 1.0634 $kgCO_2e/kg$, respectively. With palm fruit bunch for ORCs of 20 and 100 kWe, it was found that the CO_2 emission was decreased with the increasing of solar collector area due to very low emission during operation from solar energy system. The CO_2 emission was found to be in ranges of 3.96 to 1.44 $kgCO_2e/kWh$ and 2.72 to 1.90 $kgCO_2e/kWh$, respectively. Example of calculation was shown in Appendix B.

With biodiesel for ORCs of 20 and 100 kWe, the trends of the CO_2 emission were similar to the previous case. The emissions were in ranges of 1.36 to 0.50 $kgCO_2e/kWh$ and 1.36 to 1.11 $kgCO_2e/kWh$, respectively. All the results were shown in Figure 5.10.

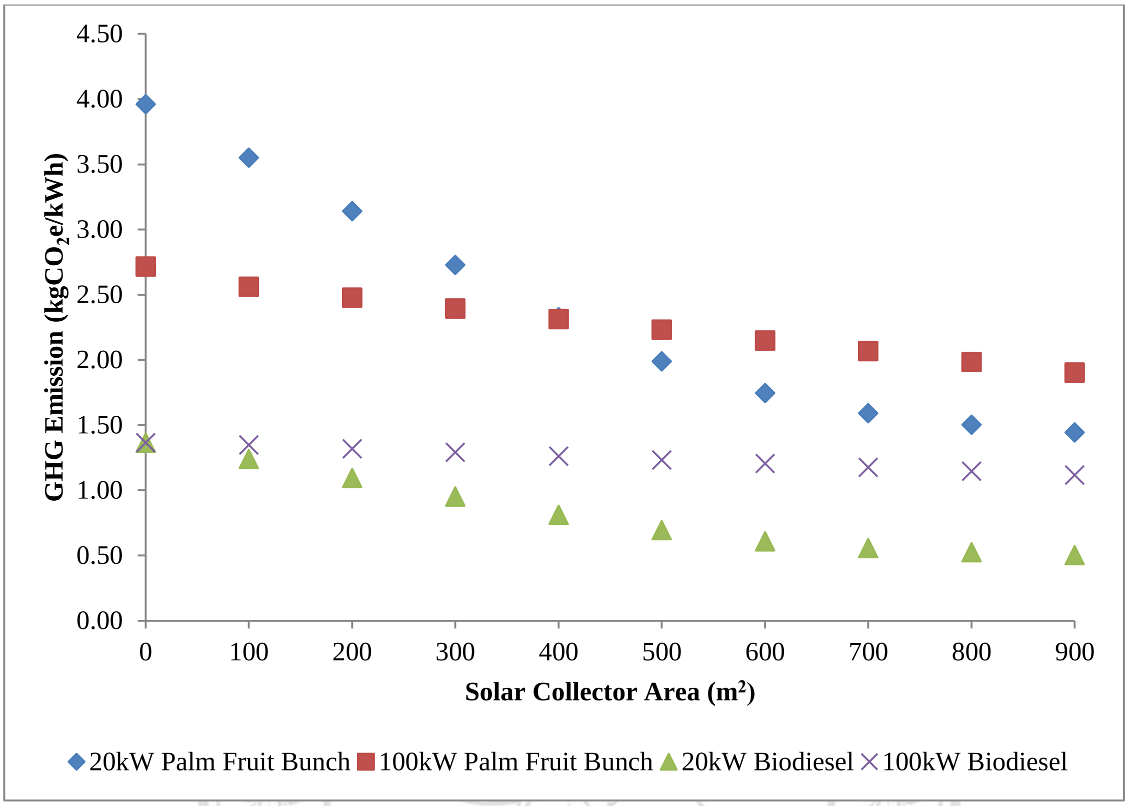

Figure 5.10 CO_2 emissions for 20 kWe and 100 kWe ORCs with hybrid solar and biofuel energy at various solar collector areas.

Figure 5.11 shows the UCE for CHP-ORC when external cost on GHG emission was included. The external cost was taken from marginal abatement cost of biofuel combustion in boiler for Thailand [Chamsilpa, 2015] which was 0.69 Baht/kWh.

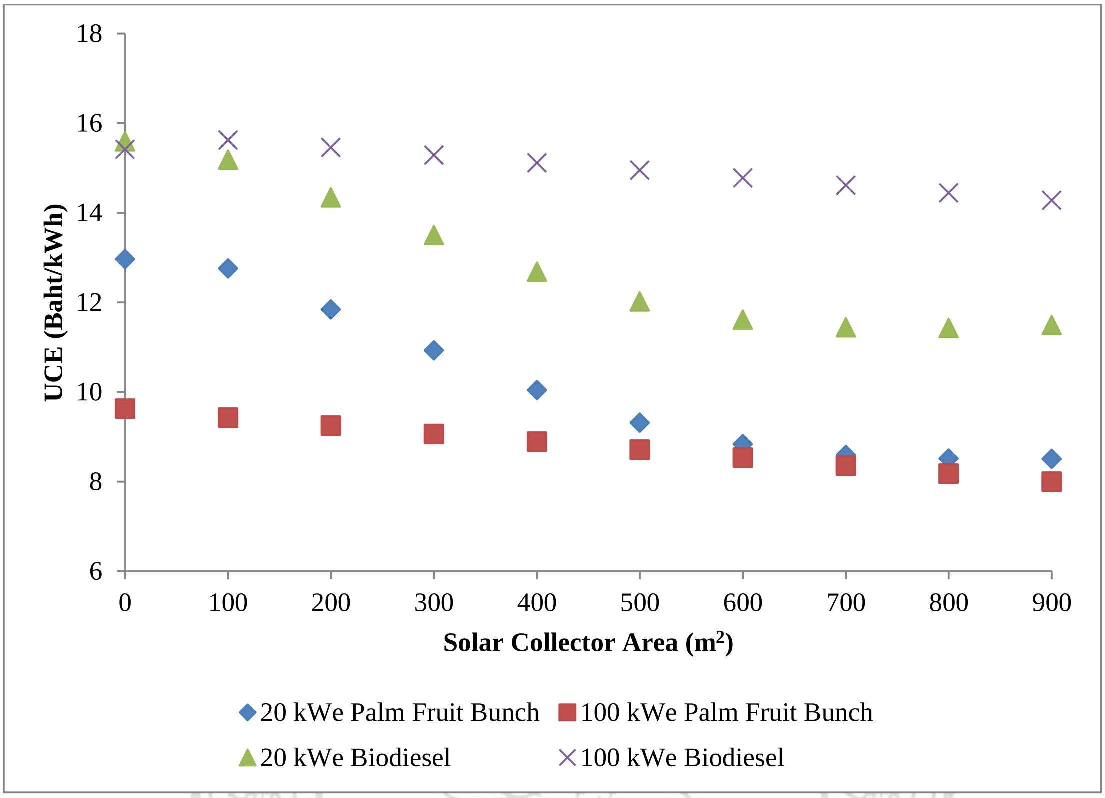

Figure 5.11 The UCE for 20 and 100 kWe CHP-ORC with hybrid solar and biofuel energy at various solar collector areas include with the external cost of GHG emission.

In Figure 5.12, for hybrid solar and biodiesel, when the biodiesel capital cost was at 20 Baht/liter (market price), it could be found that the hybrid energy could be more advantage that that of biodiesel only. The UCE of CHP ORC for 20 kWe which included the external cost of GHG emission was found to be lowest at 26.58 Baht/kWh for 800 m^2 solar collector areas, compare to those of biodiesel only, which was 31.53 Baht/kWh. But when the solar collector area was over 800m^2, the UCE tended to increase slightly due to the higher cost of the solar system with the nearly constant biodiesel consumption.

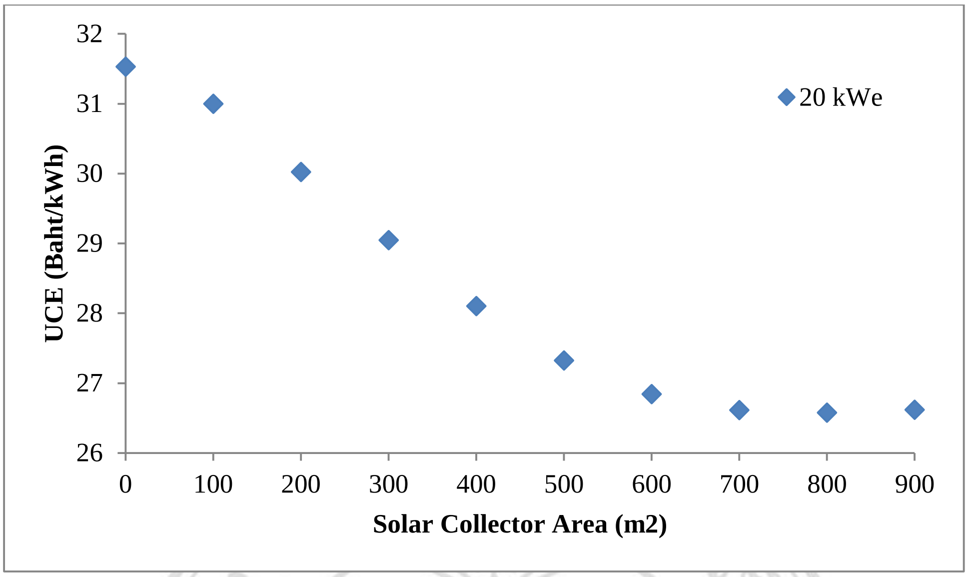

Figure 5.12 The UCE for 20 kWe CHP-ORC with hybrid solar and biodiesel (Capital cost 20 Baht/liter) at various solar collector areas include with the external cost of GHG emission.

In Figure 5.13, The UCE including external cost of GHG emission of 100 kWe CHP ORC for hybrid solar and biodiesel compared to those of biodiesel only which was 31.15 Baht/kWh and when solar collector areas over 300 m^2. The value was lower than that of the biodiesel only at 31.35 Baht/kWh. After this condition the UCE decreased with the solar collector area.

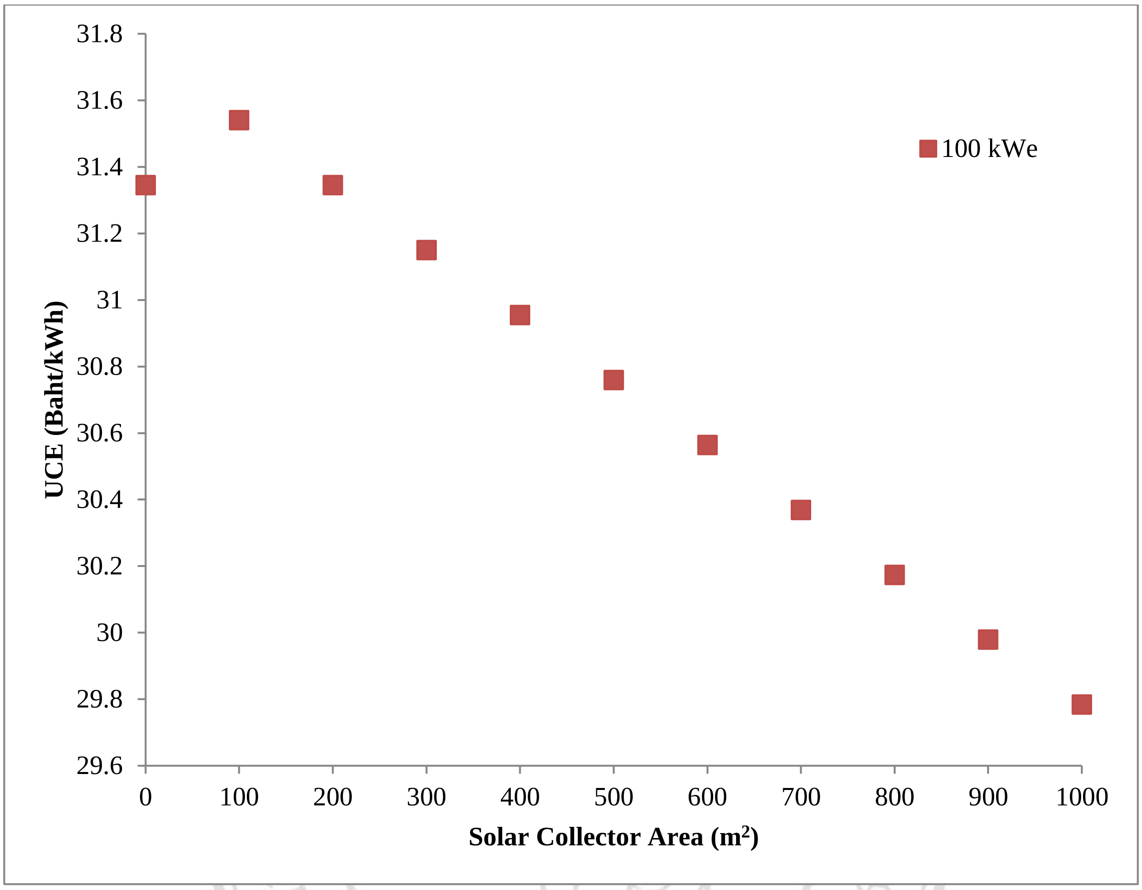

Figure 5.13 The UCE for 100 kWe CHP-ORC with hybrid solar and biodiesel (Capital cost 20 Baht/liter) at various solar collector areas include with the external cost of GHG emission.

5.6 Conclusion

The conclusions in this chapter are as follows:

1. The unit cost of electricity from hybrid solar collector area between 100 and 900 m^2 with biofuels, for biomass, the UCEs of basic ORC at 20 and 100 kWe from palm fruit bunch were found to be in a range of 4.38 to 6.54 Baht/kWh and in a range of 3.86 to 4.39 Baht/kWh for solar collector area between 100 and 900 m^2, respectively. The UCEs of 20 and 100 kWe CHP-ORCs were found to be in ranges of 3.74 to 4.84 Baht/kWh and 2.93 to 3.17 Baht/kWh, respectively.

For biodiesel cost at 5 Baht/liter (free feedstock assumption), the UCEs of basic ORC at 20 and 100 kWe were found to be in ranges of 8.39 to 10.19 Baht/kWh and 7.97 to 8.34 Baht/kWh for solar collector area between 100 and 900 m^2, respectively. The

UCEs of CHP-ORC at 20 and 100 kWe were found to be in ranges of 6.40 to 7.93 Baht/kWh and 6.07 to 6.35 Baht/kWh for solar collector area between 100 and 900 m^2, respectively.

2. The CO_2 emission of hybrid power plant with palm fruit bunch for CHP-ORCs of 20 and 100 kWe was decreased with the increase of solar collector area and the CO_2 emissions were found to be in ranges of 3.96 to 1.44 $kgCO_2e/kWh$ and 2.72 to 1.90 $kgCO_2e/kWh$, respectively. For biodiesel, the values were found to be in ranges of 1.36 to 0.50 $kgCO_2e/kWh$ and 1.36 to 1.11$kgCO_2e/kWh$, respectively.

3. For hybrid solar and biodiesel, when the biodiesel cost was at 20 Baht/liter (market price), the UCE of CHP ORC for 20 kWe including the external cost of GHG emission was found to be less with the increase of the solar collector area. The value was lowest at 26.58 Baht/kWh for 800 m^2 solar collector areas, compare to that of biodiesel only, which was 31.53 Baht/kWh. But when the solar collector area was over 800m^2, the UCE tended to increase slightly due to the higher cost of the solar system with the nearly constant biodiesel consumption.

CHAPTER 6

CONCLUSIONS

In this research, thermoeconomic analyses of a modular basic and CHP organic Rankine cycle with hybrid solar collectors/biofuels energy as heat source for power generation were presented. A dimensionless term called "Figure of Merit" for predicting cycle efficiency and suitable zeotropic working fluid were proposed. The unit cost of electricity and CO_2 emission compared between basic ORC and CHP-ORC with hybrid solar collectors/biofuels energy was also considered. The conclusions of the results were as follows:

6.1 Parametric Analysis on Modular Organic Rankine Cycle Performance

A dimensionless term, the "Figure of Merit" (FOM) was proposed, to investigate the thermal performance of a low temperature, organic Rankine cycle using six zeotropic mixtures (R245fa/R152a, R245fa/R227ea, R245fa/R236ea, R245ca/R152a, R245ca/R227ea and R245ca/R236ea) as working fluids. An empirical correlation was developed to estimate the cycle efficiency from the FOM for all working fluids at condensing temperatures of 25-40ºC and evaporating temperatures of 80-130ºC. The model results fit very well with both the experimental data and that from other researchers.

6.2 Thermoeconomic Analysis of a Modular Organic Rankine Cycle with Biofuels as Heat Source

For biomass and biodiesel, the unit costs of electricity for 20 kWe and 100 kWe CHP-ORCs were cheaper than those of the basic ORCs. With the palm fruit bunch as the energy source, the UCEs for the 20 kWe and 100 kWe CHP-ORCs were 2.91 Baht/kWh and 2.73 Baht/kWh, respectively. At biodiesel cost of 5 Baht/liter, the UCEs for the 20 kWe and 100 kWe CHP-ORCs were 5.92 Baht/kWh and 5.74 Baht/kWh, respectively.

The sensitivities on the UCE which cover palm fruit bunch unit cost, operating hour and real debt interest rate on the UCE were considered. The results showed that the palm fruit bunch unit cost and the real debt interest gave the most and the least effects on the UCE.

For biodiesel, the sensitivities on the UCE were biodiesel cost, operating hour and real debt interest rate on the UCE. It was found that the biodiesel cost gave the most sensitivity on the UCE.

6.3 Thermoeconomic Analysis of a Modular Organic Rankine Cycle with Hybrid Solar Collectors/Biofuels as Heat Source

Thermoeconomic analysis of a modular organic Rankine cycle with evacuated-tube solar collectors and bioenergy as heat source for power generation under the Chiang Mai climate was considered. The area of solar collector was between 100 and 900 m^2 and the ORC zeotropic working fluid was R245fa/R152a at composition of 70:30%. The palm fruit bunch and biodiesel were biofuels used in the thermoeconomic analyses. The conclusions of the results were as follows:

6.3.1 Thermoeconomic Analyses of the System

The unit cost of electricity from palm fruit bunch and biodiesel versus collector area between 100 and 900 m^2 was evaluated. For biomass, the UCEs of basic ORC at 20 and 100 kWe from palm fruit bunch were in ranges of 4.38 to 6.54 Baht/kWh and 3.86 to 4.39 Baht/kWh for solar collector area between 100 and 900 m^2, respectively. For 20 and 100 kWe CHP-ORC, the values were in ranges of 3.74 to 4.84 Baht/kWh and 2.93 to 3.17 Baht/kWh, respectively.

For biodiesel cost at 5 Baht/liter (free feedstock assumption), the UCEs of basic ORC 20 and 100 kWe were found in ranges of 8.39 to 10.19 Baht/kWh and 7.97 to 8.34 Baht/kWh for solar collector area between 100 and 900 m^2, respectively. In case of 20 and 100 kWe CHP-ORCs, the values were in ranges of 6.40 to 7.93 Baht/kWh and 6.07 to 6.35 Baht/kWh for solar collector area between 100 and 900 m^2, respectively.

6.3.2 CO_2 Emission of a Modular Organic Rankine Cycle with Hybrid Solar Collectors/Biofuels as Heat Source.

The CO_2 emissions of hybrid power plant with palm fruit bunch for 20 and 100 kWe CHP-ORCs were decreased with the increase of solar collector area and the CO_2 emissions were found to be in ranges of 3.96 to 1.44 $kgCO_2e$/kWh and 2.72 to 1.90 $kgCO_2e$/kWh, respectively. With biodiesel, the values were in ranges of 1.36 to 0.50 $kgCO_2e$/kWh and 1.36 to 1.11 $kgCO_2e$/kWh, respectively.

When biodiesel cost was at 20 Baht/liter (market price), the UCEs including the GHG external cost for 20 and 100 kWe CHP-ORCs, were decreased with the increase of solar collector area. The lowest UCE values for 20 kWe and 100 kWe were 26.58 Baht/kWh at 800 m^2 and 31.35 Baht/kWh at 300 m^2 of solar collectors, respectively.

6.4 Recommendation for Future Works

The long term experiment of a modular organic Rankine cycle with hybrid solar collectors/biofuels as heat source under real practice should be carried out to compare the data with the simulation results. The exhaust gas from biofuel combustion could be used to generate hot water for other process or preheat water in thermal storage before entering evaporator in the ORC to improving the cycle efficiency.

In addition, the ORC could recover heat from exhaust gas of a gas heat engine such as that in biogas or landfill gas power plants to generate secondary power thus the overall efficiency of these power plants could be improved.

REFERENCE

[Biomass Price, 2013] Energy for Environment Foundation, "Biomass Price", [online]. Available: http://www.efe.or.th/efe-book.php?task=25 [December,2013]

[Chamsilpa, 2015] Chamsilpa M., Wiriyatangsakul S., Panichayapichet P., Kittisompun B. and Lohsomboon P. "Economics analysis of power generation technology for greenhouse gas mitigation" Engineering J. CMU., Vol.22, 2015, pp. 98-106.

[Chys, 2012] Chys M., van den Broek M., Vanslambrouck B., De Paepe M. "Potential of zeotropic mixtures as working fluids in organic Rankine cycles". Energy, Vol.44, 2012, pp. 623–32.

[Department of Alternative Energy Development and Efficiency, 2013] Department of Alternative Energy Development and Efficiency, Alternative Energy Development Plan: AEDP 2012-2021 2013, http://www.dede.go.th/dede/images/stories/aedp25.pdf.

[Dong, 2014] Dong, B., Xu G., Cai Y. and Li H. "Analysis of zeotropic mixtures used in high-temperature Organic Rankine cycle". Energy Conversion & Management, Vol. 84, 2014, pp. 253-260.

[Donghong, 2006] Donghong, W., Xuesheng , L., Zhen, L., and Jianming, G., "Performance analysis and optimization of organic Rankine cycle (ORC) for waste heat recovery", Energy Conversion & Management, Vol. 48, 2007, pp. 1113-1119.

[Drescher, 2007] Drescher U. and Bruggemann D. "Fluid selection for the Organic Rankine Cycle (ORC) in biomass power and heat plants", Applied Thermal Engineering, Vol. 27, 2007, pp. 223-228.

[Duffie, 1980] Duffie, J.A., Beckman, W.A. "Solar engineering of thermal processes". New York: John Wiley & Sons, Inc, 1980.

[Energy Policy and Planning Office, 2013] Energy Policy and Planning Office, "Energy Annual Report", 2013.

[European Wood-Heating Technology Survey, 2015] "European Wood-Heating Technology Survey" [online] Available: https://www.nyserda.ny.gov/Publications/Research-and-Development-Technical-Reports/Other-Technical-Reports/European-Wood-Heating-Technology-Survey.aspx [August, 25, 2015].

[Heberle, 2012] Heberle F., Preißinger M., Brüggemann D. "Zeotropic mixtures as working fluids in organic Rankine cycles for low-enthalpy geothermal resources". Renewable Energy, Vol.37: 2012, pp. 364–70.

[Hettiarachchi, 2007] Hettiarachchi, M., Golubovic, M., Worek,W.M. and Ikegami, Y., "Optimum design criteria for an Organic Rankine cycle using low-temperature geothermal heat sources", Energy, Vol. 32, 2007, pp. 1698-1706.

[Hung, 1997] Hung T.C., Shai T.Y., Wang S.K. "A review of organic Rankine cycles (ORCs) for the recovery of low-grade waste heat". Energy, Vol. 22, 1997, pp. 661–7.

[IEA, 2003] International Energy Agency Report, Renewables for power generation, 2003

[IPCC, 2006] IPCC Guidelines for National Greenhouse Gas Inventories (2006)

[Karellas, 2011] Karellas, S., Terzis, K., Manolakos, D. "Investigation of an autonomous hybrid solar thermal ORC-PV RO desalination system. The Chalki island case". Renewable Energy, Vol.36, 2011, pp. 583-590.

[Kuo, 2009] Kuo C. R., Hsu S. W., Chang K. H., Wang C. C. "Analysis of a 50 kW organic Rankine cycle system", Energy, Vol. 36, 2011, pp. 5877-5885.

[Li, 2011] Li W., Feng X., Yu L.J., Xu J. "Effects of evaporating temperature and internal heat exchanger on organic Rankine cycle", Applied Thermal Engineering, Vol.31, 2011, pp. 4014–23.

[Li, 2014] Li Y.R., Du M.T., Wu C.M., Wu S.Y., Liu C. "Potential of organic Rankine cycle using zeotropic mixtures as working fluids for waste heat recovery", Energy, Vol.77, 2014, pp. 509-519

[Mago, 2008] Mago P. J., Chamra L. M., Srinivasan K., Somayaji C. "An examination of regenerative organic Rankine cycles using dry fluids", Applied Thermal Engineering, Vol. 28, 2008, pp. 998-1007.

[Maizza, 2001] Maizza, V. and Maizza , "Unconventional working fluids in organic Rankine-cycles for waste energy recovery systems", Applied Thermal Engineering, Vol. 21, 2001, pp. 381-390.

[Marion, 2012] Marion, M., Voicu, I. and Tiffonnet, A., "Study and optimization of a solar subcritical organic Rankine cycle", Renewable Energy, Vol. 48, 2012, pp. 100-109.

[Ministry of Energy, 2013] Ministry of Energy, "Online Publication," Historic and projected Thailand energy consumption, 1990-2030, http://www.eppo.go.th/encon/ee-20yrs/EEDP_Thai.pdf.

[Ngammuang, 2015] Ngammuang S., Kiatsiriroat T. "Performance test of agricultural diesel engine using blended fuel of Diesel/ Biodiesel/ Water emulsion", The 8th Thailand Renewable Energy for Community Conference, Bangkok, Thailand, 4-6 Nov 2015.

[Oonk, 1979] Oonk, R., D.E. Jones and Cole-Appel B.E. "Calculation of performance of N collectors in series from test data on a single collector". Solar Energy, Vol.23, 1979, p. 535.

[Pindyck, 2012] Pindyck R.,"The Climate Policy Dilemma," Working paper 10 June 2012.

[Potentials of solar power, 2006] Department of Alternative Energy Development and Efficiency, Ministry of Energy, A research report, 2006, "Potentials of concentrating solar power technologies in Thailand".

[REFPROP, 2013] REFPROP version 9, National Institute of Standard and Technology (NIST), 2013.

[Saleh, 2007] Saleh B., Koglbauer G., Wendland M., Fischer J. "Working Fluids for low-temperature organic Rankine cycles", Energy, Vol.32, 2007, pp. 1210-1221.

[Solar collector, 2014] Solar Panels Plus. Commercial Applications [online]. http://www.solarpanelsplus.com/evacuated-tube-collectors.

[Somayaji, 2006] Somayaji C., Mago, P, Chamra, L.M. "Second law analysis and optimization of organic Rankine cycle". ASME Power Conference, Paper No. PWR 2006-88061, Atlanta, GA 2-4 May 2006.

[Tchanche, 2009] Tchanche B.F., Papadakis G., Lambrinos G.,Frangoudakis A. “Fluid selection for a low-temperature solar organic Rankine cycle”, Applied Thermal Engineering, Vol. 29 , 2009, pp. 2468-2476.

[Thawonngamyingsakul, 2012] Thawonngamyingsakul, C., Kiatsiriroat, T. Potential of solar organic Rankine cycle with evacuated-tube solar collectors as heat source for power generation in Thailand. Energy Science and Technology, Vol.4, 2012, pp. 25-35.

[Thawonngamyingsakul, 2013] Thawonngamyingsakul, C. “Performance Analysis of an organic Rankine cycle with solar collectors and biomass for electricity generation”, 2013. Doctor’s thesis. Chiang Mai University.

[Thermoeconomics, 2005] Moran M.J., Shapiro H.N., Fundamentals of Engineering Thermodynamics, 5th Edition, John Wiley & Sons.

[Treasury Department, 2015] Treasury Department. “Land Price” [online]. Available: http://www.treasury.go.th/download/property_valuation/chiangmai.pdf [2015, August 2]

[Vorayos, 2009] Vorayos, N., Wongsuwan, W. and Kiatsiriroat, T. “Development of solar hot water system in Thailand. Energy. J CMU Vol.16, 2009, pp.55-69.

[Wang, 2009] Wang X.D., Zhao L. “Analysis of zeotropic mixtures used in low-temperature solar Rankine cycles for power generation”. Sol Energy, Vol.83, 2009, pp. 605–13.

[Wang, 2010] Wang J.L., Zhao L., Wang X.D. “A comparative study of pure and zeotropic mixtures in low-temperature solar Rankine cycle”. Applied Energy, Vol. 94, 2012, pp.34–40.

[Wibulswas, 1998] Research and development of solar thermal energy in Thailand. Asean J. Sci. Technol. Develop, Vol.5, 1998, pp. 15-23.

APPENDIX 1

TOTAL AND AVERAGE SOLAR RADIATION ON TILTED SURFACE AND THE AMBIENT TEMPERATURE AT CHIANG MAI

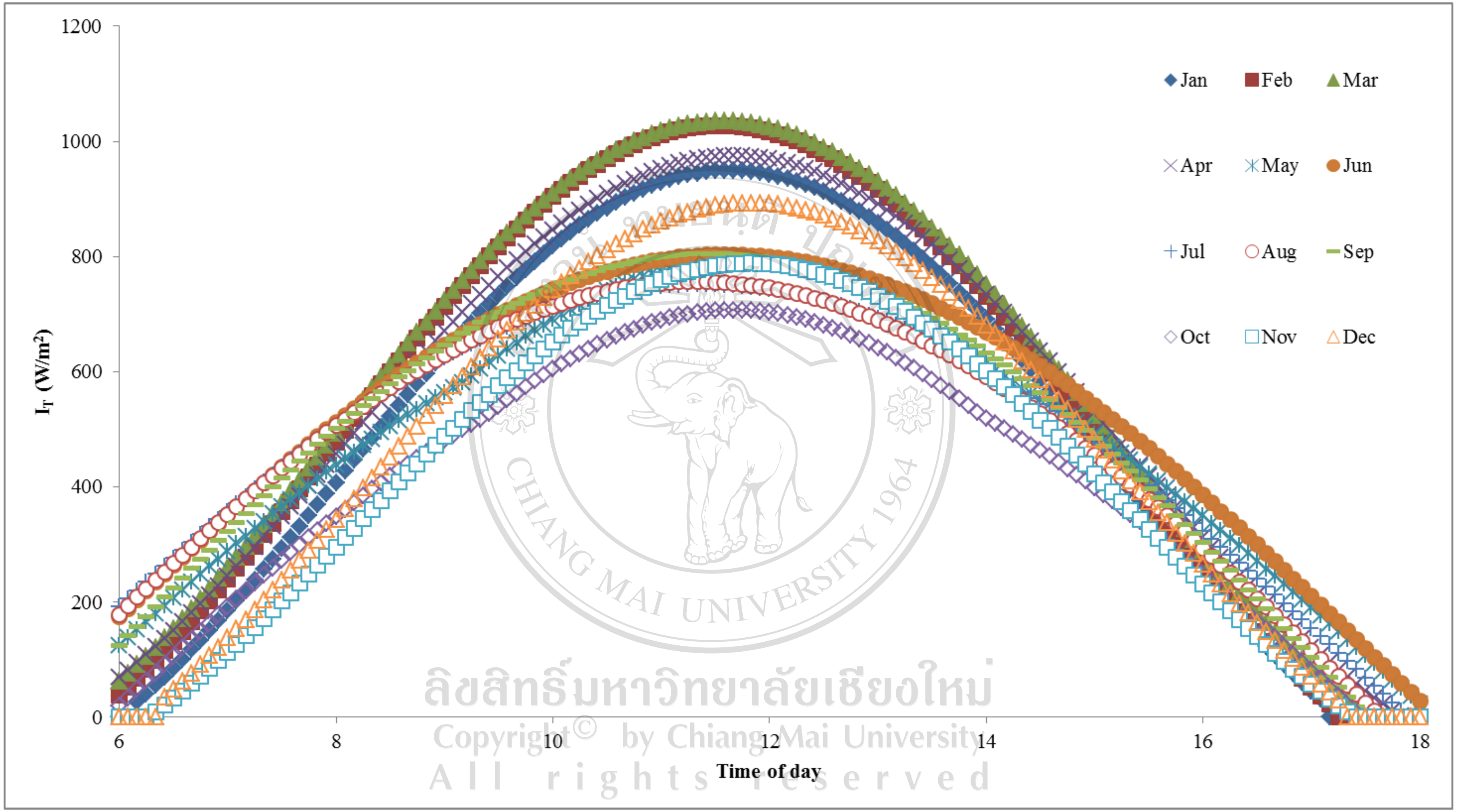

Figure A.1 Total solar radiation on the 18º titled surface at Chiang Mai.

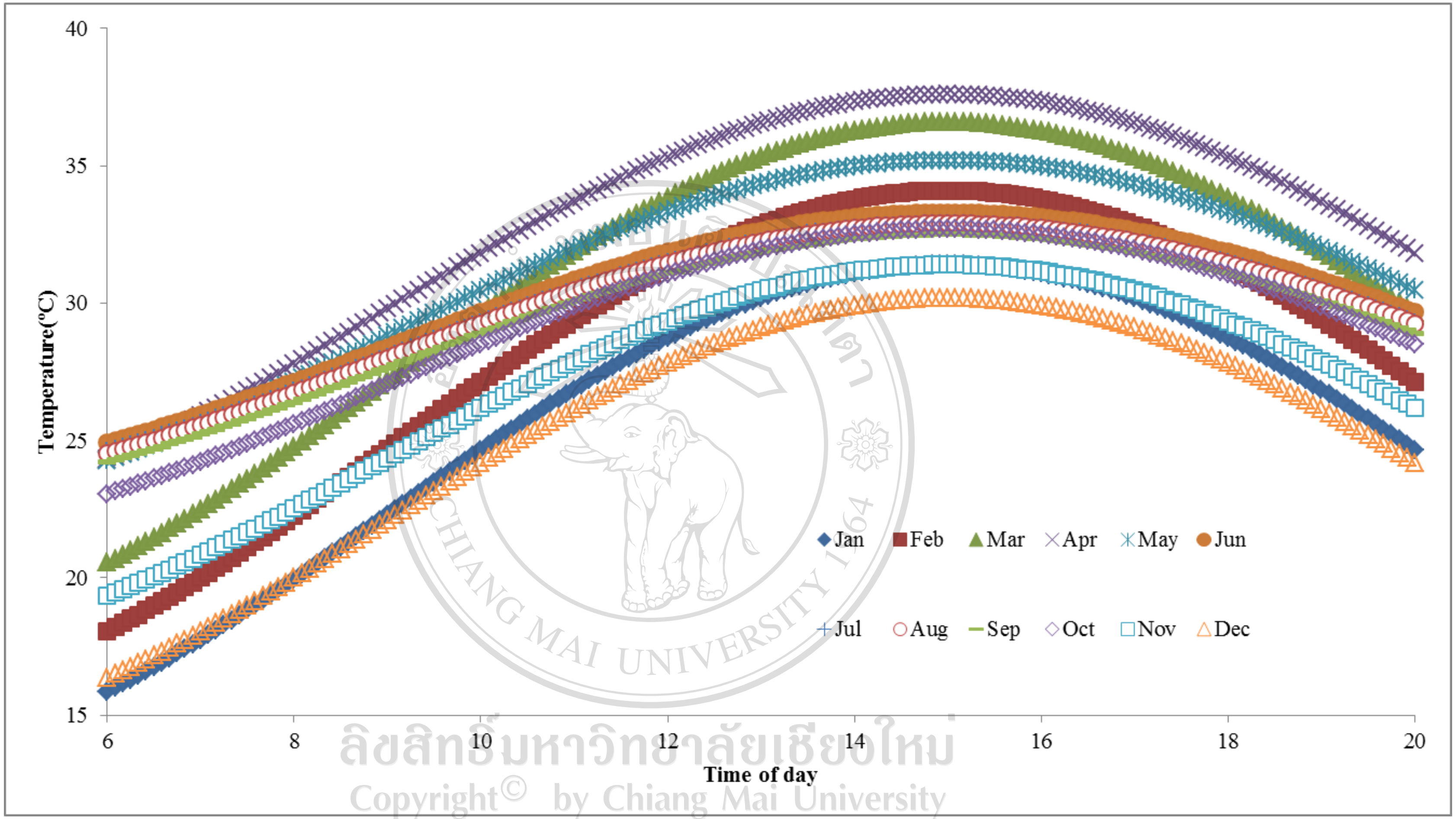

Figure A.2 The ambient temperature at Chiang Mai.

APPENDIX 2

The External Cost of GHG Emission

2.1 The External Cost of GHG Emission

Example: The hybrid solar/biomass ORC 20 kWe @ Solar Collector area 500 m^2 was used Biomass 251,311 kg/year. The external cost of GHG emission per kWh was calculated as follow:

Carbon Emission for biomass = 0.693 $kgCO_2e/kg$

Carbon Emission = 0.693x251,311 $kgCO_2/year$

= 174,158.52 $kgCO_2/year$

ORC 20 kWe, Total electricity generation =87,600 kWh/year

Carbon Emission =174,158.52/87,600 =1.988 $kgCO_2/kWh$

From [Chamsilpa *et al*., 2015]

The external cost of GHG Emission was 0.69 Baht/kWh

High heating value of palm fruit bunch was 9,196 kJ/kg

∴ The external cost of GHG emission per $kgCO_2$

=0.69x9,196/(3600x0.693)

=2.54 Baht/$kgCO_2$

APPENDIX 3

LIST OF PUBLICATIONS

LIST OF PUBLICATIONS

1) Deethayat T., Kiatsiriroat T. and Thawonngamyingsakul C. “Performance analysis of an organic Rankine cycle with internal heat exchanger having zeotropic working fluid,” Case Studies in Thermal Engineering, Vol.6, 2015, pp. 155-161(Indexed by SCOPUS).
2) Deethayat T. and Kiatsiriroat T. “Cost Analysis on Power Generation from Biomass-Fuelled Modular Organic Rankine Cycle Power Plant,” Engineering J. CMU, Vol.21, 2014, pp.84-93(Indexed by TCI).
3) Deethayat T. and Kiatsiriroat T. “Reduction of Irreversibilities in Organic Rankine Cycle by Non-Azeotropic Working Fluid,” The Fifth International Conference on Science, Technology and Innovation for Sustainable Well-Being, 4-6 September 2013, Luang Prabang, Lao PDR.
4) Deethayat T., Asanakham, A. and Kiatsiriroat T. “A Study on Modular Organic Rankine Cycle with Biomass for Power Generation in Small Community”, Asia Pacific Network for Sustainable Agriculture, Food and Energy, 17-18 November 2015, Ho Chi Minh, Vietnam.
5) Deethayat T. and Kiatsiriroat T. “Prediction of Low Temperature Organic Rankine Cycle (ORC) Thermal Efficiency by A Dimensionless FOM”, The 8th Thailand Renewable Energy for Community Conference, 4-6 November 2015, Bangkok, Thailand.
6) Deethayat T. and Kiatsiriroat T. “Performance Analysis of Low Temperature Organic Rankine Cycle with Zeotropic Refrigerant by Figure of Merit (FOM)”, Energy, Vol.96, 2016, pp. 96-102 (Thompson Reuters Impact Factor 4.844).

Deethayat T., Kiatsiriroat T. and Thawonngamyingsakul C.

"Performance analysis of an organic Rankine cycle with internal heat exchanger having zeotropic working fluid,"

Case Studies in Thermal Engineering, Vol.6, 2015, pp. 155-161(Indexed by SCOPUS).

Case Studies in Thermal Engineering 6 (2015) 155–161

Contents lists available at ScienceDirect

Case Studies in Thermal Engineering

journal homepage: www.elsevier.com/locate/csite

Performance analysis of an organic Rankine cycle with internal heat exchanger having zeotropic working fluid

Thoranis Deethayat [a], Tanongkiat Kiatsiriroat [a,*], Chakkraphan Thawonngamyingsakul [b]

[a] Department of Mechanical Engineering, Faculty of Engineering, Chiang Mai University, Chiang Mai 50200, Thailand
[b] Department of Mechanical Engineering, Faculty of Engineering, Rajamangala University of Technology Lanna Tak, Tak 63000, Thailand

ARTICLE INFO

Article history:
Received 9 April 2014
Received in revised form
12 February 2015
Accepted 13 September 2015
Available online 18 September 2015

Keywords:
Organic Rankine cycle
Internal heat exchanger
Thermal performance
Zeotropic refrigerant

ABSTRACT

In this study, performance of a 50 kW organic Rankine cycle (ORC) with internal heat exchanger (IHE) having R245fa/R152a zeotropic refrigerant with various compositions was investigated. The IHE could reduce heat rate at the ORC evaporator and better cycle efficiency could be obtained. The zeotropic mixture could reduce the irreversibilities during the heat exchanges at the ORC evaporator and the ORC condenser due to its gliding temperature; thus the cycle working temperatures came closer to the temperatures of the heat source and the heat sink. In this paper, effects of evaporating temperature, mass fraction of R152a and effectiveness of internal heat exchanger on the ORC performances for the first law and the second law of thermodynamics were considered. The simulated results showed that reduction of R245fa composition could reduce the irreversibilities at the evaporator and the condenser. The suitable composition of R245fa was around 80% mass fraction and below this the irreversibilities were nearly steady. Higher evaporating temperature and higher internal heat exchanger effectiveness also increased the first law and second law efficiencies. A set of correlations to estimate the first and the second law efficiencies with the mass fraction of R245fa, the internal heat exchanger effectiveness and the evaporating temperature were also developed.

1. Introduction

At present, demand and cost of electricity increase rapidly and moreover, higher greenhouse gas and other emissions due to power generation are obtained. Many methods have been reported to reduce the fossil fuel consumption and organic Rankine cycle (ORC) [1–4] is a promising technology to generate electricity. The cycle uses low boiling point working fluid then it could be operated with low grade heat sources such as industrial waste heat and renewable energy, for example, geothermal energy, solar energy and biomass, etc.

To improve ORC thermal performance, an internal heat exchanger could be conducted to exchange heat between the fluid leaving the turbine and that before entering the evaporator to reduce heat rate input of the cycle. Guo et al. [5] analyzed and compared performance of an ORC with internal heat exchanger to that of a basic ORC, using R600a, R245fa and R290 as working fluids. With a heat source temperature at 160 °C, compared to the basic ORC, the thermal efficiency of the

* Corresponding author.
E-mail address: kiatsiriroat_t@yahoo.co.th (T. Kiatsiriroat).

http://dx.doi.org/10.1016/j.csite.2015.09.003

Nomenclature

C_P	heat capacity, J/kg-K
h	specific enthalpy, J/kg
$\dot{I}$	irreversibility, W
M	mass fraction of R245fa, %
$\dot{m}$	mass flow rate, kg/s
P	pressure, kPa
s	specific entropy, J/kg-K
T	temperature, °C, K
$\dot{Q}$	heat input, W
$\dot{W}$	work, W
η	efficiency, %
v	specific volume, m^3/kg
ε	effectiveness

Subscripts

1, 2, 2a,…8	state point
evap	evaporator
PUMP	pump
1st	the 1st law
TUR	turbine
C	condenser
HE	heat exchanger

modified ORC could be increased by 14%.

Selection of organic working fluid must be performed carefully by considering safety and environmental properties assessment such as atmospheric life time (ALT), ozone depletion potential (ODP), global warming potential (GWP) including appropriate values of cycle temperature and pressure. Hung et al. [6] studied an ORC using different fluids among wet, dry and isentropic fluids. Dry and isentropic fluids showed better thermal efficiencies and moreover, they did not condense during expansion in the turbine thus less damage in the machine was obtained. Tchanche et al. [7] analyzed thermodynamic characteristics and performances of 20 fluids in a low-temperature solar organic Rankine cycle and R134a was recommended. Recently, there was a report showing other suitable working fluids for low temperature heat source which were R123 and R245fa.

During heat exchanging in the evaporator and the condenser of the ORC cycle, there are temperature differences between the heat exchanging fluids which generate irreversibilities at the cycle components; then some part of the cycle available work is destroyed. Use of zeotropic fluid in the ORC is one method to reduce the temperature differences during the heat exchanges. The temperature of the zeotropic fluid is changing during a phase change and the temperatures of the cycle working fluid could follow those of the heat source and the heat sink streams at the evaporator and the condenser, respectively. With smaller temperature differences compared with the single working fluid, consequently, the irreversibilities during the heat exchanges are less and higher cycle work output could be obtained. Heberle et al. [8] studied the second law efficiencies of zeotropic mixtures as the working fluids for a geothermal ORC. The results showed that the efficiency was increased up to 15% compared to that of pure fluid for heat source temperature below 120 °C. Deethayat et al. [9] studied a basic ORC using R245fa/R152a as the working fluids and the irreversibilities at the evaporator and the condenser were found to be less than those of the unit using single R245fa. Anyhow, there was a limit of R152a composition due to its high flammability when the value was over 30% [10].

In this study, performance analysis of a 50 kW ORC with internal heat exchanger was studied when the working fluid was a mixture of R245fa/R152a. A hot water stream at 115 °C was taken as a heat source at the evaporator and a cool water stream fixed at 27 °C was conducted as a heat sink at the condenser. The effects of evaporating temperature, mass fraction of R245fa and effectiveness of internal heat exchanger on the ORC performances following the first law and the second law of thermodynamics were considered.

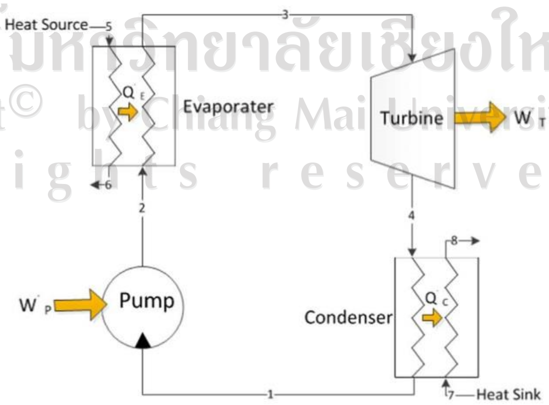

Fig. 1. The components in basic ORC.

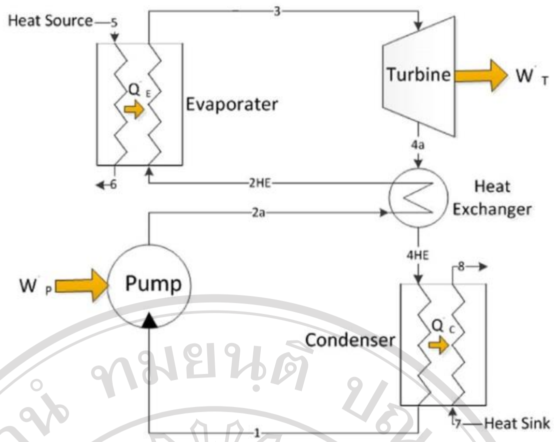

Fig. 2. The components in ORC with internal heat exchanger.

2. Methodology

The organic Rankine cycle has the same principle as the steam Rankine cycle as shown in Fig. 1 but the cycle uses organic working fluids instead of water. Fig. 2 shows the ORC with internal heat exchanger for exchanging heat between the working fluid leaving the turbine and that entering the evaporator for improving the cycle efficiency. Fig. 3 describes processes in *T–s* diagrams for single dry working fluid and zeotropic mixture. It could be noted that for the cycle with zeotropic mixture, the working fluid temperature is not constant during phase-change and follows the heat source or the heat sink temperature then the irreversibilities at the evaporator and the condenser could be less compared with those for the single fluid.

For simplicity in the analysis, some assumptions were taken as follows: steady state conditions, no pressure drops in the components. The energy equations of the all components were summarized as follows:

The basic ORCPump:

$$\dot{W}_p = \frac{\dot{m} v_1 (P_2 - P_1)}{\eta_p} \tag{1}$$

$$\dot{W}_p = \dot{m}(h_{2a} - h_1) \tag{2}$$

Evaporator:

$$\dot{Q}_E = \dot{m}(h_3 - h_{2a}) \tag{3}$$

Turbine:

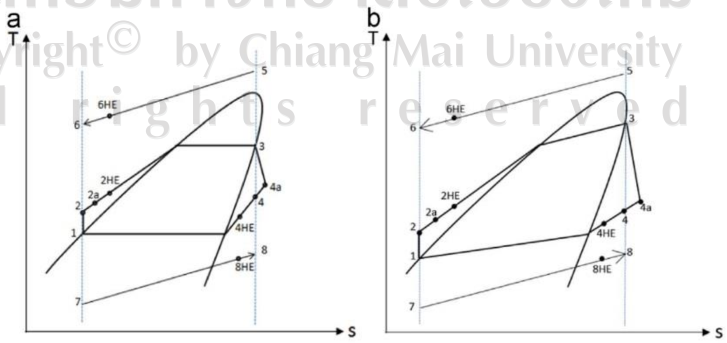

Fig. 3. *T*–s diagram of the ORC for dry working fluid.

$$\dot{W}_T = \dot{m}(h_3 - h_4)\eta_T \tag{4}$$

Condenser:

$$\dot{Q}_C = \dot{m}(h_{4a} - h_1) \tag{5}$$

The 1st law of efficiency:

$$\eta_{1st} = \frac{W_T - W_P}{Q_E} \tag{6}$$

The ORC with internal heat exchangerEvaporator:

$$\dot{Q}_E = \dot{m}(h_3 - h_{2HE}) \tag{7}$$

Condenser:

$$\dot{Q}_C = \dot{m}(h_{4HE} - h_1) \tag{8}$$

Internal heat exchanger:

$$\dot{Q}_{HE} = \dot{m}C_{p4a}(T_{4a} - T_{4HE}) = \dot{m}C_{p2a}(T_{2HE} - T_{2a}), \tag{9}$$

$$\dot{Q}_{HE} = \varepsilon(\dot{m}C_p)_{min}(T_{4a} - T_{2a}). \tag{10}$$

Irreversibilities at the evaporator and the condenser,Evaporator:

$$\dot{I} = \dot{m}_w\left[(h_5 - h_{6HE}) - T_0(s_5 - s_6)\right] - \dot{m}_R\left[(h_3 - h_2) - T_0(s_3 - s_2)\right]. \tag{11}$$

Condenser:

$$\dot{I} = \dot{m}_w\left[(h_4 - h_1) - T_0(s_4 - s_1)\right] - \dot{m}_R\left[(h_8 - h_7) - T_0(s_8 - s_7)\right]. \tag{12}$$

The 2nd law efficiencies,η_{2nd}

$$\eta_{2nd} = \frac{\dot{m}_R\left[(h_3 - h_4) - (h_2 - h_1)\right]}{\dot{m}_w\left[(h_5 - h_{6HE}) - T_0(s_5 - s_{6HE})\right]} \tag{13}$$

3. Conditions for the ORC Calculation

The conditions for the ORC calculation were:

1. The temperature of heat source was 115 °C.
2. The ambient temperature was 25 °C.
3. The cooling water temperature at the condenser was 27 °C.
4. The evaporation temperature (saturated condition) ranged from 70 to 100 °C.

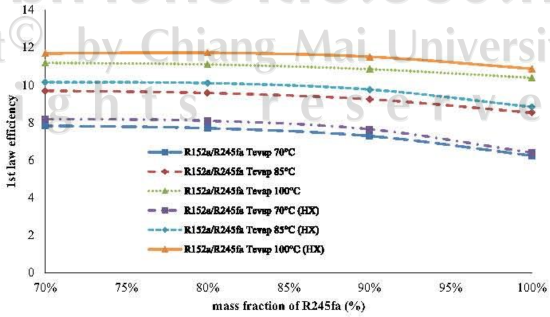

Fig. 4. The 1st law efficiencies of the basic ORC and the ORC with internal heat exchanger at various evaporating temperatures and mass fractions of R245fa. The internal heat exchanger effectiveness was 0.6.

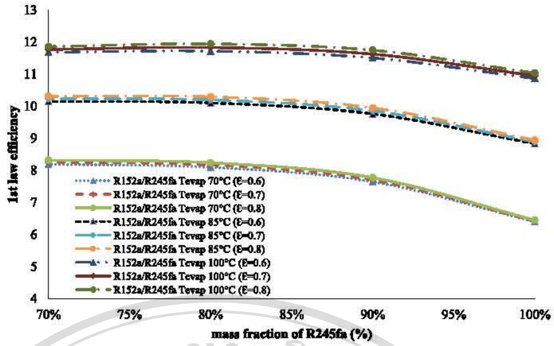

Fig. 5. The 1st law efficiency of the ORC with internal heat exchanger at various mass fractions of R245fa and various effectiveness of internal heat exchanger.

5. Isentropic efficiency of pump (η_{PUMP}) was 0.8.
6. Isentropic efficiency of turbine (η_{TUR}) was 0.85.
7. The turbine work was at 50 kW.
8. The thermal-physical properties of the working fluids were evaluated from REFPROP [11].
9. The set pinch-point temperatures between the heat exchanging fluids (ΔTPP) at the evaporator and the condenser were 6 °C and 3 °C, respectively.
10. The effectiveness (ε) of internal heat exchanger was 0.6–0.8.

4. Results and discussion

Fig. 4 shows the first law efficiencies of the basic ORC and the ORC with internal heat exchanger at various values of evaporating temperatures and mass fractions of R245fa/R152a. The effectiveness of internal heat exchanger is 0.6. Higher evaporation temperature resulted in higher efficiencies. More mass fraction of R152a or less mass fraction of R245fa gave better performance since less irreversibilities at the evaporator and the condenser were obtained. The efficiency was highest when the R245fa fraction was around 80% and the value was rather steady when the fraction was less than this value. It could be noted that the ORC with internal heat exchanger gave better performance since the internal heat exchanger reduced the heat rate input at the evaporator.

Fig. 5 shows the effect of the internal heat exchanger effectiveness on the first law efficiency of the ORC with internal heat exchanger. Higher effectiveness and evaporation temperature resulted in higher efficiency. Again, the first law efficiency was highest when the R245fa fraction was around 80%.

Figs. 6 and 7 show irreversibilities during heat exchanges at the evaporator and the condenser of the ORC with internal

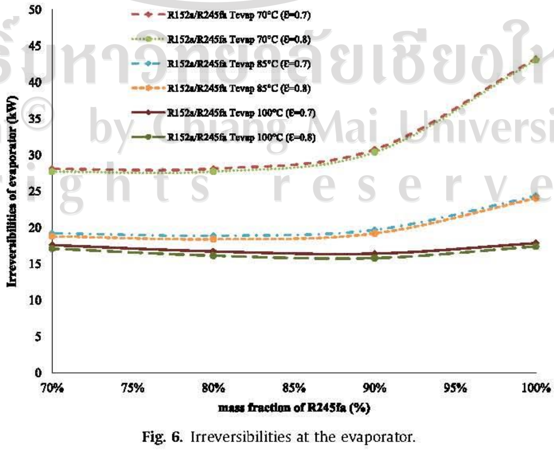

Fig. 6. Irreversibilities at the evaporator.

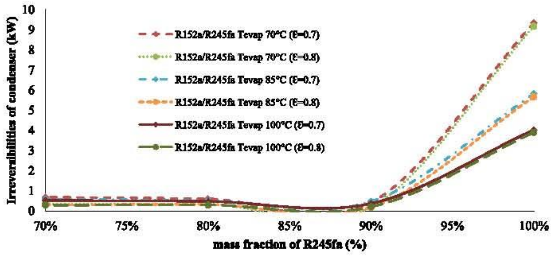

Fig. 7. Irreversibilities at the condenser.

heat exchanger, respectively. It could be seen that the irreversibilites for the mixture at the evaporator decreased compared with those for the single fluid due to lower temperature gaps between the heat exchanging fluids. For the working blend, as the R245fa composition decreased, at the evaporator, it was found that the temperature gap of the heat exchanging fluids was reduced and then less irreversibility was obtained. Anyhow, it could be found that the temperature difference slightly increased when the R245fa composition was over around 80–90% (R152a composition of 20–10%). Higher evaporator temperature also resulted in lower irreversibility since the temperature gap between the heat source and the cycle working fluid was less. The results were similar at the condenser.

Fig. 8 shows the second law efficiency of the ORC with internal heat exchanger. It could be seen that the value was highest when the R245fa composition was around 80% (R152a at 20%) since lowest irreversibilities at the evaporator and at the condenser were found. Higher evaporating temperature and higher internal heat exchanger effectiveness also resulted in higher efficiency.

Some of the simulation results were given in Table 1. A correlation to predict the first and the second law efficiencies could be given in forms of

$$\eta_{1st}=0.1758\epsilon^{0.06168}M^{-0.1543}T_{evap}^{1.065} \tag{14}$$

$$\eta_{2nd}=11.83\epsilon^{0.04906}M^{-0.1818}T_{evap}^{0.5071} \tag{15}$$

It should be noted that the model could predict all of the data within ±5% variation and the standard deviations were 0.0178 and 0.0234, respectively.

5. Conclusion

R245fa/R152a, a zeotropic refrigerant was used as a working fluid in a 50 kW ORC with internal heat exchanger. The results showed that the temperature gliding during the phase change of mixture could decrease ireversibilities at the evaporator and the condenser of the cycle thus the first law and the second law efficiencies could be improved. Decrease of R245fa or increase of R152a compositions generated higher temperature gliding of the cycle working fluid. The suitable composition of R245fa was around 80% mass fractions. When the R245fa composition was less than this, the first law, the second law efficiencies and the irreversibilities at the evaporator and the condenser were nearly steady. Higher evaporating

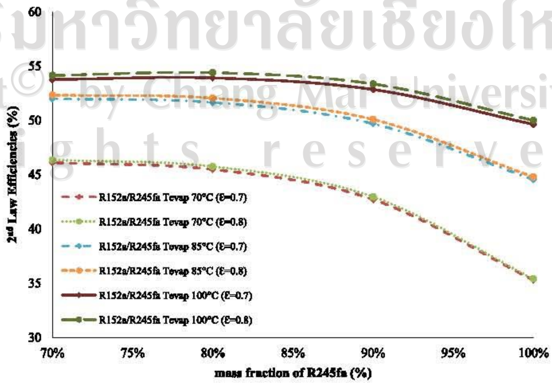

Fig. 8. The 2nd law efficiency of the ORC with internal heat exchanger.

Table 1
Simulation Data.

Working fluids	Mass fraction	T_{evap} (°C)	Effectiveness (ε)	Work (kW)	Irreversibilities at evaporator and condenser (kW)	1st law (%)	2nd law (%)
R152a/R245fa	−30/70	70	0.6	47.96	104.53	8.19	45.88
R152a/R245fa	−20/80	70	0.6	48.20	106.59	8.09	45.22
R152a/R245fa	−10/90	70	0.6	48.45	114.07	7.64	42.47
R152a/R245fa	−30/70	85	0.6	47.49	91.91	10.15	51.67
R152a/R245fa	−20/80	85	0.6	47.79	93.21	10.10	51.27
R152a/R245fa	−10/90	85	0.6	48.09	97.53	9.76	49.31
R152a/R245fa	−30/70	100	0.6	46.91	87.87	11.68	53.39
R152a/R245fa	−20/80	100	0.6	47.29	88.49	11.72	53.44
R152a/R245fa	−10/90	100	0.6	47.67	91.08	11.50	52.34
R152a/R245fa	−30/70	70	0.7	47.96	104.00	8.25	46.12
R152a/R245fa	−20/80	70	0.7	48.20	105.98	8.17	45.48
R152a/R245fa	−10/90	70	0.7	48.45	113.43	7.71	42.71
R152a/R245fa	−30/70	85	0.7	47.49	91.34	10.23	52.00
R152a/R245fa	−20/80	85	0.7	47.79	92.52	10.20	51.65
R152a/R245fa	−10/90	85	0.7	48.09	96.79	9.85	49.69
R152a/R245fa	−30/70	100	0.7	46.91	87.26	11.77	53.76
R152a/R245fa	−20/80	100	0.7	47.29	87.72	11.83	53.91
R152a/R245fa	−10/90	100	0.7	47.67	90.21	11.62	52.84
R152a/R245fa	−30/70	70	0.8	47.96	103.46	8.32	46.36
R152a/R245fa	−20/80	70	0.8	48.20	105.36	8.24	45.75
R152a/R245fa	−10/90	70	0.8	48.45	112.79	7.77	42.95
R152a/R245fa	−30/70	85	0.8	47.49	90.76	10.31	52.33
R152a/R245fa	−20/80	85	0.8	47.79	91.83	10.29	52.04
R152a/R245fa	−10/90	85	0.8	48.09	96.04	9.95	50.08
R152a/R245fa	−30/70	100	0.8	46.91	86.65	11.86	54.14
R152a/R245fa	−20/80	100	0.8	47.29	86.94	11.94	54.39
R152a/R245fa	−10/90	100	0.8	47.67	89.33	11.75	53.36

temperature and higher internal heat exchanger effectiveness also increased the cycle efficiency. A set of correlations to estimate the first law and the second law efficiencies with the mass fraction of R245fa, the internal heat exchanger effectiveness and the evaporating temperature was also developed. The results could fit very well with the experimental data.

Acknowledgment

The authors would like to thank the Graduate School and Department of Mechanical Engineering, Faculty of Engineering, Chiang Mai University for supporting facilities. In addition, the authors would like to acknowledge the Commission on Higher Education under the National Research University Project for the budget support.

References

[1] B.T. Liu, K.H. Chien, C.C. Wang, Effect of working fluids on organic Rankine cycle for waste heat recovery, Energy 29 (2004) 1207–1217.
[2] U. Drescher, D. Brüggemann, Fluid selection for the organic Rankine cycle (ORC) in biomass power and heat plants, Appl. Therm. Eng. 27 (2007) 223–228.
[3] T. Yamamoto, T. Furuhata, N. Arai, Design and testing of the organic Rankine Cycle, Energy 26 (2001) 239–251.
[4] S. Quoilin, M. Van Den Broek, S. Declaye, S. Dewallef, V. Lemort, Techno-economic survey of organic Rankine Cycle (ORC) systems, Renew. Sustain. Energy Rev. 22 (2013) 168–186.
[5] C. Guo, X. Du, L. Yang, Y. Yang, Performance analysis of organic Rankine cycle based on location of heat transfer pinch point in evaporator, Appl. Therm. Eng. 62 (2014) 176–186.
[6] T.C. Hung, S.K. Wang, C.H. Kuo, B.S. Pei, K.F. Tsai, A study of organic working fluids on system efficiency of an ORC using low-grade energy sources, Energy 35 (2010) 1403–1411.
[7] B.F. Tchanche, G. Papadakis, G. Lambrinos, A. Frangoudakis, Fluid selection for a low-temperature solar organic Rankine cycle, Appl. Therm. Eng. 29 (2009) 2468–2476.
[8] F. Heberle, M. Preißinger, D. Brüggemann, Zeotropic mixtures as working fluids in organic Rankine cycles for low-enthalpy geothermal resources, Renew. Energy 37 (2012) 364–370.
[9] T. Deethayat, T. Kiatsirriroat, Reduction of Irreversibilities in organic Rankine cycle by non-azeotropic working fluid, in: Proceedings of the STISWB V Conference, LuangPrabang, Lao PDR 2013, p. 55.
[10] J.K. Wang, L. Zhao, X.D. Wang, A comparative study of pure and zeotropic mixtures in low-temperature solar Rankine cycle, Appl. Energy 87 (2010) 3366–3373.
[11] National Institute of Standard and Technology (NIST), REFPROP Version 7, Thermodynamic Properties of Refrigerants and Refrigerant Mixtures Software, 2000.

Deethayat T. and Kiatsiriroat T.

"Cost Analysis on Power Generation from Biomass-Fuelled Modular Organic Rankine Cycle Power Plant,"

Engineering J. CMU, Vol.21, 2014, pp.84-93(Indexed by TCI).

วารสารวิศวกรรมศาสตร์
Engineering Journal
มหาวิทยาลัยเชียงใหม่
Chiang Mai University

Volume 21 (3) September - December 2014 ISSN 0857-2178

Contents

การศึกษาปริมาณแอนโธไซยานินในน้ำต้มข้าวโพดสีม่วงและการประยุกต์ใช้ในการผลิตผงสี 1-13
(A Study of Anthocyanin Content in Cooked Purple Corn Water and Its Applications in Colorant Powder Production)
รัตนา ม่วงรัตน์ จินตนา ใจมูล ทัศนีย์ ศรีวิชัย และ ตะวัน ณ ลำพูน

ศักยภาพการอนุรักษ์พลังงานและมาตรการส่งเสริมการใช้หม้อไอน้ำขนาดเล็กประสิทธิภาพสูงในโรงพยาบาล 14-26
(Potential of Energy Saving and Promotion Measure of Using Small Scale High Efficiency Boiler in Hospitals)
วัลยา กวีพรพจน์ และ วารุณี เตีย

การวิเคราะห์ต้นทุนโลจิสติกส์ในโรงงานผลิตน้ำผลไม้โดยใช้การคิดต้นทุนกิจกรรมเกณฑ์เวลา 27-36
(Logistics Cost Analysis in Fruit Juice Manufacturing Factory Using Time-Driven Activity-Based Costing)
นรเศรษฐ์ บุญเหมย และ รุ่งฉัตร ชมภูอินไหว

การลดเวลานำในการประกอบเครื่องจักรโดยการจัดกลุ่มชิ้นส่วนตามสายการผลิต 37-46
(Lead Time Reduction in Machine Assembly Using Part Routing Group)
มาณิก นิลสุวรรณ และ จรีมพร หรรษมนตร์

การบริหารโครงการโดยการสร้างข่ายงานกิจกรรมในกระบวนการผลิตเครื่องย่อยกิ่งไม้ 47-55
(The Project Management of Constructions Activity Network in Production Process Wood Split Machine)
สุรพงศ์ บางพาน และ พีรพันธ์ บางพาน

พฤติกรรมที่ไม่ปลอดภัยของคนงานในงานก่อสร้างอาคารขนาดใหญ่ในเขตจังหวัดกรุงเทพมหานครและปริมณฑล 56-64
(Unsafe behavior of workers in the construction of large buildings in Bangkok and Surrounding Areas)
จตุพล พิสิฏฐ์ศักดิ์ และ อุลาวัณย์ กุลชาติชัย

ปัจจัยที่ส่งผลกระทบต่อการตัดสินใจประยุกต์ใช้ ISO9001 ในอุตสาหกรรมก่อสร้างไทย 65-71
(Factors affecting decision making in the application of ISO 9001 in Thai Construction Industry)
ทนงศักดิ์ บุบผาถา อุลาวัณย์ กุลชาติชัย และ วัชระ สัตยาประเสริฐ

การจัดการสินค้าคงคลังสำหรับการผลิตส่วนประกอบชุดชั้นในสตรี 72-83
(Inventory Management for Lingerie Component Manufacturing)
กัญญาลักษณ์ คำซั่ง และ วิมลิน เหล่าศิริถาวร

การวิเคราะห์ต้นทุนการผลิตไฟฟ้าจากโรงไฟฟ้าวัฏจักรแรงคินสารอินทรีย์ขนาดโมดูลาร์ที่ใช้ชีวมวลเป็นเชื้อเพลิง 84-93
(Cost Analysis on Power Generation from Biomass-Fuelled Modular Organic Rankine Cycle Power Plant)
ธรณิศวร์ ดีทายาท และ ทนงเกียรติ เกียรติศิริโรจน์

Engng.J.CMU.(2014) 21 (3), 84-93

วารสารวิศวกรรมศาสตร์
มหาวิทยาลัยเชียงใหม่
Engineering Journal
Chiang Mai University

การวิเคราะห์ต้นทุนการผลิตไฟฟ้าจากโรงไฟฟ้าวัฏจักรแรงคินสารอินทรีย์ขนาดโมดูลาร์ที่ใช้ชีวมวลเป็นเชื้อเพลิง

Cost Analysis on Power Generation from Biomass-Fuelled Modular Organic Rankine Cycle Power Plant

ธรณิศวร์ ดีทายาท[1] และ ทนงเกียรติ เกียรติศิริโรจน์[2]

Thoranis Deethayat[1] and Tanongkiat Kiatsiriroat[2]

สาขาวิศวกรรมพลังงาน คณะวิศวกรรมศาสตร์ มหาวิทยาลัยเชียงใหม่[1]

ภาควิชาวิศวกรรมเครื่องกล คณะวิศวกรรมศาสตร์ มหาวิทยาลัยเชียงใหม่[2]

Energy Engineering, Faculty of Engineering, Chiang Mai University, 50200, Thailand

Department of Mechanical Engineering, Faculty of Engineering, Chiang Mai University, 50200, Thailand

E-mail: thoranisdee@gmail.com

บทคัดย่อ

งานวิจัยนี้เป็นการศึกษาต้นทุนการผลิตไฟฟ้าจากโรงไฟฟ้าที่ใช้วัฏจักรแรงคินสารอินทรีย์ขนาดโมดูลาร์ เมื่อมีการใช้ชีวมวลชนิดต่างๆ เป็นเชื้อเพลิง โดยพิจารณาจากโรงไฟฟ้า 2 ขนาด ที่มีจำหน่ายในท้องตลาด ที่กำลังการผลิตไฟฟ้าสุทธิ 35 และ 65 kW ในงานนี้ยังพิจารณาถึงอิทธิพลของอัตราการไหล และอุณหภูมิของน้ำร้อนที่ใช้ในการผลิตไฟฟ้าที่มีต่อต้นทุนการผลิตไฟฟ้า จากผลการศึกษาพบว่า เมื่อมีการเพิ่มค่าอัตราการไหลของน้ำร้อน และอุณหภูมิน้ำร้อนขาเข้าเครื่องทำระเหย พบว่าประสิทธิภาพของระบบจะเพิ่มขึ้น และต้นทุนการผลิตไฟฟ้าต่อหน่วยจะลดลง สำหรับโรงไฟฟ้า ขนาด 35 และ 65 kW ที่อัตราการไหลของน้ำร้อนที่เข้าเครื่องทำระเหย 12.6 l/s และอุณหภูมิน้ำร้อนขาเข้า 116 °C จะมีประสิทธิภาพทางความร้อนที่ 16.9% และ 16.53% ตามลำดับ เมื่อมีการใช้ชีวมวลชนิดทะลายปาล์มจะมีต้นทุนการผลิตไฟฟ้าต่ำที่สุด เทียบกับชีวมวลอื่น โดยมีค่าเท่ากับ 6.66 และ 4.85 บาท/kWh ตามลำดับ

คำสำคัญ: วัฏจักรแรงคินสารอินทรีย์ขนาดโมดูลาร์, ชีวมวล, ประสิทธิภาพ, การวิเคราะห์ต้นทุน

ABSTRACT

Economic analyses on power generations from biomass-fuelled modular organic Rankine cycle (ORC) power plants available in the market were considered. The net power generations were at 35 and 65kW. And economic analyses from effect of hot water at various flow rates and temperatures to generated power. When the supplied mass flow rate and the inlet temperature of the hot water at the cycle evaporator increased, it was found that the thermal efficiencies were increased and the unit costs of the power generation decreased. For the ORCs at 35 and 65 kW, at hot water mass flow rate of 12.6 l/s and evaporator inlet temperature of 116ºC, the thermal efficiencies were 16.9% and 16.53%, respectively. With palm bunch as feedstock for heat source, the levelized electricity unit costs were lowest compared with other biomass residues which were 6.66 and 4.85 baht/kWhe, respectively.

Keywords: Modular organic Rankine cycle, Biomass, Efficiency, Economic analysis

Received 11 November 2013
Accepted 9 December 2013

1. บทนำ

ในระยะ 20 ปีที่ผ่านมา ตั้งแต่ปี ค.ศ.1990 การใช้พลังงานของประเทศไทยเพิ่มขึ้นอย่างต่อเนื่อง ในอัตราเฉลี่ยร้อยละ 4.4 ต่อปี จนในปี ค.ศ.2010 การใช้พลังงานขั้นสุดท้าย (Final Energy) สูงขึ้นเป็น 2.32 เท่าของปี ค.ศ. 1990 หรือประมาณ 71,200 พันตันเทียบเท่าน้ำมันดิบ (ktoe) และแนวโน้มความต้องการใช้พลังงานในอนาคตช่วงตั้งแต่ปี ค.ศ.2011-2030 คาดว่าจะเพิ่มขึ้นจาก 71,200 ktoe ต่อปี ในปัจจุบัน เป็น 162,715 ktoe หรือประมาณ 2.3 เท่าของปัจจุบัน [1]

การผลิตไฟฟ้าโดยใช้วัฏจักรไอน้ำยังเป็นวิธีหลักวิธีหนึ่งในปัจจุบัน ความร้อนที่นำมาใช้มาจากเชื้อเพลิงฟอสซิล เป็นตัวการสำคัญที่ทำให้เกิดปัญหาด้านสิ่งแวดล้อมทางอากาศ คาร์บอนไดออกไซด์ (CO_2) คาร์บอนมอนออกไซด์ (CO) มีเทน (CH4) ซัลเฟอร์ไดออกไซด์ (SO_2) และ ไนโตรเจนไดออกไซด์ (NOx) ที่ปลดปล่อยออกมา ก่อให้เกิดสภาวะโลกร้อน การทำลายชั้นโอโซนและฝนกรด ในระหว่างปี ค.ศ.2008-2011 [2] พบว่าการใช้พลังงานด้านไฟฟ้ามีการปล่อยแก๊สคาร์บอนไดออกไซด์สูงที่สุด

จากเป้าหมายการใช้พลังงานทดแทนของประเทศไทย ภายในปี ค.ศ.2021 จะมีการส่งเสริมให้ชุมชนมีส่วนร่วมในการผลิตและการใช้พลังงานทดแทน โดยมีสัดส่วนเป็น 25% ของการใช้พลังงานทั้งหมด รัฐบาลส่งเสริมให้มีการผลิตไฟฟ้าจากพลังงานหมุนเวียน อีกทั้งยังมุ่งเน้นการผลิตไฟฟ้าระดับหมู่บ้าน โดยสนับสนุนการก่อสร้างโครงการไฟฟ้าระดับชุมชนให้องค์กรปกครองส่วนท้องถิ่นหรือชุมชนเจ้าของพื้นที่มีส่วนร่วมเป็นเจ้าของโครงการ สามารถบริหารงานและบำรุงรักษาเองได้ในอนาคต

วัฏจักรแรงคินสารอินทรีย์ (Organic Rankine Cycle) เป็นอีกทางเลือกหนึ่งที่น่าสนใจ เนื่องจากวัฏจักรแรงคินสารอินทรีย์ มีระบบโครงสร้างเหมือนวัฏจักรแรงคิน (Rankine Cycle) ทั่วไปที่ใช้ไอน้ำเป็นสารทำงาน โดย ORC มีการใช้สารอินทรีย์ที่มีจุดเดือดต่ำเป็นสารทำงาน ซึ่งสามารถเปลี่ยนสถานะเป็นไออิ่มตัวหรือไอร้อนยวดยิ่งเมื่อได้รับความร้อนจากแหล่งความร้อนอุณหภูมิที่ไม่สูงมาก ทำให้สามารถใช้แหล่งความร้อนได้หลายชนิด เช่น พลังงานความร้อนใต้พิภพ พลังงานจากแสงอาทิตย์ พลังงานจากชีวมวล รวมถึงความร้อนทิ้งจากอุตสาหกรรม

ชีวมวลถือเป็นแหล่งพลังงานที่มีศักยภาพสูงของไทย เนื่องจากประเทศไทยเป็นประเทศเกษตรกรรม ส่งผลให้มีผลผลิตทางการเกษตรเป็นจำนวนมาก ผลผลิตทางการเกษตรเหล่านี้จะมีวัสดุเหลือทิ้งออกมาจำนวนหนึ่งด้วย เช่น แกลบ ฟางข้าว ชานอ้อย และซังข้าวโพด เป็นต้น ปริมาณวัสดุเหลือทิ้งทางการเกษตรมีมากถึง 59,539,905.20 ตันต่อปี คิดเป็นพลังงานเทียบเท่า 504,339.40 TJ [3]

เบญจมาศและคณะ[4] ได้ศึกษาศักยภาพการผลิตไฟฟ้าจากชีวมวล 5 ชนิด ได้แก่ เศษไม้ แกลบ เหง้ามันสำปะหลัง กากอ้อย และกะลาปาล์ม พบว่า ในปี พ.ศ.2547 ปริมาณชีวมวลทั้ง 5 ชนิด เพียงพอที่จะสามารถนำไปใช้ผลิตไฟฟ้าได้ถึง 1,999.42 MW และการพยากรณ์ปริมาณชีวมวลในปี พ.ศ.2554 มีศักยภาพในการผลิตไฟฟ้ามากถึง 2,938.47 MW วีรชัยและคณะ[5] ได้ศึกษาโรงไฟฟ้าชีวมวลขนาด 100kW ใช้เทคโนโลยีแก๊สซิฟิเคชั่น พบว่าสามารถใช้เชื้อเพลิงชีวมวลได้ทุกชนิดในประเทศไทย โดยเชื้อเพลิงจากซังข้าวโพดมีต้นทุนต่ำสุด คือ 1.9 บาท/kWh รองลงมาคือ เหง้ามันสำปะหลังและไม้โตเร็ว 2.1 และ 2.2 บาท/kWh ตามลำดับ จักรพันธ์และทนงเกียรติ [6] ทำการวิเคราะห์เชิงเศรษฐศาสตร์โรงไฟฟ้าวัฏจักรแรงคินสารอินทรีย์ที่ใช้แกลบเป็นเชื้อเพลิง มีกำลังการผลิตไฟฟ้า 2.18 MW ชั่วโมงการทำงาน 8,000 ชั่วโมงต่อปี มีระยะโครงการ 25 ปี พิจารณาราคาแกลบ 400-1,600 บาทต่อตัน พบว่าต้นทุนผลิตไฟฟ้ามีค่า 2-3.65 บาท/kWh และที่ราคาแกลบต่ำกว่า 1,200 บาทต่อตัน

จากเป้าหมายการใช้พลังงานทดแทนของประเทศไทย ที่ส่งเสริมให้ชุมชนผลิตไฟฟ้าได้เอง งานวิจัยนี้จึงศึกษาสมรรถนะในการผลิตไฟฟ้า และวิเคราะห์ต้นทุนการ

ผลิตไฟฟ้าจากโรงไฟฟ้าวัฏจักรแรงคินสารอินทรีย์แบบโมดูลาร์ ขนาด 35kW และ 65kW ที่ใช้ชีวมวลต่างๆ เป็นเชื้อเพลิง และหาชนิดของชีวมวลที่มีราคาต้นทุนเหมาะสมกับโรงไฟฟ้าวัฏจักรแรงคินสารอินทรีย์ขนาดโมดูลาร์ดังกล่าว

2. ทฤษฎีที่เกี่ยวข้องกับงานวิจัย

วัฏจักรแรงคินสารอินทรีย์

วัฏจักรแรงคินสารอินทรีย์ มีระบบโครงสร้างเหมือนวัฏจักรแรงคิน (Rankine Cycle) แต่มีลักษณะโครงสร้างที่ไม่ซับซ้อน ใช้สารอินทรีย์ที่มีจุดเดือดต่ำเป็นของไหลทำงาน ซึ่งสามารถเปลี่ยนสถานะเป็นไออิ่มตัวหรือไอร้อนยวดยิ่งเมื่อได้รับความร้อนจากแหล่งความร้อนอุณหภูมิต่ำเช่น พลังงานจากแสงอาทิตย์ และพลังงานจากชีวมวล วัฏจักรพื้นฐานประกอบไปด้วยอุปกรณ์ 4 ตัว คือ ปั๊ม (Pump) เครื่องระเหย (Evaporator) เอ็กซ์แพนเดอร์ (Expander)และเครื่องควบแน่น(Condenser)ดังรูปที่ 1

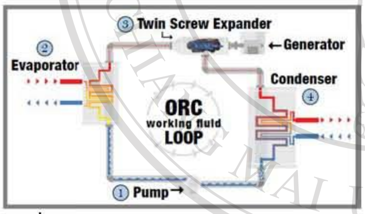

รูปที่ 1 ไดอะแกรมอุปกรณ์ของวัฏจักรแรงคินสารอินทรีย์ที่ใช้ในการศึกษา [11]

การทำงานเริ่มจากสารทำงานไหลเข้าปั๊มในสถานะของเหลวอิ่มตัวที่สภาวะที่ 1 แล้วถูกอัดจนกระทั่งมีความดันเท่ากับความดันชุดทำระเหยซึ่งเป็นความดันสูงสุดของวัฏจักร โดยสารทำงานที่ออกจากปั๊มมีสถานะของเหลวอัดตัวที่สภาวะที่ 2 จากนั้นไปรับความร้อนที่ชุดทำระเหยที่ความดันคงที่ และไหลออกมาในสถานะไออิ่มตัวที่สภาวะที่ 3 ต่อจากนั้นไหลเข้าเทอร์ไบน์เกิดการขยายตัวให้งานออกมาโดยการหมุนของเพลา ซึ่งกระบวนการนี้ความดันและอุณหภูมิของสารทำงานจะลดลง หลังจากนั้นสารทำงานไหลเข้าเครื่องควบแน่นเพื่อเปลี่ยนสถานะเป็นของเหลว โดยคายความร้อนออกมาที่ความดันคงที่ซึ่งเป็นความดันต่ำสุดของวัฏจักร จากนั้นสารทำงานไหลเข้าปั๊มทำงานเป็นวัฏจักรต่อไป ซึ่งสภาวะและสถานะต่างๆ สามารถเขียนแผนภาพอุณหภูมิ-เอนโทรปี ดังรูปที่ 2

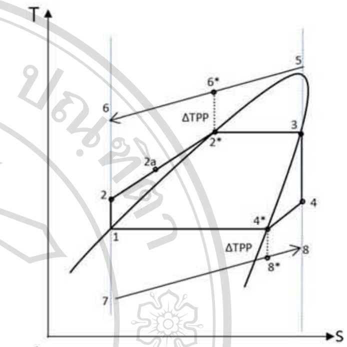

รูปที่ 2 แผนภาพอุณหภูมิ-เอนโทรปีของสารทำงานที่พิจารณาสมการเธอร์โมไดนามิกส์ สำหรับวัฏจักร

ตามรูปที่ 1 โดยพิจารณาสภาวะต่างๆ จากแผนภาพอุณหภูมิ-เอนโทรปี ตามรูปที่ 2 โดยแยกอุปกรณ์ต่างๆ จะได้ดังนี้สภาวะต่างๆ ของ ORC

ปั๊ม

$$\dot{W}_p = \frac{\dot{m}v_1(P_2-P_1)}{\eta_P} \quad (1)$$

$$\dot{W}_p = \dot{m}(h_{2a} - h_1) \quad (2)$$

เครื่องระเหย

$$\dot{Q}_E = \dot{m}_R(h_3 - h_2) = \dot{m}_{hw}C_p(T_5 - T_6) \quad (3)$$

$$\dot{m}_R(h_3 - h_{2^*}) = \dot{m}_{hw}C_p(T_5 - T_{6^*}) \quad (4)$$

เทอร์ไบน์

$$\dot{W}_T = \dot{m}_R(h_3 - h_4)\eta_T \quad (5)$$

เครื่องควบแน่น

$$\dot{Q}_C = \dot{m}_R(h_4 - h_1) = \dot{m}_{cw}C_p(T_8 - T_7) \quad (6)$$

$$\dot{m}_R(h_{4^*} - h_1) = \dot{m}_{cw}C_p(T_{8^*} - T_7) \quad (7)$$

ประสิทธิภาพเชิงความร้อน (Thermal efficiency) η_{th} ที่ใช้คำนวณในการศึกษานี้คือ

$$\eta_{th} = \frac{\dot{W}_T - \dot{W}_P}{\dot{Q}_E} \quad (8)$$

ในงานวิจัยนี้ จะใช้ข้อมูลสมรรถนะของวัฏจักรสารอินทรีย์แบบโมดูลาร์ ที่มีจำหน่ายในท้องตลาด โดยแบบโมดูลาร์จะมีอุปกรณ์ย่อยต่างๆ อยู่ในระบบรวมชุดเดียวกัน โดยระบบดังกล่าว เมื่อมีการติดตั้งระบบทำน้ำร้อน และระบบระบายความร้อน สามารถผลิตกำลังไฟฟ้าสุทธิมาใช้ประโยชน์ได้เลย ในงานนี้จะใช้ที่กำลังการผลิตไฟฟ้าที่ 35 kW และ 65 kW ข้อมูลสมรรถนะแสดงในภาคผนวก ซึ่งประกอบด้วยความสัมพันธ์ ของกำลังไฟฟ้าที่ผลิตได้ ที่อัตราการไหลของน้ำร้อนที่อุณหภูมิต่างๆ และข้อมูลการระบายความร้อนที่คอนเดนเซอร์ สารทำงานที่ใช้ในวัฏจักร เป็นสาร R245fa จากนั้นจึงนำอัตราการไหลของน้ำร้อนไปใช้ในรูปที่ 8 โดยเมื่อกำหนดผลต่างอุณหภูมิน้ำร้อนขาเข้าและขาออกเครื่องทำระเหยที่ค่าต่างๆ เทียบกับอัตราการไหลของน้ำร้อนจะสามารถหาอัตราความร้อนที่ต้องป้อนให้เครื่องระเหยได้

ชีวมวล

ชีวมวล คือ สารอินทรีย์ที่เป็นแหล่งกักเก็บพลังงานจากธรรมชาติและสามารถนำมาใช้ผลิตพลังงานได้ เช่น เศษวัสดุเหลือทิ้งทางการเกษตรหรือกากจากกระบวนการผลิตในอุตสาหกรรมการเกษตร เช่น แกลบ ได้จากการสีข้าวเปลือก ชานอ้อย ได้จากการผลิตน้ำตาลทราย เศษไม้ที่ได้จากการแปรรูปไม้ยางพาราหรือไม้ยูคาลิปตัส และบางส่วนได้จากสวนป่าที่ปลูกไว้ กากปาล์ม ได้จากการสกัดน้ำมันปาล์มดิบออกจากผลปาล์มสด กากมันสำปะหลัง ได้จากการผลิตแป้งมันสำปะหลัง ซังข้าวโพดได้จากการสีข้าวโพดเพื่อนำเมล็ดออก และกะลามะพร้าวได้จากการนำมะพร้าวมาปลอกเปลือกออกเพื่อนำเนื้อมะพร้าวไปผลิตกะทิ และน้ำมันมะพร้าว ส่าเหล้าที่ได้จากการผลิตแอลกอฮอล์ เป็นต้น

กระบวนการแปรรูปชีวมวลไปเป็นพลังงานรูปแบบต่างๆ สามารถกระทำได้โดยกระบวนการต่างๆ เช่น การเผาไหม้โดยตรง การผลิตก๊าซ การหมัก เป็นต้น แต่ในงานวิจัยนี้จะพิจารณานำชีวมวลมาผลิตน้ำร้อนโดยกระบวนการเผาไหม้โดยตรงเพียงอย่างเดียว เพื่อใช้เป็นแหล่งความร้อนให้กับวัฏจักรแรงคินสารอินทรีย์

การเผาไหม้โดยตรง (Direct combustion)

เป็นการนำชีวมวลมาเผาไหม้โดยตรงในเตาเผา ซึ่งจะได้ความร้อนออกมาตามค่าความร้อนของชนิดชีวมวลดังตารางที่ 1 ความร้อนที่ได้จากการเผาสามารถนำไปถ่ายเทให้กับหม้อต้ม เพื่อผลิตน้ำร้อนที่มีอุณหภูมิและความดันสูง โดยน้ำร้อนที่ได้จะนำไปแลกเปลี่ยนความร้อนกับสารทำงานในวัฏจักรแรงคินสารอินทรีย์ ทำให้สารทำงานมีอุณหภูมิสูงขึ้นจนเป็นไออิ่มตัวหรือไอร้อนยิ่งยวด จากนั้นจึงไปปั่นเทอร์ไบน์ เพื่อผลิตไฟฟ้าต่อไป ตัวอย่างชีวมวลประเภทนี้ คือ เศษวัสดุทางการเกษตรและเศษไม้

ตารางที่ 1 ค่าความร้อนและราคาของชีวมวลแต่ละชนิด [7, 8]

ชนิดของชีวมวล	ความชื้น (%)	Ash (%)	Higher heating value (kJ/kg)	Lower heating value (kJ/kg)	ราคา (บาท/ตัน)
แกลบ	12	12.65	14,755	13,517	1,600
ฟางข้าว	10	10.39	13,650	12,330	1,225
ยอดและใบอ้อย	9.2	6.10	16,794	15,479	1,125
ไม้ยางพารา	45	1.59	10,365	8,600	1,300
ทะลายปาล์ม	58.6	2.03	9,196	7,240	514
ซังข้าวโพด	40	0.9	11,298	9,615	1,100
เหง้ามันสำปะหลัง	59.4	1.5	7,451	5,494	950
เปลือกไม้ยูคาฯ	60	2.44	6,811	4,917	700

สำหรับการหาอัตราความร้อนที่ป้อนให้เครื่องระเหย ($\dot{Q}_E$) จะมีค่าใกล้เคียงอัตราความร้อนที่หม้อน้ำร้อนได้รับจากการเผาไหม้เชื้อเพลิง ($\dot{Q}_{heater}$) โดยกำหนดให้ประสิทธิภาพของหม้อน้ำร้อนเท่ากับ 75% ดังนั้น อัตราน้ำร้อนที่หม้อน้ำร้อนได้รับ สามารถหาได้จาก

$$\dot{Q}_{heater} = n_f(\dot{m}LHV) \quad (9)$$

การวิเคราะห์เชิงเศรษฐศาสตร์

สำหรับการวิเคราะห์เชิงเศรษฐศาสตร์ของระบบประกอบไปด้วย

1. ต้นทุนการลงทุน (Investment cost) ของระบบในงานวิจัยนี้ ได้แก่ ราคาโรงไฟฟ้าวัฏจักรแรงคินสารอินทรีย์ที่มีระบบระบายความร้อนในตัวบวกกับราคาหม้อผลิตน้ำร้อนที่ใช้เชื้อเพลิงชีวมวลแบบเผาตรง ไม่รวมต้นทุนของระบบกำจัดเถ้า, มูลค่าซากของอุปกรณ์ต่างๆ หลังสิ้นสุดระยะเวลา 20 ปี และค่าขนส่งชีวมวล

2. ค่าดำเนินการและบำรุงรักษา (Operating & maintenance cost) ของระบบ ได้แก่ บุคลากรสำหรับใช้ในการเดินเครื่องและควบคุมระบบ ค่าบำรุงรักษาระบบสามารถคำนวณได้ โดยกำหนดให้มีค่า 3.5% ของต้นทุนการลงทุน

3. ค่าชีวมวลที่ต้องใช้เป็นเชื้อเพลิงตลอดทั้งปี

ตารางที่ 2 แสดงค่าต่างๆ ที่ใช้ในการประเมินการลงทุนทางเศรษฐศาสตร์

Investment Cost, C_{invest} สำหรับ ORC 35kW [12],[14]	9,847,166.27 บาท
Investment Cost, C_{invest} สำหรับ ORC 65kW [13],[14]	11,048,857.34 บาท
Financial Parameters -Annual insurance rate, $k_{Insurance}$ -Real debt interest rate, i_d [9] - Depreciation period, n	 0.6%/ปี 6.75% 20 ปี

4. ต้นทุนการผลิตไฟฟ้าต่อหน่วยในรูป Levelized Electricity Cost (LEC) สามารถคำนวณตามสมการดังต่อไปนี้ [15]

$$LEC = \frac{(crf \times C_{invest}) + \dot{C}_{o\&m} + \dot{C}_{biomass}}{E_{Net}} \quad (10)$$

เมื่อ

$$crf = \frac{i_d(1+i_d)^n}{(1+i_d)^n - 1} + k_{Insurance} \quad (11)$$

$$E_{Net} = H \times W \quad (12)$$

เงื่อนไขในการคำนวณ

1. โรงไฟฟ้าวัฏจักรแรงคินสารอินทรีย์ที่ทำการศึกษา กำลังการผลิตไฟฟ้าสุทธิ 35 kWและ 65 kW ชั่วโมงการทำงาน 8,000 ชั่วโมงต่อปี
2. ชีวมวลถูกนำไปใช้เผาไหม้โดยตรง ให้แก่หม้อน้ำร้อน เพื่อผลิตน้ำร้อนจ่ายให้ ORC โดยประสิทธิภาพของหม้อน้ำร้อนเท่ากับ 75% [14]
3. อัตราการไหลของน้ำร้อนที่จ่ายให้วัฏจักรแรงคินสารอินทรีย์ 6.3-12.6 l/s อุณหภูมิน้ำร้อนที่เข้า 104°C , 110°C และ 116°C ตามลำดับ
4. อัตราการไหลของน้ำเย็นผสมไกลโคล 40% ที่ใช้ในการระบายความร้อน ORC ขนาด 35 kW และ 65 kW เท่ากับ 13.9 l/s และเท่ากับ 22 l/s ตามลำดับ
5. อุณหภูมิพินช์ (ΔTPP) ระหว่างการแลกเปลี่ยนความร้อนที่เครื่องระเหยและเครื่องควบแน่นคือ 3°C
6. ไม่ได้พิจารณาพลังงานที่ใช้ในการปั๊มน้ำร้อนที่เปลี่ยนแปลงตามอัตราการไหลรวมถึงการระบายความร้อนของเครื่องควบแน่นน้อยมาก
7. ค่าเชื้อเพลิงชีวมวลและค่า O&M ไม่เปลี่ยนแปลงตามเวลา ไม่พิจารณาค่า escalation rate

3. ผลการศึกษา

จากรูปที่ 3 และ 4 เมื่อมีการเพิ่มค่าอัตราการไหลของน้ำร้อน และอุณหภูมิน้ำร้อนตั้งแต่ 104°C จนถึง 116°C โดยกำหนดกำลังการผลิตไฟฟ้าสุทธิคงที่ที่ 35 kW และ 65 kW พบว่าความต้องการอัตราความร้อนลดลงเนื่องจากอัตราการไหลของของไหลมีค่าเพิ่มขึ้น โดยเมื่อความร้อนที่ใช้ในการผลิตน้ำร้อนลดลง จะส่งผลให้ประสิทธิภาพของวัฏจักรสูงขึ้น โดยวัฏจักรแรงคินสารอินทรีย์ ขนาด 35kW และ 65kW ที่อัตราการไหล 12.6 l/s อุณหภูมิของน้ำร้อนขาเข้าเครื่องทำระเหยเท่ากับ 116°C มีประสิทธิภาพของวัฏจักรสูงสุดที่ 16.9% และ 16.53% ตามลำดับ ดังนั้นในการวิเคราะห์ต้นทุนผลิตไฟฟ้าจะนำอัตราความร้อนที่ใช้

ในวัฏจักรที่อุณหภูมิของน้ำร้อนขาเข้าเครื่องทำระเหยเท่ากับ 116°C มาใช้ต่อไป

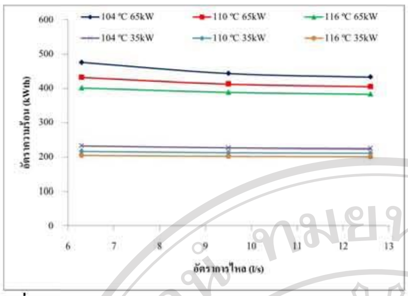

รูปที่ 3 ความสัมพันธ์ระหว่างอัตราความร้อนและอุณหภูมิของน้ำร้อนขาเข้าเครื่องทำระเหยที่อัตราการไหลของน้ำร้อนต่างๆ

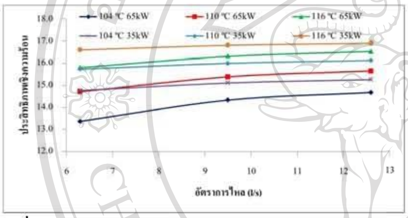

รูปที่ 4 ความสัมพันธ์ระหว่างประสิทธิภาพเชิงความร้อนและอุณหภูมิของน้ำร้อนขาเข้าเครื่องทำระเหยที่อัตราการไหลของน้ำร้อนต่างๆ

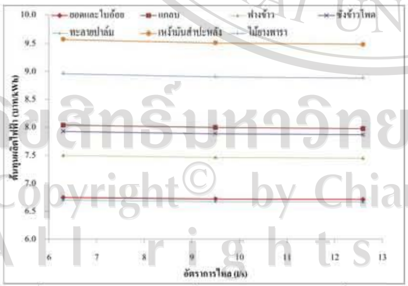

รูปที่ 5 ต้นทุนผลิตไฟฟ้าที่ชีวมวลชนิดต่างๆ ที่วัฏจักรแรงคินสารอินทรีย์ ขนาด 35 kW เมื่อมีการเปลี่ยนอัตราการไหลของน้ำร้อน ที่อุณหภูมิของน้ำร้อนขาเข้าเครื่องทำระเหย 116°C

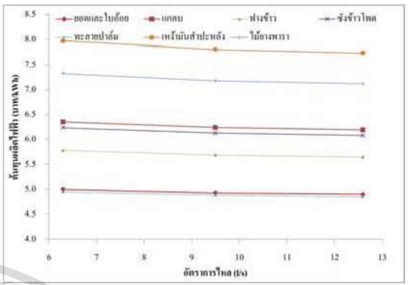

รูปที่ 6 ต้นทุนผลิตไฟฟ้าที่ชีวมวลชนิดต่างๆ ที่วัฏจักรแรงคินสารอินทรีย์ ขนาด 65 kW เมื่อมีการเปลี่ยนอัตราการไหลของน้ำร้อน ที่อุณหภูมิของน้ำร้อนขาเข้าเครื่องทำระเหย 116°C

ดังนั้นในรูปที่ 5 และ 6 เมื่อกำหนดกำลังการผลิตไฟฟ้าสุทธิที่ 35kW และ 65 kW และอุณหภูมิน้ำร้อนขาเข้าเครื่องทำระเหยให้คงที่ที่ 116°C เนื่องจากให้ค่าประสิทธิภาพเชิงความร้อนสูงที่สุด เมื่ออัตราการไหลของน้ำร้อนเพิ่มขึ้น ต้นทุนการผลิตไฟฟ้าของชีวมวลชนิดต่างๆ จะลดลง เนื่องจากความร้อนที่ใช้ในการผลิตน้ำร้อนลดลง โดยโรงไฟฟ้าวัฏจักรแรงคินสารอินทรีย์ขนาด 35 และ 65kW เมื่อมีการใช้ชีวมวลชนิดทะลายปาล์มจะมีต้นทุนการผลิตไฟฟ้าต่ำที่สุด เทียบกับชีวมวลชนิดอื่น โดยมีค่าเท่ากับ 6.66 และ 4.85 บาท/kWh ตามลำดับ

สาเหตุที่ทำให้ทะลายปาล์มมีต้นทุนการผลิตไฟฟ้าต่ำเพราะถึงแม้ว่าค่าความร้อน (LHV) ทะลายปาล์มจะมีค่าต่ำและใช้ปริมาณมากในการเผาให้ความร้อนน้ำร้อนแต่ทะลายปาล์มนั้นมีราคาต่อตันค่อนข้างถูกทำให้ต้นทุนการผลิตไฟฟ้าต่ำ โดยเมื่อเปรียบเทียบ ยอดและใบอ้อยที่มีต้นทุนการผลิตไฟฟ้าใกล้เคียงกับทะลายปาล์ม ซึ่งราคาต่อตันจะมีราคาแพงแต่สามารถชดเชยด้วยค่าความร้อนที่มีค่าสูง ทำให้ปริมาณชีวมวลที่ใช้ในโรงไฟฟ้าจึงมีค่าต่ำ ต้นทุนการผลิตไฟฟ้าจึงต่ำด้วยเช่นกัน ดังผลแสดงในตารางที่ 3 และตารางที่ 4 ในภาคผนวก

ตารางที่ 3 ตัวอย่างปริมาณชีวมวลที่ต้องใช้ตลอดทั้งปี เมื่อใช้โรงไฟฟ้าวัฏจักรแรงคินสารอินทรีย์ ขนาด 65 kW อัตราการไหลและอุณหภูมิขาเข้าของน้ำร้อนเครื่องทำระเหยเท่ากับ 12.6 l/s และ 116°C ตามลำดับ

ชนิดของชีวมวล	LHV (kJ/kg)	ราคา (บาท/ตัน)	ปริมาณชีวมวลเหลือใช้ (ตัน/ปี) [10]	ปริมาณชีวมวลที่ต้องใช้ตลอดทั้งปี (ตัน/ปี)
ทะลายปาล์ม	7,540	514	1,024,868	2033.45
ยอดและใบอ้อย	15,479	1,125	4,190,794	951.11

4. สรุปผลการศึกษา

ความร้อนจากชีวมวลที่ใช้ในการผลิตน้ำร้อนเพื่อป้อนอัตราความร้อนให้เครื่องทำระเหยจะมีปริมาณลดลงเมื่ออัตราการไหลเพิ่มขึ้น และอุณหภูมิของน้ำร้อนขาเข้าเครื่องทำระเหยมีค่าต่ำ โดยวัฏจักรแรงคินสารอินทรีย์ขนาด 35 kW และ 65 kW อัตราการไหล 12.6 l/s อุณหภูมิของน้ำร้อนขาเข้าเครื่องทำระเหยเท่ากับ 116°C มีประสิทธิภาพของวัฏจักร 16.9% และ 16.53% ตามลำดับ เมื่อทำการศึกษาเศรษฐศาสตร์พบว่าโรงไฟฟ้าวัฏจักรแรงคินสารอินทรีย์ขนาด 35 kW และ 65 kW ที่ใช้ชีวมวลชนิดทะลายปาล์มจะมีต้นทุนการผลิตไฟฟ้าต่ำที่สุดคือ 6.66 และ 4.85 บาท/kWh ตามลำดับ

5. กิตติกรรมประกาศ

ขอขอบคุณบัณฑิตวิทยาลัย มหาวิทยาลัยเชียงใหม่ และ ศูนย์ความเป็นเลิศด้านพลังงานสะอาดและการพัฒนาทรัพยากรธรรมชาติที่ยั่งยืน ภายใต้โครงการการพัฒนามหาวิทยาลัยวิจัย มหาวิทยาลัยเชียงใหม่

เอกสารอ้างอิง

[1] กระทรวงพลังงาน (2554). แผนปฏิบัติการอนุรักษ์พลังงาน 20 ปี (2554-2573). [ระบบออนไลน์] แหล่งที่มา: http://www.eppo.go.th/encon/ee-20yrs/EEDP_Thai.pdf [2556, 20 ตุลาคม].

[2] กรมพัฒนาพลังงานทดแทนและอนุรักษ์พลังงาน (2554). แผนพัฒนาพลังงานทดแทนและพลังงานทางเลือก 25% ใน 10 ปี (2555-2565). [ระบบออนไลน์] แหล่งที่มา: http://www.dede.go.th/dede/images/stories/aedp25.pdf [2556, 20 ตุลาคม].

[3] กรมพัฒนาพลังงานทดแทนและอนุรักษ์พลังงาน (2554). ศักยภาพชีวมวลในประเทศไทย. [ระบบออนไลน์] แหล่งที่มา: http://www.dede.go.th [2557, 25 พฤษภาคม].

[4] เบญจมาศ ปุยอ๊อก วิชชากร จารุศิริ และจินตนา อุบลวัฒน์ (2550). การศึกษาศักยภาพการผลิตไฟฟ้าจากเศษวัสดุเหลือใช้ทางการเกษตร. การประชุมเชิงวิชาการเครือข่ายพลังงานแห่ง ประเทศไทยครั้งที่ 3, โรงแรมใบหยกสกาย, กรุงเทพมหานคร, 23-25 พฤษภาคม 2550.

[5] วีรชัย อาจหาญ (2553). การศึกษาต้นแบบโรงงานผลิตเชื้อเพลิงชีวมวลสู่ชุมชน. *รายงานการวิจัย*, มหาวิทยาลัยเทคโนโลยีสุรนารี, สิงหาคม 2553.

[6] จักรพันธ์ ถาวรงามยิ่งสกุล และทนงเกียรติ เกียรติศิริโรจน์ (2554). การศึกษาเชิงเศรษฐศาสตร์โรงไฟฟ้าวัฏจักรแรงคินที่ใช้สารอินทรีย์ที่ใช้แกลบเป็นเชื้อเพลิง. การประชุมสัมมนาเชิงวิชาการรูปแบบพลังงานทดแทนสู่ชุมชนแห่งประเทศไทย ครั้งที่ 4, มหาวิทยาลัยราชภัฏลำปาง, ลำปาง, 28-30 พฤศจิกายน 2554.

[7] Energy for Environment Foundation. Biomass. Q print management, Bangkok, 2008.

[8] สำนักงานนโยบายและแผนพลังงาน กระทรวงพลังงาน (2556). แนวคิดการกำหนดโครงสร้างราคารับซื้อไฟฟ้า แบบ Feed-in tariff สำหรับกลุ่มพลังงานชีวภาพ. [ระบบออนไลน์] แหล่งที่มา: http://www.eppo.go.th/FIT/part2.pdf [2557, 5 มิถุนายน].

[9] ธนาคารกรุงเทพ. อัตราดอกเบี้ยเงินให้สินเชื่อ. [online] Available: http://www.bangkokbank.com [2557, 2 มิถุนายน].

[10] กรมพัฒนาพลังงานทดแทนและอนุรักษ์พลังงาน. ศักยภาพชีวมวลในประเทศไทย. [ระบบออนไลน์] แหล่งที่มา: http://www.dede.go.th/ [2557, 1 มิถุนายน].

[11] ElectraTherm's waste heat-to-power system uses a closed loop Organic Rankine Cycle [online] Available: http://electratherm.com/docs/6500Brochure20140321.pdf [2557, 15 มิถุนายน].

[12] The Green Machine 4200 Specification Sheet [Online] Available: http://electratherm.com/docs/SS-4200GreenMachine20140326.pdf [2557, 5 มิถุนายน].

[13] The Green Machine 4400 Specification Sheet [Online] Available: http://electratherm.com/docs/SS-6500GreenMachine20140326.pdf [2557, 5 มิถุนายน].

[14] European Wood-Heating Technology Survey [Online] Available: https://www.nyserda.ny.gov/Publications/Research-and-Development-Technical-Reports/Other-Technical-Reports/European-Wood-Heating-Technology-Survey.aspx [2557, 5 มิถุนายน].

[15] Pitz-Paal, R., Dersch, J., & Milow, B. European Concentrated Solar Thermal Road-Mapping Research Report on SES6-CT-2003-502578. European Commission. 2003.

สัญลักษณ์

C_{invest} = ค่าลงทุนเบื้องต้น (Baht)

$\dot{C}_{o\&m}$ = ค่าใช้จ่ายในการดำเนินงานและซ่อมบำรุง (Baht/year)

$\dot{C}_{biomass}$ = ค่าใช้จ่ายเนื่องจากเชื้อเพลิงชีวมวล (Baht/year)

E_{Net} = อัตราไฟฟ้า (kWh)

H = ชั่วโมงการทำงาน (Hour/year)

h = เอนทาลปีจำเพาะ (kJ/kg)

i_d = อัตราดอกเบี้ยทบต้น (%)

$k_{Insurance}$ = อัตราประกันภัยรายปี (%/year)

$\dot{m}_{cw}$ =อัตราการไหลของน้ำเย็น (kg/s)

$\dot{m}_{hw}$ =อัตราการไหลของน้ำร้อน (kg/s)

$\dot{m}_R$ =อัตราการไหลของของไหลทำงาน (kg/s)

n = อายุโครงการ (year)

P = ความดัน (kPa)

$\dot{Q}_C$ = อัตราความร้อนที่สูญเสียจากเครื่องควบแน่น (kW)

$\dot{Q}_E$ = อัตราความร้อนที่ให้แก่เครื่องระเหย (kW)

T = อุณหภูมิน้ำ (°C)

v_1 = ปริมาตรจำเพาะที่สภาวะที่ 1 (m^3/kg)

$\dot{W}_p$ = กำลังงานที่ป้อนเข้าปั๊ม (kW)

$\dot{W}_T$ = กำลังงานที่เทอร์ไบน์ได้จากวัฏจักร (kW)

ภาคผนวก

The Green Machine			4200 Up to 35kWe	4400 Up to 65kWe
Hot Water Input Parameters	Hot water input temp range	°F	170 - 240	170 - 240
		[°C]	[77-116]	[77-116]
	Thermal input range	MMBTU/hr	1.02-1.71	1.02-2.9
		[kWth]	[300-500]	[300-860]
	Flow rate range	gpm	50-200	50-200
		[l/s]	[3.2-12.6]	[3.2-12.6]
Water Cooled Condensing Parameters	Cooling water input temp range	°F	40 - 110	40 - 110
		[°C]	[4-43]	[4-43]
	Heat rejected to cooling water range	MMBTU/hr	1.3 - 1.4	1.3 - 2.7
		[kWth]	[380-410]	[380-795]
	Cooling water flow rate	gpm	220	350
		[l/s]	[13.9]	[22.1]
Air Condensing Conditions	Ambient air temp	°F	NA	<100
		[°C]	NA	[<38]
	Heat rejected to condenser	MMBTU/hr	NA	1.3 - 2.7
		[kWth]	NA	[380-795]

รูปที่ 7 พารามิเตอร์สมรรถนะของวัฏจักรแรงคินสารอินทรีย์ขนาด 35kW และ 65kW [12], [13]

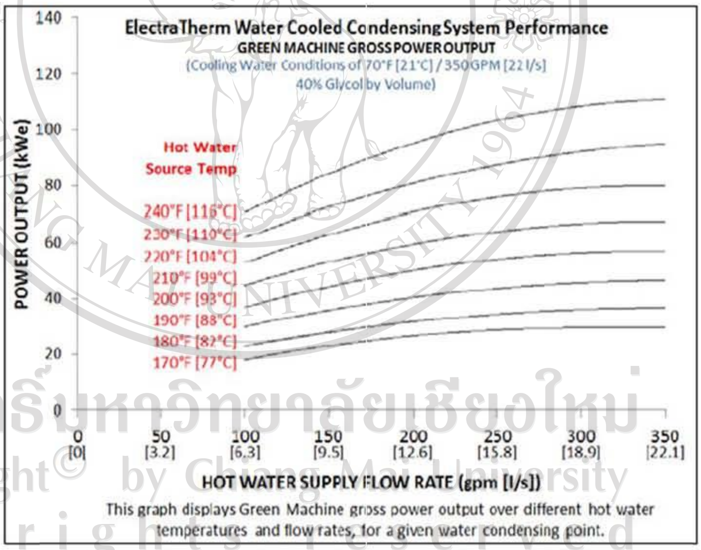

รูปที่ 8 กราฟแสดงสมรรถนะของน้ำร้อนที่อุณหภูมิและอัตราการไหลต่างๆ [11]

92

ตารางที่ 4 ตัวอย่างการคำนวณที่น้ำร้อน 116 °C และอัตราการไหล 12.6 l/s

ชีวมวล	ปริมาณชีวมวลเหลือใช้ [10]	กำลังไฟฟ้าสุทธิ	ชั่วโมงการทำงาน	ผลิตไฟฟ้าทั้งปี	ประสิทธิภาพหม้อต้ม	กระบวนการความร้อน	ปริมาณความร้อนที่ต้องใช้ตลอดทั้งปี	ปริมาณชีวมวลที่ต้องใช้ตลอดทั้งปี	ราคาชีวมวลที่ต้องจ่ายต่อปี	**Investment Cost, C_{invest}**	$\dot{C}_{o\&m}$	*crf*	*LEC*
ชนิด	ตัน/ปี	**kW**	ชม	**kWh**	**%**	**kW**	**kJ/ปี**	ตัน/ปี	บาท/ปี	บาท	บาท/ปี		**บาท/kWh**
ยอดและใบอ้อย	4,190,794							951.11	1,069,993				4.90
แกลบ	3,510,599							1089.16	1,742,654				6.19
ฟางข้าว	25,646,548							1194.01	1,462,664				5.65
ซังข้าวโพด	584,539	65	8,000	520,000	75	383.38	1.47×10^{10}	1531.17	1,684,282	11,048,857	386,710.01	0.098567	6.08
ทะลายปาล์ม	1,024,868							2033.45	1,045,192				4.85
เหง้ามันสำปะหลัง	1,834,467							2679.68	2,545,695				7.73
ไม้ยางพารา	312,118							1711.88	2,225,443				7.12

Deethayat T. and Kiatsiriroat T.

"Reduction of Irreversibilities in Organic Rankine Cycle by Non-Azeotropic Working Fluid,"

The Fifth International Conference on Science, Technology and Innovation for Sustainable Well-Being, 4-6 September 2013, Luang Prabang, Lao PDR.

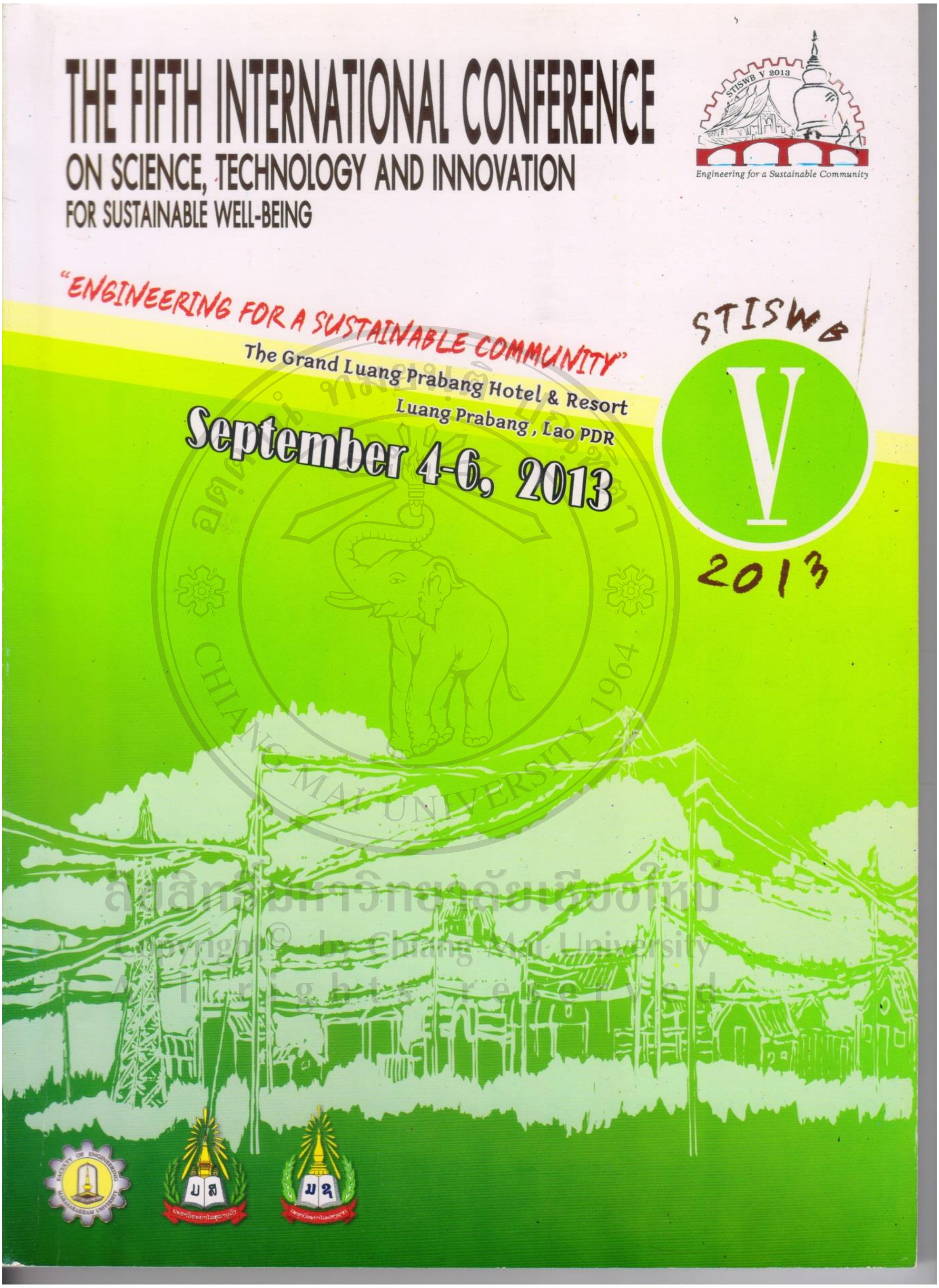
THE FIFTH INTERNATIONAL CONFERENCE
ON SCIENCE, TECHNOLOGY AND INNOVATION
FOR SUSTAINABLE WELL-BEING
STISWB V 2013
Engineering for a Sustainable Community
"ENGINEERING FOR A SUSTAINABLE COMMUNITY"
The Grand Luang Prabang Hotel & Resort
Luang Prabang, Lao PDR
September 4-6, 2013
STISWB
V
2013

14.45-15.00 CIE08 **Strength and Permeability of Fly Ash Concrete Exposed to Various Temperatures**
Natthapong Ladbut, Maneerat Ongwandee and Sahalaph Homwuttiwong
Mahasarakham University, Thailand

15.00-15.15 CIE09 **Utilization of Ceramic Waste as Coarse Aggregate in Concrete**
Wantana Papaporn and Sahalaph Homwuttiwong
Mahasarakham University, Thailand

Session ***Mechanical and Manufacturing Engineering (MME)***
Chairman ***Asst. Prof. Dr. Nitipong Soponpongpipat (SU, Thailand)***
Co-Chairman ***Asst. Prof. Bopit Bubphachot (MSU, Thailand)***
Date ***September 5,2013***
Time ***15.45-18.00***
Room ***2***

15.45-16.00 MME28 **Silver Nano-Ethanol Mixture Effect on Heat Transfer Performance in n Closed-loop Oscillating Heat-pipe with Check Valve (CLOHP/CV)**
Nipon Bhuwakietkumjohn and Thanya Parametthanuwat
King Mongkut's University of Technology North Bangkok, Thailand

16.00-16.15 MME29 **Effect of Process Parameters on Surface Roughness of Turned Parts**
On-Uma Lasunon and Nattarat Saenmeema
Mahasarakham University, Thailand

16.15-16.30 MME30 **Removal of Submicron Soot Particles in Exhaust Combustible Gas with Pulse-Energized Electrostatic Precipitator**
Vishnu Thonglek and Tanongkiat Kiatsirriroat
Chiang Mai University, Thailand

16.30-16.45 MME31 **Energy Saved by Using Cooling Pad with Split Type Air Conditioning System**
Nipon Bhuwakietkumjohn and Supachoke Saengswarng
King Mongkut's University of Technology North Bangkok, Thailand

16.45-17.00 MME32 **Reduction of Irreversibilities in Organic Rankine Cycle by Non-Azeotropic Working Fluid**
Thoranis Deethayat and Tanongkiat Kiatsiriroat
Chiang Mai University, Thailand

The Fifth International Conference on Science, Technology and Innovation for Sustainable Well-Being (STISWB V) , 4-6 September 2013, LuangPrabang, Lao PDR

Reduction of Irreversibilities in Organic Rankine Cycle by Non-Azeotropic Working Fluid

Thoranis Deetayat, Tanongkiat Kiatsirriroat
Energy Engineering Program, Faculty of Engineering, Chiang Mai University, Thailand
E-mail: thoranisdee@gmail.com

Abstract

In this study, a concept of non-azeotropic(NA) working fluid of which the temperatures during boiling and condensation are changing with the temperatures of heat source and heat sink, respectively, was considered in organic Rankine cycle (ORC) for power generation. Due to the temperature differences in the cycle evaporator and condenser were less than those of the single working fluid during heat exchanging then the irreversibilities in these components could be reduced which resulted in higher work output. In this paper, R 245fa/R152anon-azeotropic refrigerant at different compositions was used as a working in a 50 kW ORC. The thermodynamic properties were used to evaluate the cycle performances and the results were compared with those of R245fa which was a single component working fluid. The simulated results showed that the irreversibilities at the evaporator and the condenser of the ORC with the NA working fluid were less than those of the single component which resulted in higher cycle efficiency. Higher the composition of R152a could reduce the irreversibilites but there was a limit of the R 152a composition due to its high flammability and GWP.

Keywords: organic Rankine cycle, non-azeotropic working fluid, irreversibilities, power generation

1. Introduction

Organic Rankine cycle (ORC) is a kind of Rankine cycle of which the working fluid has a low boiling point thus the unit could operate with a low heat source temperature such as low temperature waste heat, geothermal heat, solar energy or biomass combustion for generating electricity.Various groups of working fluids, wet, isentropic and dry fluids, such as benzene, ammonia, and some CFC, HFC refrigerants have been analyzed to be used in the cycle [1, 2]. For small ORC with solar energy application, R 134a was found to be one of the most suitable working fluid in terms of cycle efficiency, mass flow rate, pressure ratio, toxicity, flammability, ODP and GWP [2]. Recently, there was a report showed that the suitable working fluids for low temperature heat source were R123 and R245fa [3].

During heat exchanging in the evaporator and the condenser of the ORC cycle, there were temperature difference between the streams of the heat source and the heat sink with the ORC working fluid, respectively. The temperature differences generate irreversibilities at the cycle components then some part of the cycle work was destroyed.

Use of non-azeotropic (NA) fluid in the ORC is one method to reduce the temperature differences between those of the heat source and the heat sink with the ORC working fluid. Since the temperature of the NA fluid is changing during a phase change then the temperature of the working fluid could follow those of the heat source and the heat sink streams at the evaporator and the condenser, respectively with smaller temperature differences compared with the single working fluid. Consequently, the irreversibilities during the heat exchanges are less which results in higher cycle work output. Moreover, some working fluid blend might be more friendly to the environment. The ODP or GWP will be less than those of the single component [4].

In this study, performance analyses of a 50 kW ORC with R245fa/R152a at various compositions were studied. With a hot water stream at 85-115℃ as a heat source at the evaporator and a cool water stream fixed at 40℃ was a heat sink at the condenser, the irreversibilities during the heat exchanging and the cycle efficiency were evaluated. The results were compared with that when R245fa was the working fluid.

2. Organic Rankine Cycle Model

A diagram of the basic ORC system is shown in Fig. 1. The system consists of an evaporator, a turbine, a condenser and a pump. The working fluid leaves the condenser is designated as saturated liquid (state 1) and the pump supplies the working fluid to the evaporator (state 2) where it is heated and vaporized by a heat source. The generated high pressure vapor or high pressure superheated vapor (state 3) flows through the turbine to produce power. The low pressure vapor then exits the turbine (state 4) and enters into the condenser to reject heat to a heat sink. The condensed working fluid at the condenser outlet is pumped back to the evaporator. The described processes are shown in a T-s diagram in Fig. 2. It could be noted that the temperature differences between the heat source and the heat sink streams with cycle working fluid for the NA fluid were less than those of the single fluid.

Detailed analysis of the ORC system is summarized as follows:

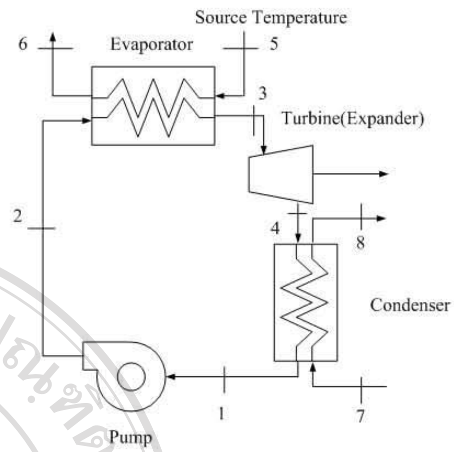

Fig. 1 The components in a basic ORC.

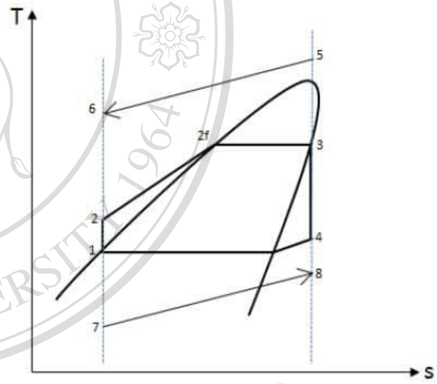

a. For single working fluid

2

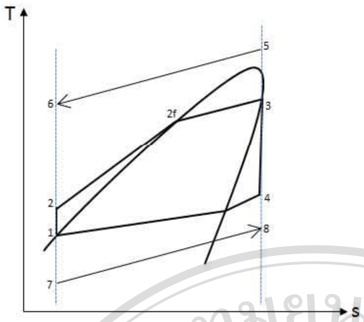

b. For NA fluid

Fig.2 T-s diagrams of the ORC.

The 1st law efficiency, η:

$$\eta = \frac{(h_3-h_4)-(h_2-h_1)}{(h_3-h_2)}. \quad (1)$$

Irreversibilities, I,
at evaporator:

$$I = \dot{m}_w[(h_5-h_6)-T_0(s_5-s_6)]\text{-}\dot{m}_R[(h_3-h_2)-T_0(s_3-s_2)]. \quad (2)$$

at condenser:

$$I = \dot{m}_w[(h_4-h_1)-T_0(s_4-s_1)]\text{-}\dot{m}_R[(h_8-h_7)-T_0(s_8-s_7)]. \quad (3)$$

The 2nd law efficiencies, ε:

$$\varepsilon = \frac{\dot{m}_R[(h_3-h_4)-(h_2-h_1)]}{\dot{m}_w[(h_5-h_6)-T_0(s_5-s_6)]}. \quad (4)$$

The conditions for the ORC analysis were as follows:

1. Cooling water temperature at the condenser was at 28°C.
2. Evaporation temperatures ranged from 85 to 115°C.
3. The saturation liquid temperatures at the evaporator and the condenser pressures were at 70 and 40°C, respectively.
4. Isentropic efficiency of pump (η_{PUMP}) was 1.
5. Isentropic efficiency of turbine (η_{TUR}) was 1.
6. The turbine work was at 50 kW.
7. The thermal-physical properties of the working fluids were evaluated from REFPROP [5].
8. The set pinch-point temperatures between the heat exchanging fluids (ΔTPP) at the evaporator and the condenser were 6°C and 3°C, respectively.
9. The compositions of the R245fa/R152a were 95%/5%, 90%/10% and 85%/5% by mass.

3. Results and Discussions

Fig. 3 showed the first law efficiencies of the ORC with R245fa and R245fa/R152a as working fluids. Higher heat source temperature resulted in higher efficiencies. It could be noted that the NA fluid gave better performance since there were gliding temperatures during heat exchanges in the evaporator and the condenser thus the total area in the T-s diagram which represented the total work output was higher than that of the single fluid.

Fig. 4 and 5 showed irreversibilities in the evaporator and the condenser of the ORC, respectively, when the cycle working fluids were R245fa and R245fa/R152a. It could be seen that the irreversibilities at the evaporator decreased compared with those of the single fluid due to lower temperature gaps between the heat exchanging fluids. For the working fluid blend, as the composition of R152a increased, it was found that the temperature gap was reduced then less irreversibility was obtained. The results were similar for the condenser.

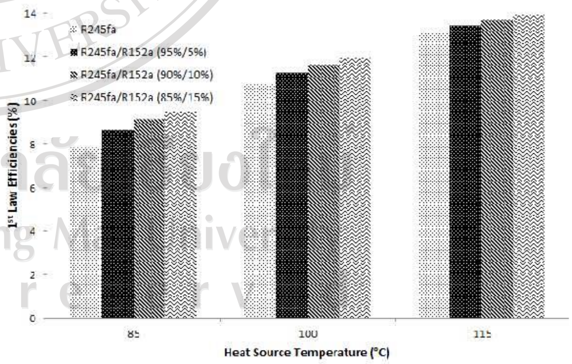

Fig.3 The 1st law efficiencies of the ORC.

3

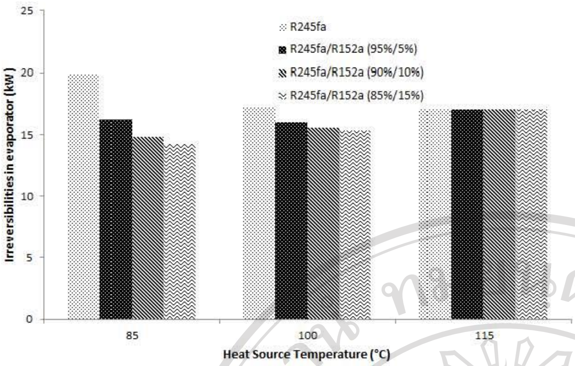

Fig.4 Irreversibilities in the evaporator

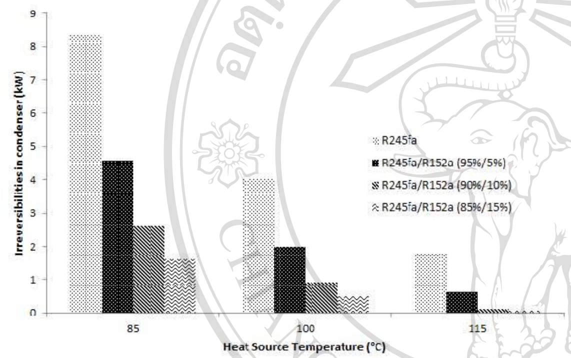

Fig.5 Irreversibilities in the condenser

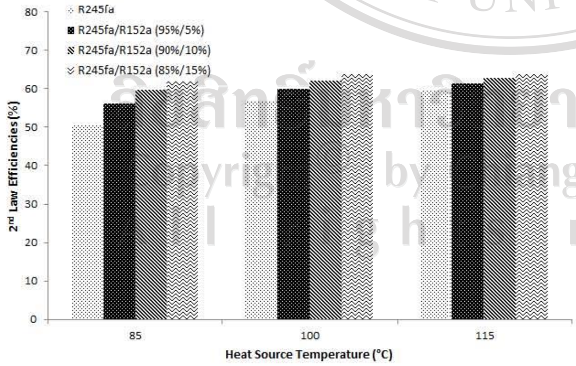

Fig.6 The 2nd efficiencies of the ORC.

Fig.6 showed the second law efficiency of the ORC with the above working fluids. Due to lower irreversibilities in the evaporator and the condenser for the NA working fluid, higher cycle work was obtained compared with the single working fluid. Again, as the composition of R152a was higher, better cycle performance was obtained. Anyhow, there is a limit of R152a composition that the value should not over 30 % by mass due to its high flammability and it also generates high GWP [6].

4. Conclusion

R245fa/R152a, a non-azeotropic refrigerant was used as a working in a 50 kWe ORC. The thermodynamic properties at various compositions of R 152a were used to evaluate the cycle performances and the results were compared with those of R245fa. The simulated results showed that the irreversibilities at the evaporator and the condenser of the ORC with the NA working fluid were less than those of the single component. Higher the composition of R152a could reduce the irreversibilites and increase the cycle efficiency. However, a limit of the R 152a composition due to its high flammability and GWP should be considered.

5. Acknowledgement

The authors would like to acknowledge the Commission on Higher Education, Thailand for the financial support; Graduate School, and Faculty of Engineering, Chiang Mai University for the testing facilities and some partial supports.

6. References

[1] Hung, T. C., Shai, T. Y. and Wang, S. K., A review of organic Rankine cycles (ORCs) for the recovery of low-grade waste heat, Energy, Vol. 22, pp. 661-667, 1997..
[2] Bertrand, F. T., George, P., Gregory, L. and Antonios, F., Fluid selection for a low temperature solar Organic Rankine cycle, Applied Thermal Engineering, vol. 29, pp. 2468-2476, 2009.
[3] Thawonngamyingsakul, C. and Kiatsiriroat, T., Working fluid selection for a low-to-intermediate temperature Organic Rankine cycle, The 2nd Conference on Science, Agriculture, Engineering and Environment,

August 25, 2010, Payao University, Thailand (in Thai).
[4] Mohanraj, M., Muraleedharan, C. and Jayaraj, S., A review on recent developments in new refrigerant mixtures for vapour compression-based refrigeration, air-conditioning and heat pump units, International Journal of Energy Research, vol. 35, pp.647-669, 2011.
[5] National Institute of Standard and Technology (NIST). REFPROP Version 7, Thermodynamic Properties of Refrigerants and Refrigerant Mixtures Software. 2000.
[6] Wang, J.K., Zhao, L., Wang, X.D., A comparative study of pure and zeotropic mixtures in low-temperature solar Rankine cycle, Applied Energy, vol. 87, pp.3366-73, 2010.

Deethayat T., Asanakham, A. and Kiatsiriroat T.

"A Study on Modular Organic Rankine Cycle with Biomass for Power Generation in Small Community"

Asia Pacific Network for Sustainable Agriculture, Food and Energy, 17-18 November 2015, Ho Chi Minh, Vietnam.

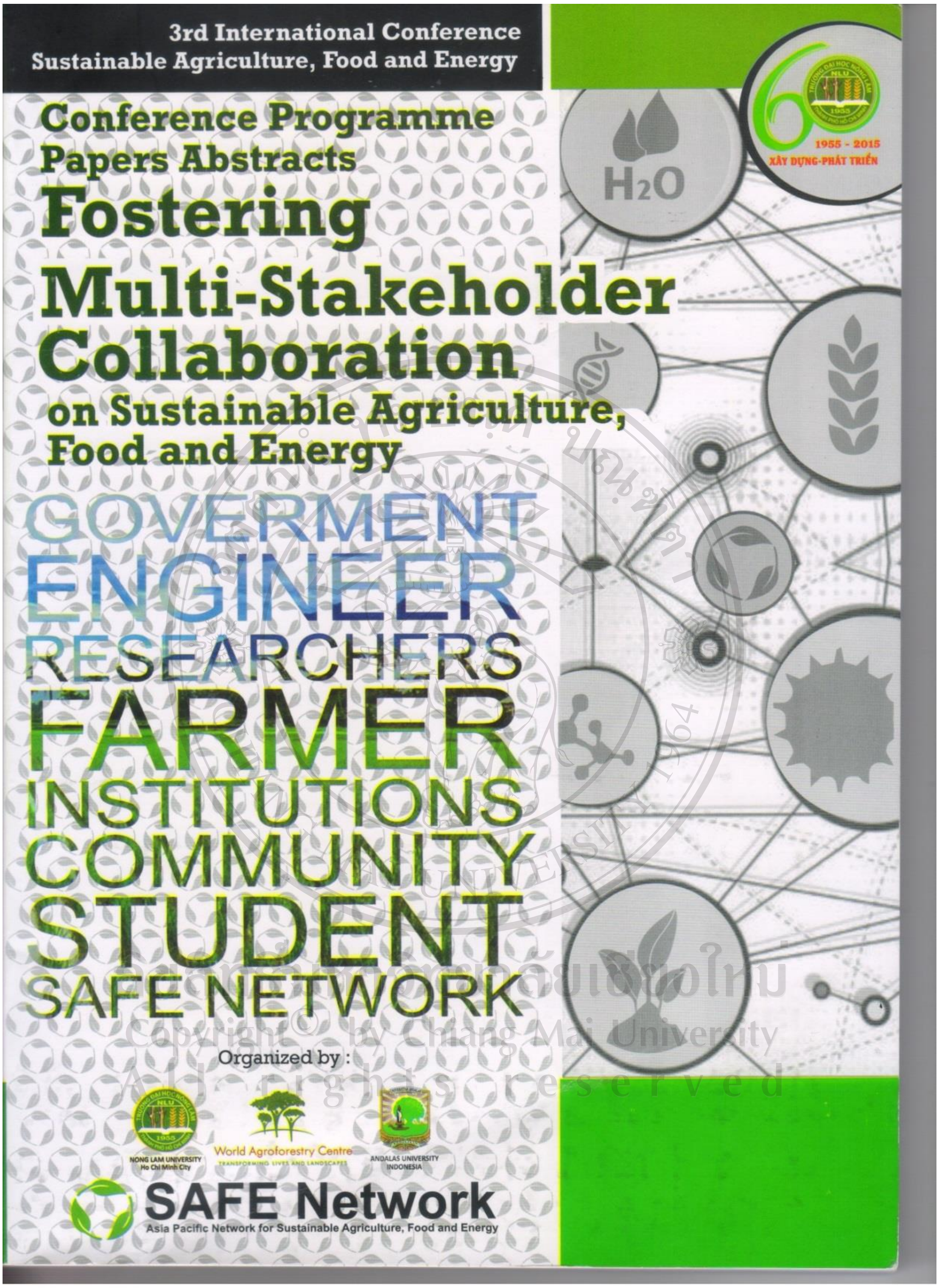
3rd International Conference
Sustainable Agriculture, Food and Energy
Conference Programme
Papers Abstracts
Fostering
Multi-Stakeholder
Collaboration
on Sustainable Agriculture,
Food and Energy
GOVERMENT
ENGINEER
RESEARCHERS
FARMER
INSTITUTIONS
COMMUNITY
STUDENT
SAFE NETWORK
Organized by :
NONG LAM UNIVERSITY Ho Chi Minh City
World Agroforestry Centre
ANDALAS UNIVERSITY INDONESIA
SAFE Network
Asia Pacific Network for Sustainable Agriculture, Food and Energy
H2O
1955 - 2015
XÂY DỰNG-PHÁT TRIỂN

E-03

A Study on Modular Organic Rankine Cycle with Biomass for Power Generation in Small Community

Thoranis Deetayat[#], Attakorn Asanakham[*], Tanongkiat Kiatsiriroat[*]
[#] Energy Engineering Program, Faculty of Engineering, Chiang Mai University, Thailand
[*] Department of Mechanical Engineering, Faculty of Engineering, Chiang Mai University, Chiang Mai, 50200, Thailand
corresponding author : thoranisdee@gmail.com

Abstract: In this study, a potential on power generation from a modular organic Rankine cycle (ORC) power plant with biomass as fuel was considered. The scales on net power generation were at 20 kW_e and 100 kW_e and thesesizes could be implemented in small community. The values of unit cost of generated electricity (UCE) for the basic ORC and the ORC in a form of combined heat and power (CHP-ORC) were evaluated with various biomass fuels. The operating period was 8 hr/day and the real debt interest rate was 6%. For palm fruit bunch compared with other biomass residues, the UCEs were found to be lowest. For the basic ORC, and the CHP-ORC, the UCEs of 20 kW_e were 6.65 and 4.44 Baht/kWh, respectively. The UCEs of 100 kW_e were cheaper which were 4.69 and 3.88 Baht/kWh, respectively. By sensitivity analysis, it was found that the UCE was decreased when the operating hour was increased and the value increased following the unit cost of palm fruit bunch and the real debt interest rate.

Keywords : Modular organic Rankine cycle; Sensitivity Analysis; Unit cost of electricity; Biomass fuel

---

E-04

Chemical Kinetics in Biodiesel Production from Used Cooking Oil with Methanol/Ethanol Reagent under Electric Field

Attakorn Asanakham[#], Supakrit Ngammuang[*] and Tanongkiat Kiatsiriroat[#]
[#]Department of Mechanical Engineering, Faculty of Engineering, Chiang Mai University,
[*]Energy Engineering Program, Faculty of Engineering and Graduate School, Chiang Mai University Chiang Mai 50200, Thailand
corresponding author : attakorn_asanakham@hotmail.com

Abstract: In Thailand, biodiesel production process uses methanol or ethanol in biodiesel transesterification. Methanol is imported andsince it comes from petroleum product therefore it gives some impact to the environment. On the other hand, ethanol comes from agricultural feedstock thus it is more friendly to the environment. Anyhow, it could be found that consumption of ethanol volume was rather high and longer reaction time for biodiesel production compared with methanol and in addition, the ethanol is more expensive.Suitable compositions of methanol/ethanol should be found to get the biodiesel production of which the cost is not expensive and the process is green. This research is to study chemical kinetics on transesterification reaction of used cooking oil with methanol/ethanol reagent to generate biodiesel in term of mixture of esters. The process was performed under a barrier discharge electric field of which very short reaction period could be performed with very low energy consumption. The electric field at ~10 kV was generated by a rod electrode mounted at the cylinder axis and a set of a spiral electrode coil wrapped around a cylindrical glass reactor. In each experiment, 1000 ml of used vegetable cooking oil was taken as a feedstock for the reaction and KOH at 5 g was taken as the catalyst. The tests were performed with various compositions of the reagent mixture (methanol/ethanol, %mol/mol), 100:0, 80:20, 70:30 and 60:40 and the starting temperatures were controlled in range of 43-44°C. It was found that higher percentage of ethanol resulted in lower biodiesel yield and longer the reaction time. The biodiesel yields were found to be 92.73, 80.48, 78.98and 74.94% of the used cooking oil amount, respectively. The chemical kinetics of the transesterification could be found as follows: Ratio of methanol/ethanol (100:0) k = 0.0045 s-1 , Ea = 15.201 kJ/mol; Ratio of methanol/ethanol (80:20) k = 0.0021 s-1 , Ea = 19.611 kJ/mol; Ratio of methanol/ethanol (70:30) k = 0.0018 s-1 , Ea = 30.683 kJ/mol; Ratio of methanol/ethanol (60:40) k = 0.0013 s-1 , Ea = 37.860 kJ/mol where k and Ea are reaction constant in s-1and activation energy in kJ/mol, respectively.

Keywords : Biodiesel, Methanol/ethanol reagent, Electric field, Chemical kinetics.

A Study on Modular Organic Rankine Cycle with Biomass for Power Generation in Small Community

Thoranis Deethayat[#], Attakorn Asanakham*, Tanongkiat Kiatsiriroat*

[#] *Energy Engineering Program, Faculty of Engineering, Chiang Mai University, Chiang Mai, 50200, Thailand*
E-mail: thoranisdee@gmail.com

* *Department of Mechanical Engineering, Faculty of Engineering, Chiang Mai University, Chiang Mai, 50200, Thailand*

Abstract— **In this study, a potential on power generation from a modular organic Rankine cycle (ORC) power plant with biomass as fuel was considered. The scales on net power generation were at 20 kW_e and 100 kW_e and these sizes could be implemented in small community.**

The values of unit cost of generated electricity (UCE) for the basic ORC and the ORC in a form of combined heat and power (CHP-ORC) were evaluated with various biomass fuels. The operating period was 8 hr/day and the real debt interest rate was 6%. For palm fruit bunch compared with other biomass residues, the UCEs were found to be lowest. For the basic ORC, and the CHP-ORC, the UCEs of 20 kW_e were 6.65 and 4.44 Baht/kWh, respectively. The UCEs of 100 kW_e were cheaper which were 4.69 and 3.88 Baht/kWh, respectively.

By sensitivity analysis, it was found that the UCE was decreased when the operating hour was increased and the value increased following the unit cost of palm fruit bunch and the real debt interest rate.

Keywords— Modular organic Rankine cycle; Sensitivity Analysis; Unit cost of electricity; Biomass fuel

I. Introduction

Acceleration of fossil fuel consumption has led to a serious problem such as global warming, ozone layer depletion and air pollution. Hence, recovering waste heat from energy conversion process is quite essential to reduce the fuel consumption. Combined Heat and Power (CHP) is an effective method with simultaneous production of electricity and heat from one fuel source could be obtained. The fuel source could come from biomass, biogas or waste heat. The total cost of the CHP plant, including capital cost, fuel and maintenance cost of capital is normally less than the costs of purchased fuel and power separately. Moreover, the air pollution and the greenhouse gas emission could be reduced.

Various conversion technologies have been used for CHP applications such as steam Rankine cycle, organic Rankine cycle (ORC), gas turbine and internal combustion engine [1].

Focusing on small community application, the ORC having organic fluid as working fluid has been prospected as a suitable conversion technology since it could be used with different kinds of energy sources such as solar thermal energy [2], geothermal energy [3], biomass [4] and waste heat from industrial process [5]. It can recover low grade heat into electricity with sufficient high efficiency.

Biomass is a high potential energy source in Thailand. Agricultural residues or wastes such as rice straw, bagasse and corn cob have a volume of about 59,539,905 tons per year with an energy equivalent to 504,339.40 TJ [6].

In Thailand, very few data on ORC performance has been reported. Thawornngamyingsakul and Kiatsiriroat [7] presented economic consideration of a 2.18 MW organic Rankine cycle with rice husk as heat source. The annual operating hour was 8,000 hr/year and the plant lifespan was 25 year. With the rice husk unit cost of 400-1,600 Baht/ton, the unit cost of electricity (UCE) was 2-3.65 Baht/kWh.

From the previous information, it could be seen that there was a high potential to generate power through the ORC for small community of which the ORC scale could be in a range of 20 – 100 kW. In this paper, a basic ORC for power generation only and an ORC to generate both electricity and thermal heat (combined heat and power, CHP-ORC) with heat source from various kinds of biomass were considered. The selected scales for power generation were 20 kW and 100 kW. Sensitivity analysis of the parameters affecting the UCE was also carried out.

II. THE ORC SYSTEM

Organic Rankine Cycle

A diagram of the basic ORC system is shown in Fig. 1. The system consists of an evaporator, a turbine, a condenser and a pump. The working fluid leaves the condenser is designated as saturated liquid (state 1) and the pump supplies the working fluid to the evaporator (state 2) where it is heated and vaporized by a heat source. The generated high pressure vapor (state 3) flows through the turbine to produce power. The low pressure vapor then exits the turbine (state 4) and enters into the condenser to reject heat to a heat sink. The condensed working fluid at the condenser outlet is pumped back to the evaporator. The described processes are shown in a T-s diagram in Fig. 2.

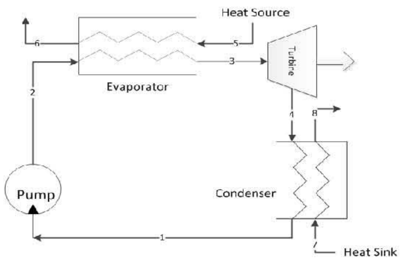

Figure 1 The components in a basic ORC.

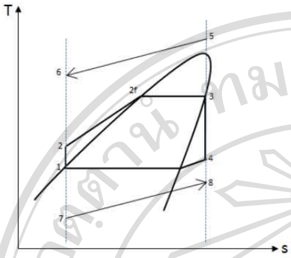

Figure 2 T-s diagram of a basic ORC.

It could be noted that the ORC working fluid in this study was a dry fluid of which the slope of the saturated vapor line was positive in thermodynamic T-s diagram. Then all the fluid during expansion was in superheat region which did not give strong corrosion effect to the expansion device as the two phase fluid.

Combined Heat and Power (CHP)

Combined heat and power (CHP) is an effective energy conversion since simultaneous electricity and useful heat could be generated from one source of energy. In our CHP-ORC as shown in Figure 3, the exhausted gas from biomass combustion could be used for water heating, therefore, higher overall efficiency could be obtained compared with the basic ORC.

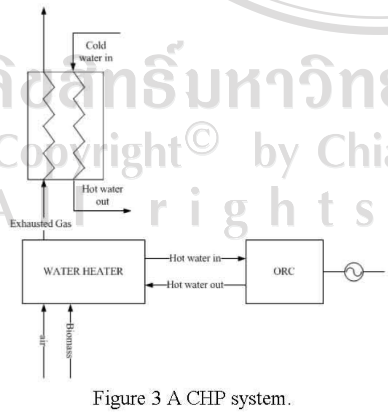

Figure 3 A CHP system.

Biomass

Biomass is organic material that stores energy from natural sources and can be used for energy production such as agricultural waste or residues from production in the agriculture industry such as rice husk from rice milling process, fibrous bagasse from sugar production and wood chips from sawn timber or eucalyptus wood, etc.

Biomass could be converted into energy by various processes such as direct combustion, gasification and fermentation. In this study, thermal heat from biomass to generate electricity and hot water through an ORC was performed by direct combustion in a furnace.

The biomass residues for direct combustion were shown in Table 1. The heating values and the prices of the residues were given. The combustion heat was used to generate hot water for supplying heat at the ORC evaporator as shown in Fig. 3. The exhaust gas was also used to generate hot water for other thermal process.

Table 1. Heating values and prices of biomass residues [8].

Type of Biomass	Ash (%)	Higher heating value (kJ/kg)	Lower heating value (kJ/kg)	Price (Baht/ton)
Rice Husk	12.65	14,755	13,517	1,600
Rice Straw	10.39	13,650	12,330	1,225
Sugar Cane Leaves and Tops	6.10	16,794	15,479	1,125
Rubber wood	1.59	10,365	8,600	1,300
Palm Fruit Bunch	2.03	9,196	7,240	514
Corncob	0.9	11,298	9,615	1,100
Cassava	1.5	7,451	5,494	950
Eucalyptus Bark	2.44	6,811	4,917	700

The heat rate at the ORC evaporator ($\dot{Q}_E$) was assumed to be the same as the heat rate from fuel combustion ($\dot{Q}_{heater}$). The heating efficiency in this study was assumed to be 80% [9] then the heat rate from fuel combustion could be calculated by

$$\dot{Q}_{heater} = n_{WH}(\dot{m}LHV). \quad (1)$$

III. Exergy Analysis

Exergy analysis is generally taken as a tool to analyze energy quality of thermal systems including the energy cost in term of exergy cost rate or exergy costing.

For basic ORC

$$c_e\dot{W}_e = c_{fuel}\dot{E}_{fuel} + \dot{Z}_{WH} + \dot{Z}_{ORC} + \dot{Z}_{O\&M} \quad (2)$$

For CHP ORC

$$c_e(\dot{W}_e + \dot{E}_{HWout}) = c_{fuel}\dot{E}_{fuel} + \dot{Z}_{WH} + \dot{Z}_{ORC} + \dot{Z}_{HX} + \dot{Z}_{O\&M} \quad (3)$$

c_e is the exergy costing. It could be noted that the exergy costings of the power and exergy in hot water generated were assumed to be the same.

Table 2. Cost data used for the thermoeconomic analyses of basic ORC and CHP-ORC.

Investment cost for ORC 20kW	
ORC power plant 20 kW (Baht/unit)	1,500,000
Biomass Hot Water Heater (Baht/unit)	200,000
Heat Exchanger for exhaust gas from biomass (Baht/unit)	20,000
Investment cost for ORC 100kW	
ORC power plant 100 kW (Baht/unit)	4,000,000
Biomass Hot Water Heater (Baht/unit)	2,700,000
Heat Exchanger for exhaust gas from biomass (Baht/unit)	100,000
Operating & Maintenance (O&M) cost	
Operating & maintenance equipment cost (% of investment cost per year)	1
Financial parameters	
Real debt interest rate, i_d (%)	6
Depreciation period, n (year)	20

The conditions for the basic ORC and the CHP-ORC analyses were

1. The power outputs of the ORC were 20 kW and 100 kW.
2. The water heating efficiency from biomass combustion was 80%.
3. Evaporating temperature were 95°C and 125°C for 20 kW_e and 100 kW_e, respectively. Condensing temperature was 35°C
4. Isentropic efficiencies of pump and turbine were 0.7 and 0.8, respectively.
5. Exhausted gas from biomass combustion was 50% of $\dot{Q}_{load}$.
6. Hot and cold water temperature at heat exchanger was 80°C and 28°C, respectively.
7. Effectiveness of heat exchanger (ε) for hot water 80 °C was 0.85.
8. The ORC working fluid was R245fa and the properties were based upon REFPROP [10].

IV. Results

Fig. 4 and Fig. 5 show UCEs of basic ORC and CHP- ORC having net power generations of 20 kW and 100 kW, respectively. The daily operating hour was 8 hr per day, the real debt interest rate was 6% and heat sources of ORC came from various biomasses.

For basic ORC of 20 kW and 100 kW, it could be found that UCE with palm fruit bunch was lowest as 6.65 and 4.69 Baht/kWh, respectively. Even though the LHV of palm fruit bunch was low but the price per ton was cheapest as given in Table 3.

When the exhausted gas from biomass combustion was used to generate hot water in other process (CHP-ORC), for 20kW and 100 kW, it could be found that UCE was decreased. For palm fruit bunch, the UCE was decreased from 6.65 to 4.44 Baht/kWh (20kW ORC) and 4.69 to 3.88 Baht/kWh (100kW ORC).

Since CHP system could generate total output including electricity and useful heating, therefore UCE of the CHP-ORC was cheaper than that of the basic ORC. It could also be found that, when net power generation was increased. The investment cost per kWh was cheaper.

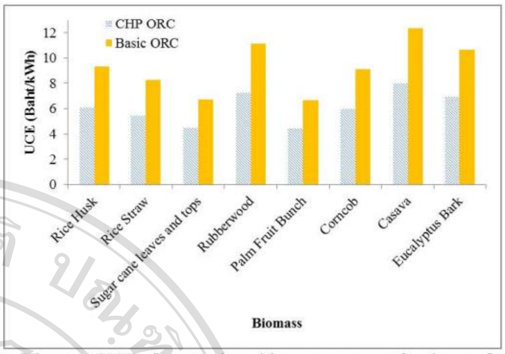

Figure 4 UCEs from various biomass at operating hour of 8hr/day, i_d=6%, the ORC capacity of 20 kW.

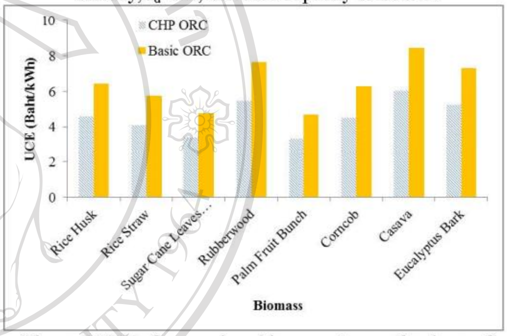

Figure 5 UCEs from various biomass at operating hour of 8hr/day, i_d=6%, the ORC capacity of 100 kW.

Table 3 Utilized biomass for the 100 kW CHP-ORC with operating hour of 8 hr/day.

Biomass Type	LHV (kJ/kg)	Price (Baht/ton)	Residual Potential (ton/year)	Biomass Utilized (ton/year)
Palm Fruit Bunch	7,540	514	1,024,868	1446.99

V. Sensitivity Analysis

In this section, sensitivity analyses of the parameters those affect the electricity unit cost of the CHP-ORC system were considered. The parameters were the palm fruit bunch unit cost of 300-700 Baht/ton, the operating hour of 8-12 hour/day and the real debt interest rate of 6-10%. From Fig. 6, it was found that the palm fruit bunch unit cost and the real debt interest gave the most and least sensitivities on the UCE.

If the 20kW and 100kW CHP-ORCs operated at 12 hours/day, 8% real debt interest rate and palm fruit bunch unit cost of 300 Baht/ton, the unit cost of electricity was 2.75 Baht/kWh and 2.26 Baht/kWh, respectively.

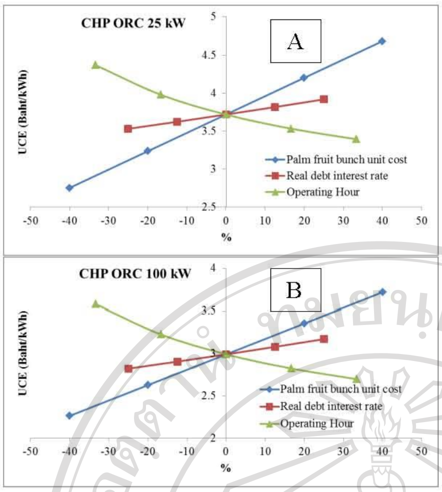

Figure 5 Sensitivity analyses on UCE with varying unit costs of biomass, operating hours and interest rates. The reference conditions are: Palm fruit bunch unit cost = 514 Baht/ton, operating hour= 12hr/day and real debt interest rate =8%.

VI. Conclusion

The unit costs of electricity from the 20 kW and 100 kW CHP-ORCs were cheaper than those of the basic ORC. It was found that with the palm fruit bunch as the energy source, the UCEs for the 20kW and 100kW CHP-ORCs were 4.44 Baht/kWh and 3.88 Baht/kWh, respectively.

The sensitivities on the UCE which were palm fruit bunch unit cost, operating hour and real debt interest rate on the UCE were considered. The results showed that the palm fruit bunch unit cost and the real debt interest gave the most and least effects on the UCE.

VII. Acknowledgements

The authors would like to thank the Graduate School and Thermal System Research Unit, Department of Mechanical Engineering, Chiang Mai University for providing facilities. In addition, the authors would like to acknowledge the Commission on Higher Education under the National Research University Project for the financial support.

VIII. References

[1] Prando D.,Patuzzi F., Pernigotto G., Gasparella A., Baratieri M. (2014). Biomass gasification systems for residential application: an integrated simulation approach, Applied Thermal Engineering, 71:152-60

[2] Wang X.D., Zhao L., Wang J.L. (2011). Experimental investigation on the low-temperature solar Rankine cycle system using R245fa. Energy Conversion and Management, 52 : 946-952.

[3] Heberle F., Bruggemann D. (2010). Exergy based fluid selection for a geothermal Organic Rankine Cycle for combined heat and power generation. Applied Thermal Engineering, 30 : 1326-1332.

[4] Drescher U., Bruggemann D. (2007) Fluid selection for the organic Rankine cycle in biomass power and heat plants. Applied Thermal Engineering, 27:223-8.

[5] Zhou N.J., Wang X.Y., Chen Z., Wang Z.Q. (2013) Experiment study on organic Rankine cycle for waste heat recovery from low-temperature flue gas. Energy, 55:216-25.

[6] Department of Alternative Energy Development and Efficiency. (2015) Biomass Potential in Thailand]online] Available: http://www.dede.go.th [August, 25, 2015].

[7] Thawonngamyingsakul C., Kiatsiriroat T. (2011) Economic analysis of an organic Rankine cycle with rice husk as heat source. The 4th Thailand Renewable Energy for Community Conference, Lampang Rajabhat University, Lampang, Thailand 28-30 November 2011.

[8] Energy Policy and Planning Office, Ministry of Energy. Feed-in tariff for Biomass in Thailand. [online] Available: http://www.eppo.go.th/FIT/part2.pdf [August, 25, 2015].

[9] "European Wood-Heating Technology Survey" [online] Available: https://www.nyserda.ny.gov/Publications/Research-and-Development-Technical-Reports/Other-Technical-Reports/European-Wood-Heating-Technology-Survey.aspx [August, 25, 2015].

[10] National Institute of Standard and Technology (NIST), (2013) REFPROP Version 9, Thermodynamic Properties of Refrigerants and Refrigerant Mixtures Software, 2013.

IX. Nomenclature

c_e = cost of electricity (Baht/kWh)
c_{fuel} = cost of fuel (Baht/kWh)
LHV = low heating value (kJ/kg)
$\dot{E}_{HWout}$ = Exergy of hot water (kW)
$\dot{E}_{fuel}$ = Exergy of fuel (kW)
$\dot{Q}_{heater}$ = heat rate from fuel combustion (kW)
$\dot{m}$ = mass flow rate (kg/s)
n_{HW} = water heater efficiency
$\dot{W}_e$ = rate of work (kW)
$\dot{Z}_{WH}$ = cost rate of water heater (Bath/hr)
$\dot{Z}_{ORC}$ = cost rate of ORC (Bath/hr)
$\dot{Z}_{HX}$ = cost rate of heat exchanger (Bath/hr)
$\dot{Z}_{O\&M}$ = cost rate of operating & maintenance equipment (Bath/hr)

Deethayat T. and Kiatsiriroat T.

"Prediction of Low Temperature Organic Rankine Cycle (ORC) Thermal Efficiency by A Dimensionless FOM"

The 8th Thailand Renewable Energy for Community Conference, 4-6 November 2015, Bangkok, Thailand.


มหาวิทยาลัยเทคโนโลยีราชมงคลธัญบุรี
40th Anniversary
ENGINEERING
RMUTT
สมาคมพลังงานทดแทนสู่ชุมชนแห่งประเทศไทย
การประชุมสัมมนาเชิงวิชาการ
รูปแบบพลังงานทดแทนสู่ชุมชนแห่งประเทศไทย ครั้งที่ 8
4-6 พฤศจิกายน 2558
คณะวิศวกรรมศาสตร์
มหาวิทยาลัยเทคโนโลยีราชมงคลธัญบุรี
TREC 8
Thunya
Power Co.,Ltd.
บ้านสินทรัพย์
โครงการ 3
GH BANK
ptt
Group
IRPC
IRPC Public Company Limited
RMUTT
IRD

CP007

การทำนายประสิทธิภาพทางความร้อนของวัฏจักรแรงคินสารอินทรีย์แบบอุณหภูมิต่ำจากตัวแปรไร้มิติ FOM

Prediction of Low Temperature Organic Rankine Cycle (ORC) Thermal Efficiency by A Dimensionless FOM

ธรณิศวร์ ดีทายาท [1] และ ทนงเกียรติ เกียรติศิริโรจน์[2]

[1]สาขาวิชาวิศวกรรมพลังงาน คณะวิศวกรรมศาสตร์ และบัณฑิตวิทยาลัย มหาวิทยาลัยเชียงใหม่
[2]ภาควิชาวิศวกรรมเครื่องกล คณะวิศวกรรมศาสตร์ มหาวิทยาลัยเชียงใหม่
Email : thoranisdee@gmail.com

บทคัดย่อ

งานวิจัยนี้ได้สร้างสมการที่ใช้ในการทำนาย ประสิทธิภาพทางความร้อนของวัฏจักรแรงคินสารอินทรีย์ (organic Rankine cycle, ORC) ทำงานที่อุณหภูมิต่ำ โดยใช้ตัวแปรไร้มิติในรูป Figure of Merit, FOM ซึ่งครอบคลุมตัวแปรได้แก่ จาคอบนัมเบอร์, อุณหภูมิควบแน่นและอุณหภูมิระเหย สารทำงานที่พิจารณามี 6 ชนิด ได้แก่ R245fa, R245ca, R227ea, R236ea และ R152a โดยอุณหภูมิสารทำงานในช่วงการทำระเหย 80-130°C และอุณหภูมิควบแน่น 25-40°C

ผลการศึกษาพบว่า เมื่อนำประสิทธิภาพทางความร้อนของ ORC จากข้อมูลการทดสอบจริงและงานวิจัยที่ผ่านมา ไปเปรียบเทียบกับค่าที่ได้จากสมการที่พัฒนาพบว่า ค่าความคลาดเคลื่อนไม่เกิน 3.66% เทคนิคดังกล่าวสามารถนำไปหากำลังงานที่ผลิตได้ เมื่อกำหนดอุณหภูมิและอัตราการไหล ของน้ำร้อนที่เป็นแหล่งความร้อนให้แก่วัฏจักร และอุณหภูมิและอัตราการไหลของน้ำเย็นที่ระบายความร้อน

คำสำคัญ: วัฏจักรแรงคินสารอินทรีย์, ประสิทธิภาพทางความร้อน, Figure of Merit

Abstract

This paper proposed a model to predict thermal efficiency of low temperature organic Rankine cycle (ORC) in a form of dimensionless term namely Figure of Merit, FOM. The term combines Jacob number with condensing temperature and evaporating temperature. The considered working fluids are R245fa, R245ca, R227ea, R236ea and R152a. The evaporating temperature and the condensing temperature are in ranges of 80-130°C and 25-40°C, respectively.

The results from the model were compared to those from some testing data and existing literature. It was found that the results fitted very well of which the deviation was less than 3.66%. This technique also used to calculate power generation from ORC when the temperatures and the flow rates of the hot and the cold water as the heat source and heat sink, respectively were defined.

Keywords: organic Rankine cycle, thermal efficiency, Figure of Merit

บทนำ

การผลิตไฟฟ้าโดยใช้วัฏจักรไอน้ำ ยังเป็นวิธีหลักวิธีหนึ่งในปัจจุบัน ข้อเสียของการใช้น้ำเป็นสารทำงานในวัฏจักรแรงคินนั้น คือต้องให้ความร้อนที่สูงถึงประมาณ 600°C [1] เพื่อให้สามารถเปลี่ยนน้ำเป็นไอน้ำอิ่มตัว และ ในระดับไอร้อนยวดยิ่ง เพื่อลดการควบแน่นระหว่างการขยายตัว เชื้อเพลิงที่ใช้ในการให้ความร้อนแก่วัฏจักรในปัจจุบัน ยังเป็นเชื้อเพลิงฟอสซิล ก่อให้เกิดปัญหาด้านสิ่งแวดล้อม เช่น มลพิษทางอากาศ ได้แก่ คาร์บอนไดออกไซค์ (CO_2) คาร์บอนมอนออกไซค์ (CO) มีเทน (CH_4) ซัลเฟอร์ไดออกไซค์ (SO_2) และ ไนโตรเจนออกไซค์ (NO_x) ทำให้เกิดสภาวะโลกร้อน การทำลายชั้นโอโซนและฝนกรด ในระหว่างปี ค.ศ.2010-2014 [2] พบว่าการใช้พลังงานด้านไฟฟ้ามีการปล่อยก๊าซคาร์บอนไดออกไซด์สูงที่สุด ซึ่งก๊าซดังกล่าวเป็นสาเหตุหลักของปรากฏการณ์เรือนกระจก

จากเป้าหมายการใช้พลังงานทดแทนของประเทศไทย ภายในปี ค.ศ. 2021 [3] จะมีการส่งเสริมให้ชุมชนมีส่วนร่วมในการผลิตและการใช้พลังงานทดแทนโดยมีสัดส่วนเป็น 25% ของการใช้พลังงานทั้งหมด รัฐบาลส่งเสริมให้มีการผลิตไฟฟ้าจากแสงอาทิตย์, พลังน้ำและชีวมวลค่อนข้างสูง อีกทั้งยังมุ่งเน้นผลิตไฟฟ้าระดับหมู่บ้านให้แก่ราษฎรที่ไม่มีไฟฟ้าใช้ โดยสนับสนุนการก่อสร้างโครงการไฟฟ้าระดับชุมชน ให้องค์กรปกครองส่วนท้องถิ่นหรือชุมชนเจ้าของพื้นที่มีส่วนร่วม เป็นเจ้าของโครงการ สามารถบริหารงานและบำรุงรักษาเองได้ในอนาคต

วัฏจักรแรงคินสารอินทรีย์ (Organic Rankine Cycle) ดังรูปที่ 1 เป็นวัฏจักรผลิตไฟฟ้าที่น่าสนใจ สำหรับแผนพัฒนาพลังงานทดแทนและพลังงานทางเลือก เนื่องจากวัฏจักรแรงคินสารอินทรีย์ มีระบบโครงสร้างเหมือนวัฏจักรแรงคินไอน้ำ โดยมีลักษณะโครงสร้างที่ไม่ซับซ้อน และบำรุงรักษาง่าย มีการใช้สารอินทรีย์ที่มีจุดเดือดต่ำเป็นสารทำงาน ซึ่งสามารถเปลี่ยนสถานะเป็นไออิ่มตัวหรือไอร้อนยวดยิ่งเมื่อได้รับความร้อนจากแหล่งความร้อนอุณหภูมิไม่สูงมากนัก ทำให้สามารถใช้แหล่งความร้อนได้หลายชนิด เช่น พลังงานจากการเผาขยะ พลังงานจากแสงอาทิตย์ พลังงานจากชีวมวล ซึ่งพลังงานเหล่านี้สามารถหาได้ในชุมชนรวมถึงความร้อนทิ้งจากอุตสาหกรรมเป็นต้น

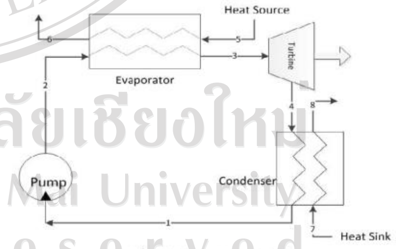

รูปที่ 1. วัฏจักรแรงคินสารอินทรีย์

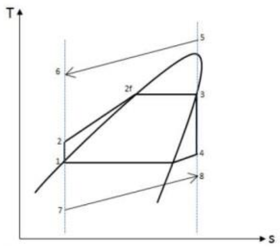

รูปที่ 2 แผนภาพอุณหภูมิ-เอนโทรปีสำหรับสารทำงานใน ORC

ประสิทธิภาพทางความร้อนของระบบ ORC เกี่ยวข้องกับสมบัติทางกายภาพทางเธอร์โมไดนามิกส์หลายๆตัว ในงานวิจัยทั่วไปนั้นต้องคำนวณหาประสิทธิภาพทางความร้อนโดยใช้สมบัติทางเธอร์โมไดนามิกส์ ซึ่งมีความยุ่งยากและใช้เวลานาน Kuo et al. 2009 [4] ได้เสนอตัวแปรไร้มิติในรูป "Figure of Merit"(FOM) ที่ประกอบด้วยจาคอบ นัมเบอร์ (Jacob number) อุณหภูมิระเหยและอุณหภูมิควบแน่น ซึ่งส่งผลต่อประสิทธิภาพทางความร้อนที่ใช้สารทำงานชนิดต่างๆโดยตรง อีกทั้งยังสามารถเลือกสารทำงานเพื่อทำให้ประสิทธิภาพของ ORC มีค่าสูง โดยประสิทธิภาพเชิงความร้อนจะลดลงเมื่อ FOM มีค่าสูงขึ้น

ในงานวิจัยนี้ เทคนิคการคำนวณ FOM ที่นำเสนอโดย Kuo et al. 2009 [4] ได้ถูกนำมาหาประสิทธิภาพทางความร้อนของ ORC ที่ใช้อุณหภูมิระเหยอยู่ในช่วง 80-130°C อุณหภูมิควบแน่น 25-40°C ทั้งนี้วิธีการดังกล่าวไม่ต้องใช้สมบัติทางเธอร์โมไดนามิกส์ ทำให้การคำนวณสะดวกและรวดเร็ว โดยมีความแม่นยำสูง

ทฤษฎี

วัฏจักรแรงคินสารอินทรีย์

วัฏจักรแรงคินสารอินทรีย์ มีระบบโครงสร้างเหมือนวัฏจักรแรงคินไอน้ำ วัฏจักรพื้นฐานประกอบไปด้วยอุปกรณ์ 4 ตัว คือ ปั๊ม (Pump) เครื่องระเหย (Evaporator) เทอร์ไบน์ (Turbine) และเครื่องควบแน่น (Condenser) ดังรูปที่ 1 และสมการที่คำนวณพลังงานในรูปของงานและความร้อนที่อุปกรณ์ต่างๆ สามารถพิจารณาจากสมบัติทางเธอร์โมไดนามิกส์ตามสภาวะต่างๆ จากแผนภาพอุณหภูมิ-เอนโทรปี ตามรูปที่ 2 ดังนี้

ปั๊ม:

$$\dot{W}_p = \frac{\dot{m}v_1(P_2-P_1)}{\eta_P} \quad (1)$$

$$\dot{W}_p = \dot{m}(h_{2a} - h_1). \quad (2)$$

เครื่องระเหย:

$$\dot{Q}_E = \dot{m}(h_3 - h_{2a}). \quad (3)$$

เทอร์ไบน์:

$$\dot{W}_T = \dot{m}(h_3 - h_4)\eta_T. \quad (4)$$

เครื่องควบแน่น:

$$\dot{Q}_C = \dot{m}(h_{4a} - h_1). \quad (5)$$

ประสิทธิภาพทางความร้อน

$$\eta_{th} = \frac{\dot{W}_T - \dot{W}_P}{\dot{Q}_E}. \quad (6)$$

สำหรับวัฏจักรในอุดมคติ งานจาก การขยาย (expansion) และการอัด (compression) เป็นกระบวนการที่ย้อนกลับได้โดยไม่มีการถ่ายเทความร้อนหรือที่เรียกว่า ไอเซนทรอปิก สถานะของสารทำงานที่ทางเข้าปั๊มและเทอร์ไบน์อยู่ในสภาวะอิ่มตัว

แต่ในทางปฏิบัติ ประสิทธิภาพไอเซนทรอปิกที่การอัดและการขยายน้อยกว่า 100% เพื่อให้ง่ายต่อการคำนวณ จึงกำหนดให้งานที่เกิดจากแรงอัดนั้นถือว่าน้อยมาก ดังนั้นประสิทธิภาพจริงของวัฏจักรสามารถคำนวณได้ดังนี้

$$\eta_{actual\ cycle} = \eta_{th\ ideal} \times \eta_T \quad (7)$$

ประสิทธิภาพทางความร้อนของวัฏจักรของแต่ละสารทำงานนั้น สามารถคำนวณได้จากอุณหภูมิระเหยและอุณหภูมิควบแน่น โดย Kuo et al. 2009 [4] ได้เสนอพารามิเตอร์ที่รวมกันให้อยู่ในรูปของตัวแปรไร้มิติในเทอมที่เรียกว่า "Figure of Merit, FOM" โดยใช้ทำนายประสิทธิภาพทางความร้อนของ ORC ที่ได้ดังสมการต่อไปนี้

$$Figure\ of\ Merit\ (FOM) = Ja^{0.1}\left(\frac{T_{cond}}{T_{evap}}\right)^{0.8} \quad (8)$$

โดยที่

Ja = Jacob number

T_{cond} = อุณหภูมิควบแน่น (°C)

T_{evap} = อุณหภูมิระเหย (°C)

เงื่อนไขของวัฏจักรแรงคินสารอินทรีย์ และขอบเขตสำหรับการประมวลผล มีดังนี้

ตารางที่ 1. เงื่อนไขที่ใช้ในการคำนวณ

พารามิเตอร์	ข้อมูล
ประสิทธิภาพไอเซนทรอปิกปั๊ม (η_p)	1
ประสิทธิภาพไอเซนทรอปิกเทอร์ไบน์ (η_T)	1
อุณหภูมิทำระเหย	80-130°C
อุณหภูมิควบแน่น	25-40°C
อุณหภูมิสิ่งแวดล้อม	25°C

สำหรับสารทำงานที่เลือกใช้ในงานวิจัยนี้จะพิจารณาจากปัจจัยต่างๆ เช่น เวลาที่สารตกค้างในบรรยากาศ ศักยภาพในการทำลายโอโซน ศักยภาพในการทำให้โลกร้อน อุณหภูมิวิกฤติ ซึ่งในการศึกษาครั้งนี้ได้เลือกสารทำงาน 6 ชนิด คือ R245fa, R245ca, R227ea, R236ea และ R152a โดยมีคุณสมบัติต่างๆ ดังตารางที่ 2 และในการคำนวณตามสมการทางเธอร์โมไดนามิกส์ คุณสมบัติสารทำงานอ้างอิงตาม REFPROP [5]

ตารางที่ 2 คุณสมบัติต่างๆของสารทำงาน

สารทำงาน	Physical Data		Environmental Data			ชนิดสารทำงาน
	อุณหภูมิวิกฤติ(°C)	อุณหภูมิจุดเดือดที่ความดันบรรยากาศ (°C)	ALT (ปี)	ODP	GWP (100 ปี)	
R245fa	154.01	15.14	7.6	0	710	แห้ง
R245ca	174.42	25.13	6.2	0	693	แห้ง
R227ea	101.75	-16.34	34.2	0	3220	แห้ง
R152a	113.3	-24	1.4	0	124	เปียก

R123	183.7	27.8	1.3	0.02	77	ไอเซนทรอปิก
R236ea	139.29	6.19	8	0	710	แห้ง

ผลการศึกษาและอภิปราย

วัฏจักรอุดมคติ

ในรูปที่ 3 แสดงถึงความสัมพันธ์ระหว่างประสิทธิภาพทางความร้อนในอุดมคติและ FOM โดยใช้สารทำงานต่างๆ ที่อุณหภูมิเครื่องทำระเหยและอุณหภูมิเครื่องควบแน่นต่างๆกัน พบว่าเมื่อ ค่า FOM จะมีค่าลดลง ประสิทธิภาพทางความร้อนจะมีค่าสูงขึ้น

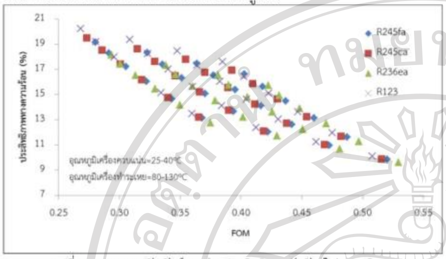

รูปที่ 3 แสดงความสัมพันธ์ระหว่างประสิทธิภาพวัฏจักรในอุดมคติและ FOM สำหรับสารทำงานต่างๆ ที่อุณหภูมิควบแน่นและอุณหภูมิทำระเหย

จากรูปที่ 3 เราสามารถสร้างสมการที่ใช้ในการทำนายประสิทธิภาพทางความร้อน (η_{th}) โดยทำให้อยู่ในรูปของอุณหภูมิควบแน่น (T_{cond}) และ FOM ได้ ดังสมการ

$$\eta_{th\,ideal} = [40.44 - 0.17T_{cond} + 0.0035T_{cond}^2] + [-132.76 + 3.604T_{cond} - 0.0428T_{cond}^2]FOM. \quad (9)$$

$80°C \leq T_{evap} \geq 130°C$ และ $25°C \leq T_{cond} \geq 40°C$

วัฏจักรจริง

เพื่อตรวจสอบความถูกต้องของเทคนิคดังกล่าว จึงได้นำสมการที่ 9 มาทำนายประสิทธิภาพทางความร้อนของสารทำงานแบบสารเดี่ยว แล้วคูณด้วยประสิทธิภาพทางไอเซนทรอปิกของเทอร์ไบน์ เพื่อประเมินวัฏจักรจริงของสารทำงาน R245fa ORC ซึ่งมีข้อมูลทดลองดังตารางที่ 3

ตารางที่ 3 ข้อมูลการทดสอบของ 245fa ORC 20kW รุ่น Hanbell model : RC2-300 hot water source, 3P380V50Hz Induction generator

รายละเอียด	เงื่อนไข 1	เงื่อนไข 2	เงื่อนไข 3	หน่วย
เครื่องทำระเหย				
อุณหภูมิน้ำร้อนขาเข้า	116	107.8	97	°C
ความจุแหล่งความร้อน	244	238.3	228.8	kW
เครื่องควบแน่น				
อุณหภูมิน้ำเย็นขาเข้า	28	28	28	°C
ความจุแหล่งระบายความร้อน	219	215.6	210.9	kW
เทอร์ไบน์				
ความดันขาเข้าเทอร์ไบน์	1097	1120	1074	kPa-Abs
ความดันขาออกเทอร์ไบน์	227.4	227.4	227	kPa-Abs
อุณหภูมิขาเข้าเทอร์ไบน์	93.7	94.6	92.8	°C
อุณหภูมิขาออกเทอร์ไบน์	37.1	37	37	°C
ประสิทธิภาพไอเซนทรอปิกของเทอร์ไบน์	71.4	67.9	56.6	%
ประสิทธิภาพวัฏจักร	9.40	8.81	7.37	%

จากสมการที่ 9 ประสิทธิภาพทางความร้อนทางอุดมคติของวัฏจักร ORC ที่สภาวะเดียวกันกับตารางที่ 3 คือ 12.92%, 13.08% และ 12.80% ตามลำดับ เมื่อนำมาคูณกับประสิทธิภาพไอเซนทรอปิกของเอ็กซ์แพนเดอร์ 71.4%, 67.9% และ 56.6% ดังสมการที่ 7ดังนั้น ประสิทธิภาพทางความร้อนของวัฏจักรจริงจะได้ 9.23%, 8.88% และ 7.25% ตามลำดับ ซึ่งเมื่อเทียบกับข้อมูลทดสอบในตารางที่ 3 มีค่าใกล้เคียงกัน พบว่าเปอร์เซ็นต์ค่าความคลาดเคลื่อนมีค่าไม่เกิน 1.81% ดังรูปที่ 4

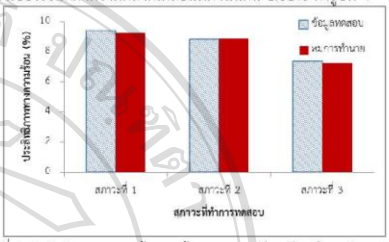

รูปที่ 4 ประสิทธิภาพทางความร้อนของข้อมูลทดสอบเปรียบเทียบกับการทำนายจากโมเดล

สมการที่ 9 ยังนำมาใช้เปรียบเทียบประสิทธิภาพทางความร้อนกับงานวิจัยของ Saleh et al.[6] โดยสภาวะที่ใช้คือ อุณหภูมิเครื่องทำระเหยสำหรับ R245fa, R245ca และ R236ea คือ 100°C, อุณหภูมิเครื่องทำระเหยสำหรับ R152 และ R227ea คือ72.59°C และ 83.88°C ตามลำดับ ส่วนอุณหภูมิควบแน่นคือ 30 °C โดยมีประสิทธิภาพไอเซนทรอปิกของเทอร์ไบน์คือ 85%

ในรูปที่ 5 แสดงประสิทธิภาพทางความร้อนของสารทำงานต่างๆเปรียบเทียบระหว่างงานของ Saleh et al. กับงานปัจจุบัน พบว่าสมการที่ 9 สามารถใช้ทำนายประสิทธิภาพทางความร้อนได้ใกล้เคียงกับงานของ Saleh et al. โดยค่าความคลาดเคลื่อนสูงสุดมีค่าเท่ากับ 3.66%

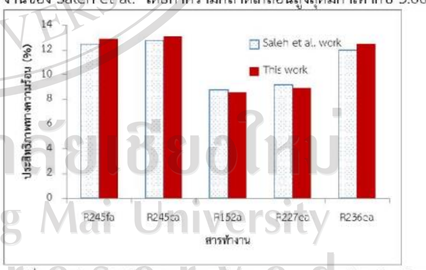

รูปที่ 5 กราฟแสดงประสิทธิภาพทางความร้อนของ Saleh et al. เปรียบเทียบกับการทำนาย

เทคนิคที่พัฒนายังสามารถนำไปประเมินกำลังงานที่ผลิตได้จากวัฏจักร เมื่อกำหนดอุณหภูมิน้ำร้อนและอัตราการไหลของน้ำร้อนในการแลกเปลี่ยนความร้อนกับวัฏจักร ดังแสดงในรูปที่ 6

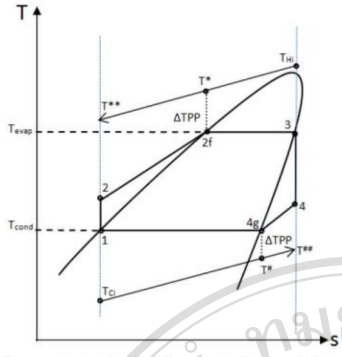

รูปที่ 6 แผนภาพอุณหภูมิ-เอนโทรปี ในการวิเคราะห์สมรรถนะวัฏจักร ORC

จากรูปที่ 6 เมื่อกำหนดพินช์พ้อยท์ (Δ_{TPP}) ในการแลกเปลี่ยนความร้อนที่เครื่องทำระเหยและเครื่องควบแน่น, อัตราการไหลของน้ำร้อน, อุณหภูมิของน้ำร้อน (T_{Hi}) และอุณหภูมิของน้ำเย็น (T_{Ci})

กำหนด T_{evap}

$$T^{*} = T_{evap} + \Delta TPP \quad (10)$$

$$(\dot{m}C_p)(T_{Hi} - T^{*}) = \dot{m}_R(h_{2f} - h_3) \quad (11)$$

$$(\dot{m}C_p)(T^{*} - T^{**}) = \dot{m}_R(h_{2f} - h_2) \quad (12)$$

กำหนด T_{cond}

$$T^{\#} = T_{cond} - \Delta TPP \quad (13)$$

$$(\dot{m}C_p)(T^{\#} - T_{Ci}) = \dot{m}_R(h_{4g} - h_1) \quad (14)$$

$$(\dot{m}C_p)(T^{\#\#} - T^{\#}) = \dot{m}_R(h_4 - h_1) \quad (15)$$

จากสมการที่ 6 และ 9 เมื่อทราบ η_{th} และกำหนดให้ $\dot{W}_P$ มีค่าน้อยมาก ดังนั้น เราสามารถทราบ $\dot{W}_T$ ได้จาก

$$\dot{W}_T = \eta_{th} \times (\dot{m}C_p)(T_{Hi} - T^{**}) \quad (16)$$

ผลที่ได้แสดงดังตัวอย่างในตารางที่ 4

ตารางที่ 4 ตัวอย่างการคำนวณหากำลังงานที่ได้จากวัฏจักร ORC

รายละเอียด	สภาวะ	หน่วย
สารทำงาน	R245fa	-
อุณหภูมิน้ำร้อนขาเข้า (T_{Hi})	150	°C
อัตราการไหลน้ำร้อน ($\dot{m}$)	5	Kg/s
อุณหภูมิระเหย (T_{evap})	90	°C
พินช์พ้อยท์ (ΔTPP)	10	°C
อุณหภูมิควบแน่น (T_{cond})	40	°C
ประสิทธิภาพไอเซนทรอปิกของเทอร์ไบน์	80	%
ประสิทธิภาพของวัฏจักร (η_{th})	9.23	%
กำลังงานที่ได้จากวัฏจักร ($\dot{W}_T$)	115.57	kW

จากตัวอย่างการคำนวณ เมื่อทราบอุณหภูมิน้ำร้อน อัตราการไหลของน้ำร้อน โดยกำหนดอุณหภูมิระเหยและอุณหภูมิควบแน่น จะสามารถทำให้ทราบกำลังงานที่ได้จากวัฏจักรได้ ซึ่งจะช่วยลดเวลาในการคำนวณเทียบกับการวิเคราะห์โดยการคำนวณตามสมการเธอร์โมไดนามิกส์

สรุปผลการศึกษา

ประสิทธิภาพทางความร้อนของ ORC ทำงานที่อุณหภูมิต่ำ สามารถประเมินได้จากตัวแปรไร้มิติในรูป FOM ซึ่งครอบคลุมตัวแปรได้แก่ จาคอบนัมเบอร์, อุณหภูมิควบแน่นและอุณหภูมิระเหย สารทำงานที่พิจารณามี 6 ชนิด ได้แก่ R245fa, R245ca, R227ea, R236ea และ R152a โดยอุณหภูมิสารทำงานในช่วงการทำระเหย 80-130°C และอุณหภูมิควบแน่น 25-40°C ซึ่งเมื่อนำไปทดสอบเทียบกับข้อมูลการทดสอบจริงและงานวิจัยที่ผ่านมา พบว่ามีความแม่นยำสูง เทคนิคดังกล่าวสามารถนำไปหากำลังงานที่ผลิตได้ เมื่อกำหนดอุณหภูมิและอัตราการไหล ของน้ำร้อนที่เป็นแหล่งความร้อนให้แก่วัฏจักร และอุณหภูมิและอัตราการไหลของน้ำเย็นที่ระบายความร้อน โดยไม่ต้องใช้สมบัติทางเธอร์โมไดนามิกส์ ทำให้การคำนวณทำได้สะดวกและรวดเร็ว

กิตติกรรมประกาศ

ขอขอบคุณ บัณฑิตวิทยาลัย มหาวิทยาลัยเชียงใหม่ ที่ให้การสนับสนุนงานวิจัย และขอขอบคุณหน่วยวิจัยระบบทางอุณหภาพ ภาควิชาวิศวกรรมเครื่องกล คณะวิศวกรรมศาสตร์ มหาวิทยาลัยเชียงใหม่ ที่ให้เอื้อเฟื้อสถานที่ทำงานวิจัย

เอกสารอ้างอิง

[1] O. Badr, S.D. Probert, P.W. O'Callaghan., "Selecting a working fluid for a Rankine-cycle engine", Applied Energy, 21(1), pp.1-42, 1985

[2] กระทรวงพลังงาน (2554) "แผนพัฒนาพลังงานทดแทน (2554-2573)."http://www.eppo.go.th/encon/ee-20yrs/EEDP_Thai.pdf [2558, 14 กรกฎาคม].

[3] กรมพัฒนาพลังงานทดแทนและอนุรักษ์พลังงาน (2558)" แผนพัฒนากำลังผลิตไฟฟ้าของประเทศไทย พ.ศ.2558–2579 (PDP2015)" http://www.eppo.go.th/PDP_hearing/PDP2015_FG.pdf [2558, 15 กรกฎาคม].

[4] Kuo C. R., Hsu S. W., Chang K. H., Wang C. C. "Analysis of a 50 kW organic Rankine cycle system". Energy, 36, pp.5877-85, 2011.

[5] National Institute of Standard and Technology (NIST). REFPROP Version 9, Thermodynamic Properties of Refrigerants and Refrigerant Mixtures Software. 2013.

[6] Tchanche BF, Papadakis G, Lambrinos G, Frangoudakis A. "Fluid selection for a low-temperature solar organic Rankine cycle". Applied Thermal Engineering, 29, pp.2468-76, 2009.

สัญลักษณ์

h_1 เอนทาลปีที่สภาวะที่ 1 (kJ/kg)
h_2 เอนทาลปีที่สภาวะที่ 2 (kJ/kg)
h_{2a} เอนทาลปีที่สภาวะที่ 2a (kJ/kg)
h_3 เอนทาลปีที่สภาวะที่ 3 (kJ/kg)
h_4 เอนทาลปีที่สภาวะที่ 4 (kJ/kg)
h_{4a} เอนทาลปีที่สภาวะที่ 4a (kJ/kg)
$\dot{m}$ อัตราการไหลของสารทำงานในวัฏจักร (kg/s)

P_1 ความดันที่สภาวะที่ 1 (kPa)
P_2 ความดันที่สภาวะที่ 2 (kPa)
$\dot{Q}_C$ อัตราความร้อนที่สูญเสียจากเครื่องควบแน่น(kW)
$\dot{Q}_E$ อัตราความร้อนที่ให้แก่เครื่องระเหย (kW)
v_1 ปริมาตรจำเพาะที่สภาวะที่ 1 (m^3/kg)
$\dot{W}_T$ กำลังงานที่เทอร์ไบน์ได้จากวัฏจักร (kW)
$\dot{W}_p$ กำลังงานที่ป้อนเข้าปั๊ม (kW)
η_{th} ประสิทธิภาพทางความร้อน

ประวัติโดยย่อ
นายธรณิศวร์ ดีทายาท
ได้รับปริญญาวิศวกรรมศาสตรบัณฑิต
สาขาวิศวกรรมเครื่องกล
และวิศวกรรมศาสตรมหาบัณฑิต
สาขาวิศวกรรมพลังงาน คณะวิศวกรรมศาสตร์
มหาวิทยาลัยเชียงใหม่ ในปีการศึกษา 2551 และ 2556 ตามลำดับ
ปัจจุบันเป็นนักศึกษาปริญญาเอกสาขาวิศวกรรมพลังงานในมหาวิทยาลัยเดียวกัน
งานวิจัยที่สนใจ
Biofuels; Combined Cooling, Heat and Power, Energy Efficiency

ประวัติโดยย่อ
นายทนงเกียรติ เกียรติศิริโรจน์
ปัจจุบันเป็นศาสตราจารย์ทางเทคโนโลยีอุณหภาพ คณะวิศวกรรมศาสตร์มหาวิทยาลัยเชียงใหม่
งานวิจัยที่สนใจ การพัฒนาน้ำมันจากชีวมวลและการเพิ่มประสิทธิภาพในระบบพลังงาน

Deethayat T. and Kiatsiriroat T.

“Performance Analysis of Low Temperature Organic Rankine Cycle with Zeotropic Refrigerant by Figure of Merit (FOM)”

Energy, Vol.96, 2016, pp. 96-102 (Thompson Reuters Impact Factor 4.844).

Energy 96 (2016) 96–102

Contents lists available at ScienceDirect

Energy

journal homepage: www.elsevier.com/locate/energy

Performance analysis of low temperature organic Rankine cycle with zeotropic refrigerant by Figure of Merit (FOM)

Thoranis Deethayat*, Attakorn Asanakham, Tanongkiat Kiatsiriroat

Department of Mechanical Engineering, Faculty of Engineering, Chiang Mai University, Chiang Mai 50200, Thailand

ARTICLE INFO

Article history:
Received 28 September 2015
Received in revised form
15 November 2015
Accepted 12 December 2015
Available online xxx

Keywords:
Organic Rankine cycle
Performance analysis
Figure of Merit
Zeotropic refrigerant

ABSTRACT

This paper proposed a dimensionless term, the "Figure of Merit" (FOM), to investigate the thermal performance of a low temperature, organic Rankine cycle using six zeotropic mixtures (R245fa/R152a, R245fa/R227ea, R245fa/R236ea, R245ca/R152a, R245ca/R227ea and R245ca/R236ea) as working fluids. An empirical correlation was developed to estimate the cycle efficiency from the FOM for all working fluids at condensing temperatures of 25–40 °C and evaporating temperatures of 80–130 °C. The model results fit very well with both the experimental data and that from other researchers.

1. Introduction

Excessive utilization of fossil fuels has led to many severe environmental problems, including global warming, ozone layer depletion, acid rain and air pollution. Hence, recovering waste heat from energy conversion or using renewable energy to reduce fossil fuel consumption is essential.

The organic Rankine cycle (ORC), a type of Rankine cycle, uses a working fluid with a low boiling point, and thus can generate electricity from low-temperature heat sources, such as low temperature waste heat, geothermal energy, solar energy or biomass combustion.

The first commercial ORC plant was installed in 1970. After that the ORC market is growing rapidly. According to Quoilin et al. [1], ORC is a mature technology for waste heat recovery and other sources from biomass and geothermal energy. ORC also has the potential to be developed for use with solar heat. Manolakosa et al. [2] designed and built a low-temperature (35–75.8 °C), solar ORC for reverse osmosis desalination. Nguyen et al. [3] designed and developed a small-scale, low temperature solar ORC to generate electricity with an efficiency of 4.3%. Velez et al. [4] reviewed the primary ORC manufacturers and found that most units were on a MW scale. However, the number of small ones (in the kW range) had increased significantly.

To improve ORC efficiency, some researches have focused on zeotropic working fluids with boiling and condensing temperatures changing with heat source and heat sink temperatures, respectively. With temperature differences during heat exchanges at the cycle evaporator and condenser less than those of the single working fluid, then the thermodynamic irreversibilities in these components can be reduced, resulting in a higher work output. Wang et al. [5] experimentally compared the performance of low temperature ORCs using pure fluid (R245fa) and its mixture (R245fa/R152a); the thermal efficiency of the zeotropic mixture was higher than that of pure R245fa. Dong et al. [6] found similar results with a high temperature ORC (heat source at 280 °C) using zeotropic mixtures of siloxanes as working fluids. For heat sources at temperatures of 150–250 °C, Chys et al. [7] found that the cycle efficiency increased 6–16% in ORC systems using zeotropic mixtures as the working fluids. Heberle et al. [8] found that the second law efficiency of an ORC with isobutane/isopentane and R227ea/R245fa as working fluids increased 4.3%–15% for the zeotropic mixtures compared with single isopentane and single R245fa.

The thermal efficiency of an ORC system is directly related to many thermophysical properties. Recently, Kuo et al. [9] studied the relationships of the thermodynamic properties of many working single fluids that affected ORC thermal efficiency. The properties could be consolidated in a dimensionless group, called Figure of Merit (*FOM*), which included the Jacob number and evaporating

* Corresponding author.
E-mail address: thoranisdee@gmail.com (T. Deethayat).

http://dx.doi.org/10.1016/j.energy.2015.12.047
0360-5442/

and condensing temperatures. The lower the *FOM* value, the higher the ORC thermal efficiency could be achieved. The *FOM* could also be used to screen working fluids to achieve higher ORC performance.

In this paper, a technique proposed by Kuo et al. [9] was modified to determine a correlation between the cycle efficiency for small-scale ORC and FOM at evaporating temperatures of 80–130 °C and condensing temperatures of 25–40 °C with zeotropic mixtures in the case of the ideal cycle. A factor to allocate the zeotropic fluid properties in a form of FOM similar to that of single fluids was created and set up in the term of gliding temperature of the working fluid. It could be noted that only dry fluids having positive slope of the saturated vapor line in T-s diagram or isentropic fluid were considered thus the fluids during expansion were superheat.

2. Thermodynamics cycle

Fig. 1(a) shows the ORC configuration, which consists of a pump, an evaporator, an expander and a condenser. The working fluid leaves the condenser as a saturated liquid (state 1) and it is pumped to the evaporator (state 2) to be heated and vaporized by various heat sources, such as waste heat, hot water from solar heat or geothermal energy. The generated high-pressure vapor (state 3) flows into the expander to generate power and, thereafter, the low pressure vapor exits the expander (state 4) to the condenser, where the vapor is condensed by rejecting heat to cooling water. The condensed working fluid at the condenser outlet is pumped back to the evaporator, and a new cycle begins. All of the above described processes are shown in a temperature versus entropy diagram for ideal ORCs with single and zeotropic working fluids in Fig. 1(b) and (c), respectively.

It can be seen in Fig. 1(c), during heat exchange at the evaporator and condenser of the ORC, there were temperature differences between the streams of the heat source and heat sink with the ORC working fluid, respectively. The temperature differences generated irreversibilities at the cycle components, and then some part of the cycle work was destroyed. As an example, the isothermal phase change during states 2f-3 for the single fluid after replacing by the non-isothermal zeotropic fluid, the temperature difference between the hot fluid stream and the phase change temperature is less and the irreversibility due to the heat exchange is smaller. Similar result is found at the condenser.

The energy balance at each component can be summarized as follows:

Pump:

$$\dot{W}_p = \frac{\dot{m}v_1(P_2 - P_1)}{\eta_P} \quad (1)$$

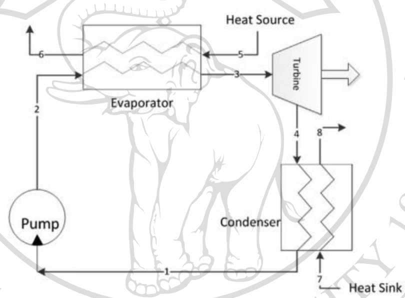

a. ORC basic components.

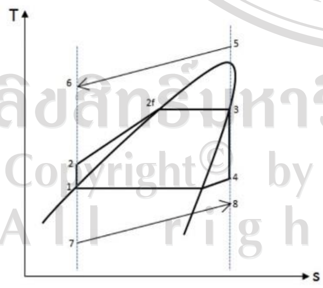

b. T-s diagram of ORC for single fluid.

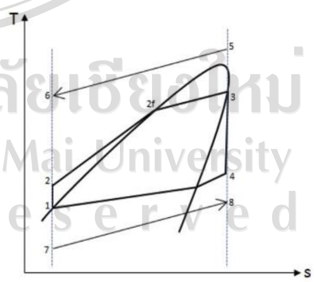

c. T-s diagram of ORC for zeotropic fluid.

Fig. 1. Thermodynamic cycles of ideal ORC for single and zeotropic working fluids.

$$\dot{W}_P = \dot{m}(h_2 - h_1). \quad (2)$$

Evaporator:

$$\dot{Q}_E = \dot{m}(h_3 - h_2). \quad (3)$$

Turbine:

$$\dot{W}_T = \dot{m}(h_3 - h_4)\eta_T. \quad (4)$$

Condenser:

$$\dot{Q}_C = \dot{m}(h_{4a} - h_1). \quad (5)$$

Thermal efficiency:

$$\eta_{th} = \frac{\dot{W}_T - \dot{W}_P}{\dot{Q}_E}. \quad (6)$$

For the ideal cycle, the expansion work and the compression work are isentropic. The states of the working fluid entering the expander and pump are saturated.

In real practice, the isentropic efficiencies during expansion and compression are less than 100%. For simplicity, the compression work is rather small; if assumed negligible, then the actual cycle efficiency can be calculated by:

$$\eta_{actualcycle} = \eta_{thideal} \times \eta_{isentropicturbine} \quad (7)$$

The cycle efficiency for each working fluid can be calculated from the above equations at various evaporating and condensing temperatures. The calculation steps are shown in Fig. 2.

Kuo et al. [9] consolidated the related parameters in a term named "Figure of Merit" (*FOM*) that affects the ORC thermal efficiency. The *FOM* was defined as:

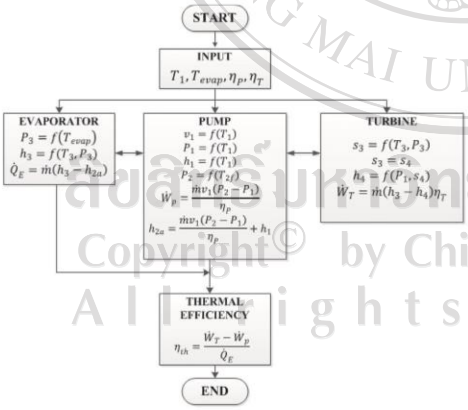

Fig. 2. Flow chart for calculating the thermal efficiency of the ORC from thermodynamic properties. The condition at the turbine inlet was saturated vapor.

$$Figure\ of\ Merit(FOM) = Ja^{0.1}\left(\frac{T_{cond}}{T_{evap}}\right)^{0.8}. \quad (8)$$

This dimensionless term includes the Jacob number (Ja), the evaporating and the condensing temperatures. The Jacob number is defined as $Ja = \frac{C_p \Delta T}{h_{fg}}$, where C_p represents the average specific heat evaluated from the mathematical mean of the condensing and the evaporating temperatures, ΔT is the temperature difference between the evaporator and the condenser temperatures, and h_{fg} denotes the latent heat at the evaporating temperature. *FOM* increases when the evaporating temperature decreases or the condensing temperature increases. These also result to the decreases in the output work and the cycle efficiency.

The cycle efficiency can be calculated from thermodynamic properties following equations (1)–(7) at various condensing and evaporating temperatures. The cycle efficiency depended strongly on the *FOM*; the lower the value of *FOM*, the higher the thermal efficiency of the ORC could be achieved.

This study considered various single and zeotropic working fluids. The conditions for the calculation of ideal ORC performance are given in Table 1.

3. Working fluids

For low temperature ORCs, a variety of low temperature heat sources – waste heat, geothermal heat, solar heat or biomass combustion – can be used to generate a hot water stream (80–130 °C) that supplies heat to the ORC evaporator. The ORC working fluids should be screened for: environmental impact – low ozone depression potential (ODP) low global warming potential (GWP) and low atmospheric life time (ALT); chemical stability in the operating temperature range; and thermal stability. Five working fluids – R245fa, R152a, R227ea, R245ca and R236fa – and their blending in the form of zeotropic fluids were selected. The physical and environmental properties of the fluids are shown in Tables 2 and 3. The thermodynamic properties of the single fluids and their mixtures can be obtained from REFPROP 9.0 [10].

4. Results and discussion

4.1. Single fluids

Ideal Cycles:

Fig. 3 shows the correlation between the ideal cycle efficiency calculated from equations (1)–(6) and the *FOM* for various single working fluids, when the evaporating and the condensing temperatures are prescribed. For each selected working fluid, *Ja* can be estimated, followed by the *FOM*. It could be seen that if the evaporating temperature increased, then the *FOM* was decreased which resulted in higher the thermal efficiency. Thus, the *FOM* term could be used to screen working fluids for high thermal efficiency at the same evaporating and condensing temperatures.

Table 1
The conditions for calculating ideal ORC performance.

Parameter	Data
Isentropic efficiency of pump (η_p)	1
Isentropic efficiency of turbine (η_T)	1
Evaporating temperature	80–130 °C
Condensing temperature	25–40 °C
Ambient temperature	25 °C

Table 2
Physical and environmental properties of the working fluids [11,12].

Substance	Physical properties				Environmental properties			Type
	M (kg/kmol)	T_{cri}(°C)	P_{cri} (Mpa)	T_b (°C)	ALT (yr)	ODP	GWP (100 yr)	
R245fa	134.05	154.01	3.65	15.14	7.6	0	710	Dry
R245ca	134.05	174.42	3.93	25.13	6.2	0	693	Dry
R236ea	152.04	139.29	3.5	6.19	8	0	710	Dry
R227ea	170.03	101.75	2.925	−16.34	34.2	0	3220	Dry
R152a	66.05	113.3	4.52	−24	1.4	0	124	Wet
R123	152.93	183.7	3.67	27.8	1.3	0.02	77	Isentropic

Table 3
Physical properties of the zeotropic working fluids [10].

Substance	Mass fraction	Physical properties		
		M (kg/kmol)	T_{cri} (°C)	P_{cri} (Mpa)
R245fa/R152a	90/10	121.54	147.44	3.91
R245fa/R152a	80/20	111.16	141.36	4.07
R245fa/R152a	70/30	102.42	136.29	4.20
R245fa/R227ea	90/10	136.95	149.57	3.65
R245fa/R227ea	80/20	139.97	144.86	3.63
R245fa/R227ea	70/30	143.13	139.89	3.59
R245ca/R236ea	90/10	135.65	170.98	3.93
R245ca/R236ea	80/20	137.3	167.42	3.90
R245ca/R236ea	70/30	138.98	163.77	3.85
R245ca/R227ea	90/10	136.95	169.37	3.98
R245ca/R227ea	80/20	139.97	163.64	3.97
R245ca/R227ea	70/30	143.13	157.35	3.94
R245ca/R152a	90/10	121.54	166.05	4.30
R245ca/R152a	80/20	111.16	157.57	4.49
R245ca/R152a	70/30	102.42	149.19	4.57
R245fa/R236ea	90/10	135.65	151.88	3.63
R245fa/R236ea	80/20	137.3	149.82	3.61
R245fa/R236ea	70/30	138.98	147.85	3.58

From Fig. 3, the thermal efficiency (η_{th}) can be expressed as a function of the condensing temperature (T_{cond}) and *FOM* as:

$$\eta_{thideal} = \left[40.44 - 0.17T_{cond} + 0.0035T_{cond}^2\right] + \left[-132.76 + 3.604T_{cond} - 0.0428T_{cond}^2\right] FOM. \quad (9)$$

The calculation steps for evaluating the thermal efficiency was shown in Fig. 4.

4.2. Experimental cycle

Single Fluid:

From equation (7), the actual thermal efficiency for single fluids can be evaluated by multiplying $\eta_{thideal}$ by the isentropic efficiency of expander. A set of experimental data from a commercial modular ORC was taken to verify the calculation from the proposed method. The specification of the commercial modular ORC was given in Table 4. The testing results were shown in Table 5.

From equation (9), the ideal ORC cycle efficiencies (at the same conditions as given in Table 3) were found to be 12.92%, 13.08%, and 12.80%, respectively. With the isentropic efficiencies at the expander, the actual cycle efficiencies could be calculated and the values were close to those of the experimental cycle. The results were shown in Table 6.

The *FOM* from our method were also used to evaluate the ORC cycle efficiencies studied by Saleh et al. [13] and very good agreement of the results were found as shown in Table 7.

4.3. Zeotropic mixture

Ideal Cycle

This paper considered six zeotropic mixtures: R245fa/R152a, R245fa/R227ea, R245fa/R236ea, R245ca/R152a, R245ca/R227ea and R245ca/R236ea. The mass fractions of R245fa and R245ca were recommended to be at least 70% [5,12]. Fig. 5 shows the correlation

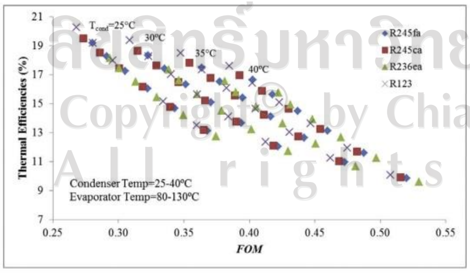

Fig. 3. The correlation between the ideal cycle efficiency and the *FOM* for various single working fluids and condensing and evaporating temperatures.

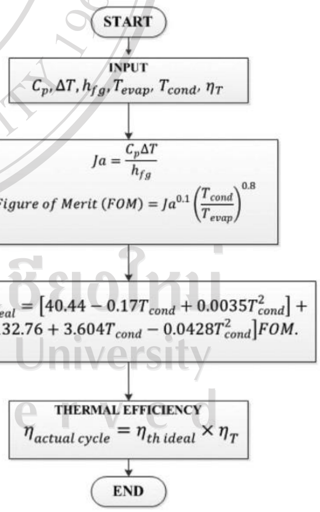

Fig. 4. Flow chart for calculating the thermal efficiency of the ORC from *FOM*. The condition at the turbine inlet was saturated vapor.

Table 4
The specification of the commercial modular ORC.

ORC type	R245fa hot water source, 3P 380 V 50 Hz induction generator	
	Gross power:20 kW	Net power:16 kW
Refrigerant	R245fa	
Expander	Semi-hermetic twin screw type expander with direct drive induction generator	
	Model:RC2-300	300CMH displacement volume
Evaporator	SUS 316 plate type heat exchanger, Z400H × 136	
	Hot water inlet 110 °C	flow rate:150LPM
	Capacity:260 kW	Hot water connection:3″ JIS10K
Condenser	Shell and tube heat exchanger	
	Shell: Carbon steel 12″ × 3000 mmL	
	Tube:3/4″ copper tube with inner and outer low fin tube	
	Cooling water: inlet 30 °C	Outlet 35 °C
	Flow rate: 810 LPM	Water connection:4″ Flange

Table 5
Testing data of the commercial modular ORC.

Descriptions	Condition 1	Condition 2	Condition 3	Unit
Evaporator				
Hot water inlet	116	107.8	97	°C
Heat source capacity	244	238.3	228.8	kW
Condenser				
Cool water inlet	28	28	28	°C
Heat sink capacity	219	215.6	210.9	kW
Expander				
Expander inlet pressure	1097.1	1120	1074	kPa-Abs
Expander outlet pressure	227.4	227.4	227	kPa-Abs
Expander inlet temperature	93.7	94.6	92.8	°C
Expander outlet temperature	37.1	37	37	°C
Isentropic efficiency of the expander	71.4	67.9	56.6	%
Cycle Efficiency	9.40	8.81	7.37	%

Table 6
Comparison of the results from the proposed method with real cycle efficiency.

Descriptions	Condition 1	Condition 2	Condition 3	Unit
Ideal cycle efficiency from eqn. (9)	12.92	13.08	12.8	%
Isentropic efficiency of the expander	71.4	67.9	56.6	%
Cycle efficiency (from the present method)	9.23	8.88	7.25	%
% Difference from experimental cycle in Table 4.	1.81	0.79	1.63	%

Table 7
Comparison of the results calculated from this study with Saleh et al. [13].

Working fluid	η_{th}		% Difference from Saleh et al.
	Saleh et al. [13]	This study	
R245fa	12.52	12.89	2.96
R245ca	12.79	13.13	2.66
R152a	8.82	8.59	2.61
R227ea	9.2	8.90	3.26
R236ea	12.02	12.46	3.66

Operating conditions: The evaporating temperature for R245fa, R245ca and R236ea was 100 °C; the evaporating temperatures for R152a and R227ea were 7259 °C and 83.88 °C, respectively. The condensing temperature was 30 °C and the isentropic efficiency of the turbine was 0.85.

between the ideal cycle efficiency with $FOM_{zeotropic}$ for these zeotropic refrigerants compared with that for single R245fa. The evaporating and the condensing temperatures for the $FOM_{zeotropic}$ calculation were taken from the saturated liquid at the evaporating pressure and the saturated vapor at the condensing pressure, respectively. It could be seen that the data points were highly disordered with the zeotropic working fluids.

The deviation of cycle efficiency from the single fluid was mainly due to the gliding temperatures of the zeotropic fluids, as shown in Table 8.

Fig. 6 shows the deviation of $FOM_{zeotropic}$ for zeotropic working fluids from FOM for the main single fluids (FOM_{single}): the higher the gliding temperature, the higher the deviation from the single fluid. The deviation (D) empirically related to the gliding temperature (T_g) as:

$$D = 0.0004T_g^2 + 0.0004T_g + 0.0047. \tag{10}$$

The $FOM_{zeotropic}$ for zeotropic mixture then could be modified as:

$$FOM_{zeotropic} = F\left(FOM_{single}\right). \tag{11}$$

where F is the correction factor: $F = (1 - D) = [1 - (0.0004T_g^2 + 0.0004T_g + 0.0047)]$.

From equation (11), with the gliding temperature of a selected zeotropic fluid, the $FOM_{zeotropic}$ could be calculated from the FOM_{single}. The correlation between the ideal thermal efficiency and the $FOM_{zeotropic}$ at various condensing and evaporating temperatures could be developed as shown in Fig. 7. Now the data points could be presented orderly. Again, a lower $FOM_{zeotropic}$ resulted in a higher thermal efficiency.

We expressed the thermal efficiency (η_{th}) as a function of the condensing temperature (T_{cond}) and the $FOM_{zeotropic}$ as:

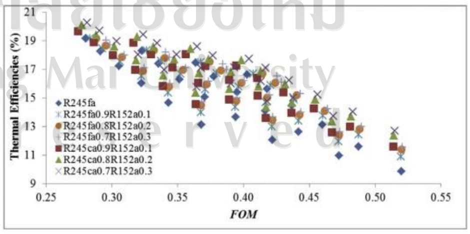

Fig. 5. The correlation between the ideal cycle efficiency with $FOM_{zeotropic}$ for zeotropic refrigerants.

Table 8
Gliding temperatures when the evaporation temperature was 80–130 °C and the condensing temperature was 25–40 °C.

Working fluid	Mass fraction	Evaporating temperature (°C)					
		80	90	100	110	120	130
R245fa/R152a	90/10	6.66	6.12	5.56	4.96	4.29	3.48
R245fa/R152a	80/20	8.76	8.02	7.23	6.35	5.32	3.99
R245fa/R152a	70/30	8.92	8.12	7.23	6.22	4.99	3.20
R245fa/R227ea	90/10	3.19	2.92	2.64	2.36	2.05	1.71
R245fa/R227ea	80/20	5.19	4.75	4.29	3.79	3.25	2.59
R245fa/R227ea	70/30	6.25	5.69	5.09	4.45	3.70	2.73
R245ca/R236ea	90/10	1.44	1.36	1.28	1.20	1.11	1.01
R245ca/R236ea	80/20	2.35	2.22	2.09	1.94	1.79	1.61
R245ca/R236ea	70/30	2.81	2.66	2.49	2.31	2.11	1.89
R245ca/R227ea	90/10	5.43	5.06	4.69	4.31	3.93	3.51
R245ca/R227ea	80/20	8.93	8.34	7.73	7.09	6.41	5.66
R245ca/R227ea	70/30	10.94	10.21	9.43	8.60	7.67	6.61
R245ca/R152a	90/10	11.63	10.90	10.14	9.33	8.46	7.50
R245ca/R152a	80/20	15.08	14.12	13.08	11.93	10.64	9.14
R245ca/R152a	70/30	15.36	14.29	13.11	11.78	10.24	8.34
R245fa/R236ea	90/10	0.46	0.43	0.39	0.35	0.31	0.27
R245fa/R236ea	80/20	0.69	0.63	0.58	0.52	0.46	0.38
R245fa/R236ea	70/30	0.74	0.68	0.61	0.55	0.48	0.40

Note: The main single fluids are R245fa and R245ca.

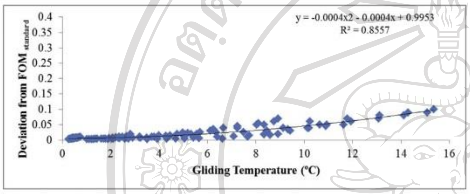

Fig. 6. The deviations of *FOM* for all zeotropic working fluids in this study from that of the single fluids.

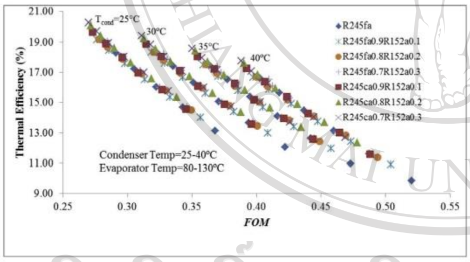

Fig. 7. The correlation of the cycle efficiency with the $FOM_{zeotropic}$ for R245fa/R152a and R245ca/R152a at various compositions.

$$\eta_{th} = \left[40.44 - 0.17T_{cond} + 0.0035T_{cond}^2\right] + \left[-132.76 + 3.604T_{cond} - 0.0428T_{cond}^2\right]FOM_{zeotropic}. \quad (12)$$

The calculation steps for evaluating the thermal efficiency was shown in Fig. 8.

For zeotropic working fluids, we compared the calculated efficiency from eqn. (12) with the results of Li et al. [14] of which the efficiencies were calculated from thermodynamic properties. The ORC used the zeotropic mixture R245fa/R152a (0.8/0.2) at an

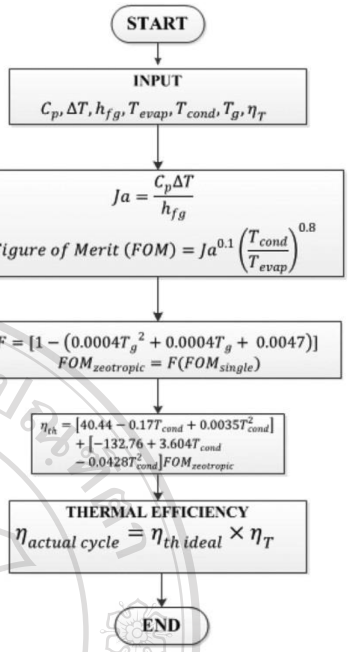

Fig. 8. Flow chart for calculating the thermal efficiency of the ORC from $FOM_{zeotropic}$. The condition at the turbine inlet was saturated vapor.

evaporating temperature of 90–110 °C and a condensing temperature of 25 °C. Our results from eqn. (12) agreed well with the literature, as shown in Table 9.

From the above results, it could be noted that with η_{th} -FOM chart, if the evaporating temperature, the condensing temperature and the working fluid properties are prescribed, the FOM could be calculated and the cycle efficiency could be estimated without any information of thermodynamic properties. The process is very simple and the results are very accurate. In addition the FOM could also be used to screen the working fluid including its operating temperature to get high thermal efficiency.

5. Conclusion

The thermal efficiency of an ORC system could be indicated by a dimensionless term namely "Figure of Merit (*FOM*)", which covered parameters such as the Jacob number and the evaporating and the condensing temperatures of the ORC. The *FOM* could be used to

Table 9
Comparison of the results calculated from this study with Li et al. [14].

Evaporating temperature (°C)	η_{th}		% Difference from Li et al.
	Li et al. [14]	This study	
90	11.65	10.97	5.86
100	12.45	12.00	3.61
110	13.12	12.83	2.20

screen the working fluids for high thermal efficiency at prescribed evaporating and condensing temperatures. A lower *FOM* resulted in higher thermal efficiency.

For zeotropic working fluids, *FOM* must be modified by multiplying a correction factor *F* that relied on the gliding temperature of the zeotropic mixture.

A model to predict the zeotropic ORC efficiency was developed. The results fitted very well with those from the literature.

Acknowledgments

The authors would like to thank the Graduate School and Thermal System Research Unit, Department of Mechanical Engineering, Chiang Mai University for providing facilities. In addition, the authors would like to acknowledge the Commission on Higher Education under the National Research University Project for their financial support.

References

[1] Quoilin S, Van Den Broek M, Declaye S, Dewallef S, Lemort V. Thermo-economic optimization of waste heat recovery organic Rankine cycles. Appl Therm Eng 2011;31:2885–93.
[2] Manolakos D, Papadakis G, Kyritsis S, Bouzianas K. Experimental evaluation of an autonomous low-temperature solar Rankine cycle system for reverse osmosis desalination. Desalination 2007;203:366–74.
[3] Nguyen VM, Doherty PS, Riffat SB. Development of a prototype low-temperature Rankine cycle electricity generation system. Appl Therm Eng 2001;21:169–81.
[4] Vélez F, Segovia JJ, Carmen Martín M, Antolín G, Chejne Farid, Quijano A. A technical, economical and market review of organic Rankine cycles for the conversion of low-grade heat for power generation. Renew Sustain Energy 2012;16:4175–89.
[5] Wang XD, Zhao L. Analysis of zeotropic mixtures used in low-temperature solar Rankine cycles for power generation. Sol Energy 2009;83:605–13.
[6] Dong B, Xu G, Cai Y, Li H, Haiwang L. Analysis of zeotropic mixtures used in high-temperature organic Rankine cycle. Energy Convers Manag August 2014;84:253–60.
[7] Chys M, van de Broek M, Vanslambrouck B, De Paepe M. Potential of zeotropic mixtures as working fluids in organic Rankine cycles. Energy 2012;44:623–32.
[8] Heberle F, Preißinger M, Brüggemann D. Zeotropic mixtures as working fluids in organic Rankine cycles for low-enthalpy geothermal resources. Renew Energy 2012;37:364–70.
[9] Kuo CR, Hsu SW, Chang KH, Wang CC. Analysis of a 50 kW organic Rankine cycle system. Energy 2011;36:5877–85.
[10] National Institute of Standard and Technology (NIST). REFPROP version 9.1, thermodynamic properties of refrigerants and refrigerant mixtures software. 2013.
[11] Tchanche BF, Papadakis G, Lambrinos G, Frangoudakis A. Fluid selection for a low-temperature solar organic Rankine cycle. Appl Therm Eng 2009;29:2468–76.
[12] Li Z, Junjiang B. Thermodynamic analysis of organic Rankine cycle using zeotropic mixtures. Appl Energy October 2014;130:748–56.
[13] Saleh B, Koglbauer G, Wendland M, Fischer J. Working fluids for low-temperature organic Rankine cycles. Energy 2007;32:1210–21.
[14] Li YR, Du MT, Wu CM, Wu SY, Liu C. Potential of organic Rankine cycle using zeotropic mixtures as working fluids for waste heat recovery. Energy 2014;77:509–19.

Nomenclature

C_p: heat capacity, J/kg-K
h: specific enthalpy, J/kg
$\dot{m}$: mass flow rate, kg/s
P: pressure, kPa
T: temperature, °C, K
$\dot{Q}$: heat input, W
$\dot{W}$: work, W
η: efficiency, %
v: specific volume, m^3/kg

Subscripts

1, 2, 2a, … 4: state points
b: boiling point
cond: condenser
cri: critical point of temperature
g: gliding temperature
E: evaporator
P: pump
T: turbine
th: thermal

Acronyms

ALT: atmospheric life time
GWP: global warming potential
ODP: ozone depletion potential

CURRICULUM VITAE

Author's Name	Mr. Thoranis Deethayat
Date/Year of Birth	16 September 1986
Education	2009: B.Eng. (Mechanical Engineering) Chiang Mai University, Thailand
	2013:M.Eng. (Energy Engineering) Chiang Mai University, Thailand